Université de Lille

Doctoral School **Sciences Pour l'Ingénieur**
University Department **CRIStAL**

Thesis defended by

Manarshhjot Singh

on **22 April 2021**

In partial fulfilment of the requirements for PhD degree from Université de Lille

Academic field **Automatique et Industrial computer science**

Energy Activity: a common metric to perform diagnosis and prognosis.

Thesis supervised by	Belkacem Ould Bouamama	-	Supervisor
	Anne-Lise Gehin	-	Co-Supervisor
Composition of jury			
Referees:	Dominique Sauter	-	Professor, University of Nancy, Loraine (France)
	Aziz Naamane	-	Associate Professor, HDR, Université Aix-Marseille (France)
Examiners:	Loucas S. Louca	-	Associate Professor, University of Cyprus (Cyprus)
President of jury:	Kamal Medjaher	-	Professor, ENI de Tarbes (France)

Université de Lille

Ecole doctorale **Sciences Pour l'Ingénieur**
Unité de recherche **CRIStAL**

Thèse présentée par

Manarshhjot Singh

Soutenue le **22 Avril 2021**

En vue de l'obtention du grade de docteur de Université de Lille

Discipline **Automatique et Industrial computer science**

Energy Activity: une métrique commune pour effectuer le diagnostic et le pronostic.

Thèse dirigée par	Belkacem OULD BOUAMAMA	-	Directeur de thèse
	Anne-Lise GEHIN	-	Co-directeur de thèse
Composition de jury			
Rapporteurs:	Dominique SAUTER	-	Professor, University of Nancy, Loraine (France)
	Aziz NAAMANE	-	Associate Professor, HDR, Université Aix-Marseille (France)
Examinateurs:	Loucas S. LOUCA	-	Associate Professor, University of Cyprus (Cyprus)
Président du jury:	Kamal MEDJAHER	-	Professor, ENI de Tarbes (France)

Acknowledgements

Firstly, I would like to express my sincere gratitude to my supervisors **Prof. Belkacem Ould-Bouamama** and **Dr. Anne-Lise Gehin** for their continuous support, patience, motivation, and immense knowledge. Their guidance helped me in through every aspect of research and writing of this thesis. I could not have imagined to complete my PhD thesis without their extraordinary support.

I would also like to thank **Prof. Dominique Sauter** and **Prof. Aziz Namaane** for reviewing this thesis. Their recommendations and suggestions were very helpful in improving the structure of this thesis.

I would also like to thank **Prof. Rochdi Merzouki** for giving me opportunities to learn and grow by allowing me to work on projects outside my thesis.

I am immensely thankful to my lab and office colleagues **Houria Chaabna, Mahdi Boukerdja, Ismail Benzekrane, Abdelkader Belarouci and Othman Lakhal** for their interesting conversations, discussions, suggestions.

My parents **Prof. Daljeet Singh Prof. Mrs. Parwinder Kaur**, my sister **Dr. Anantroop Kaur** and **Jarvis** have been my greatest support all this while. Their love and care for me, knows no bounds. I am immensely grateful to them for everything. Daily video call with them was always the highlight of my day. I also thank my uncles Jatinder Singh Dr. Tejpreet Singh for their advises and my cousins Manamrit Singh Hitraj Singh constantly sharing memes.

I would like to thank close friends **Sumit Sood, Inderjeet Singh and Sepaldeep Singh Dhaliwal** for being with me though thick and thin. They always kept my motivation and confidence higher than eiffel tower. Special thanks to **Diksha Mukhija, Shivani Shisodia, Dr. Anuradha Tewari, Ramandeep Kaur, Shilpa Sonar, Dr. Tanushree Kane, Dr. Om Prakash, Dr. Pushpendra Kumar, Dr. Arun, Dr. Devdas Bhat and Dr. Umber Nooreen, Dr. Himani Garg, Dr. Dharmendra Pratap Singh, Asmita Shah and Akash**. Our regular meets (especially for food) have always made me happy. Sorry to those of you who tried, and then failed to teach me proper french. You had a really bad student. So, it is not your fault. Congratulations to those who taught me cooking. You did a wonderful job.

Last but not the least I thank the '*Lillua ke nayyab heere*' family (**Raghav, Ankita, Obaid, Ghazala, Kanika**).

Finally, I thank **god** for everything.

Abstract

Prognosis and Health Management (PHM) is a very useful tool for improving the overall safety, reliability and cost of a system. Fault diagnosis and prognosis are two pillars of a successful PHM. Both have their own challenges and are mostly studied independent of each other. Therefore, performing both fault diagnosis and prognosis using a common metric can greatly ease the overall implementation of PHM process and hence make the system more safe and reliable. This work proposes an innovative integrated framework for performing fault diagnosis and prognosis using a common metric i.e. Energy Activity (EA). The underlying framework is in the first step validated using simulated spring-mass-damper system. The proposed framework is further improved to addresses a major challenge to PHM i.e. robustness of decision considering both system parameter uncertainties and measurement uncertainties. The improved framework is successfully applied to a real hydraulic two-tank system test bed system under uncertain conditions.

Key words: Prognosis, Fault Diagnosis, Prognosis and Health Management (PHM), Bond Graph, End of Life (EOL), Remaining Useful Life (RUL)

Abstract

Les approches "Prognosis and Health Management" sont très utiles pour améliorer la sécurité globale, la fiabilité et le coût d'un système. Le diagnostic et le pronostic des pannes sont les deux piliers pour la conception d'un système sûr de fonctionnement. Chacun d'eux a ses propres défis et est pour la plupart du temps, étudié indépendamment l'un de l'autre. Par conséquent, effectuer à la fois le diagnostic et le pronostic des pannes à l'aide d'une métrique commune peut grandement faciliter le processus global d'implémentation des méthodes PHM et donc rendre le système plus sûr et plus fiable. Ce travail propose un nouveau formalisme intégrée pour effectuer le diagnostic et le pronostic des pannes en utilisant une métrique commune, à savoir l'activité énergétique (EA). La méthodologie développée est appliquée à un système ressort-masse-amortisseur. Les outils proposés sont enrichis pour relever un défi majeur pour le PHM, à savoir la robustesse de la décision en tenant compte à la fois des incertitudes paramétriques et de de mesure. La méthodologie complète est dans une deuxième phase appliquée avec succès à un système hydraulique de régulation de niveau dans des conditions incertaines.

Mots clés: Prognosis, Fault diagnosis, Prognosis et Health Management (PHM), Bond Graph, End of Life (EOL), Remaining Useful Life (RUL)

Contents

List of Figures

List of Tables

Chapter 1

General Introduction

Contents

1.1 Introduction to maintenance

Maintenance is one of the most crucial and one of the most under-recognised phase in the working of any plant. This is partly due to the fact that as long as the system remains in a good operating condition, the importance of maintenance is not recognised. However, the importance of this activity can be fully understood when any system goes to failure leading to financial loss on account of loss in revenue, loss in working hours, loss due to inventory accumulation etc. Many times, especially in an assembly line, a failure in any one stage leads to halt in the whole manufacturing line and leads to loss in production.. Therefore a great amount of brain power is used for optimization of maintenance activities. Over the years many strategies of maintenance have been developed. The various strategies of maintenance can be understood using fig 1.1.

The first strategy of maintenance is called **Corrective Maintenance**. Under this strategy, maintenance is performed only after a system or a subsystem experiences failure and ceases to work. This strategy has high monitory loss associated with it because a failure in crucial components can be very expensive. Therefore, this strategy is generally used in systems or machines which are in surplus and experience failures rarely.

The second and most commonly used strategy for maintenance is called **Preventive maintenance**. In this strategy, we do not wait for a system failure and the various components in the system undergo maintenance action at regular intervals of time. The time period of maintenance action is fixed either by the component manufacturer or by experience. This strategy is planned by considering a very conservative estimate of the machine life cycle, therefore the monetary losses by using this strategy is majorly due to the cost of the maintenance action itself and scheduling instead of losses due to failure.

The third and the upcoming strategy is **Condition based maintenance**. This strategy neither waits for failure nor recommends maintenance at regular intervals. In this strategy, the condition of machine is constantly monitored and as soon as a fault is observed, maintenance activity is performed. Therefore, the cost associated with this strategy is lower than both corrective and preventive maintenance.

Based on the extent of utilization, Condition based maintenance can be categorised into three levels

- Monitored Maintenance: This is the very basic level of condition based maintenance. At this level, only fault symptoms can be recognised and machine maintenance is performed when these symptoms are observed. This requires the least amount of monitoring equipment and hence the monitoring cost is the least. However, it has the highest maintenance cost among the three levels.

- Isolated Maintenance: This is the second level of condition based maintenance. At this level, the root cause of fault is isolated and maintenance action is recommended only for the faulty component. This requires a higher amount of sensors for proper fault isolation, therefore, has a higher set-up cost. However, higher set-up cost can be recovered by reduced maintenance cost.

- Identified Maintenance: This is the deepest level condition based monitoring. In addition to the outputs provided by isolated maintenance, this level also recognises the type of fault and recommends a suitable maintenance action. This level requires accurate data analytic databases and tools however no extra hardware is usually required.

The various strategies of maintenance can be understood using an example. Let's consider a simple rotary pump. According to corrective maintenance strategy, all maintenance actions are performed when the pump stops working. In preventive maintenance, a maintenance time period is fixed and all the maintenance actions are performed after this time period irrespective of the working condition of the pump. In monitored maintenance, a minimum number of sensors are placed in the system for condition monitoring e.g. flow sensor at the output. Therefore whenever the flow reduces from a predetermined level all maintenance actions are performed on the pump. In isolated maintenance, additional sensors are placed in the system like current sensor in the coil and r.p.m sensor at the shaft. Additional sensors allow for proper fault isolation. For e.g. if the fault is isolated in the shaft bearing then the other components of the pump do not require any maintenance action. This saves both maintenance time and cost. Continuing further, if identified maintenance is used, in addition to the previous, the system also informs about the type of fault. Using the previous example, the identified maintenance system can indicate a misalignment in the bearing which can be rectified by hammering, without the need of replacing the whole bearing. Hence, reducing the maintenance cost even further.

A lot of improvement in the available maintenance strategies is evident from the above example. A further monitory improvement is possible if maintenance scheduling can be optimized. Even at the identified maintenance level, the user only has information regarding the current state of the system, hence to reduce major losses, immediate intervention is required for maintenance. Sometimes the immediate intervention can incur losses of it's own, hence, optimized scheduling of the maintenance activity is the next step forward in the progression of maintenance strategies. For optimal scheduling, the point of actual failure of machine is more important than the current fault level. If the time of failure is known, then the maintenance action can be scheduled more conveniently. This is the basis of **Predictive Maintenance**. In this maintenance strategy, the end of life of the machine under the current faulty state is predicted. This is usually achieved using information from Identified Maintenance stage and physical laws governing the fault progression.

Before continuing further it is important to distinguish between fault and failure. Failure is a state of the system when the system fails to perform its intended operation. On the other

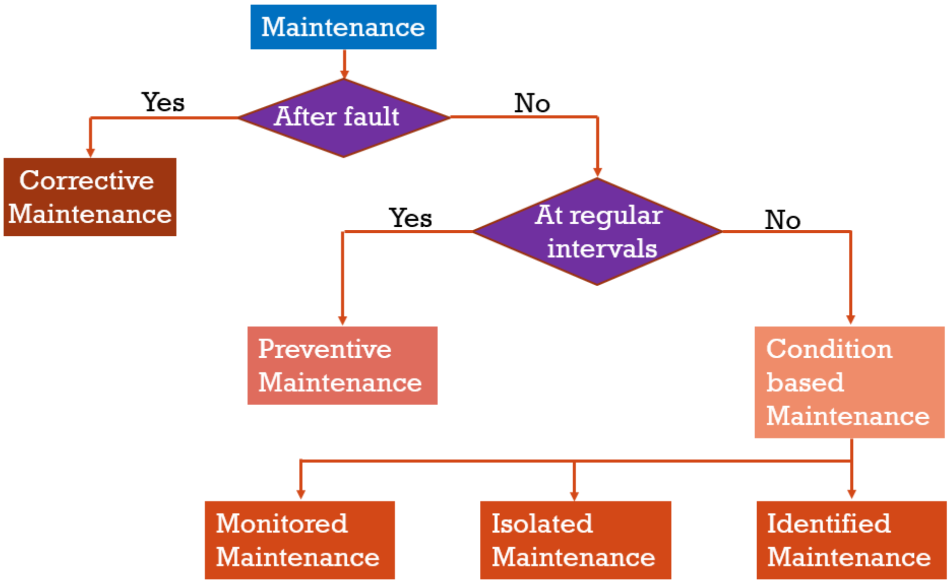

Figure 1.1: Maintenance Strategies

hand a fault is a state of a component when it interacts with the remaining components in sub optimal manner. Fault in a component can remain steady or increase i.e. continue to deviate more from the optimum state. A system with a faulty component can still function however only till a certain extent of fault. A fault in a component can evolve and progress, leading to the failure of system. For realisation of predictive maintenance, both the current state of health and the future state of health of system should be known. The field of study which deals with the current health estimation of the system is called Fault Detection and Identification (FDI) and the field of study dealing with the evolution of current health state in future is called Prognostics.

1.2 Definitions

Maintenance: Maintenance being a general term is used by practitioners of every field. Therefore, everyone has a general idea regarding maintenance. However, European Federation of Maintenance Societies defines it as "*All actions which have the objective of retaining or restoring an item in or to a state in which it can perform its required function. The actions include the combination of all technical and corresponding administrative, managerial, and supervision actions.*"

Some of the parameters used in maintenance system evaluation are:

Availability: It is the probability that of a system to operate satisfactorily at any point of time. It is measured using Mean Time To Repair (MTTR)

$$MTTR = \frac{1}{\mu} \text{ where } \mu \text{is rate of repair}$$

Reliability: It is the ability of a system to complete a required task under stated conditions. It is measured using Mean Time Before Failure (MTBF)

$$MTBF = \frac{1}{l_a} \text{ where } l_a \text{ is rate of failure}$$

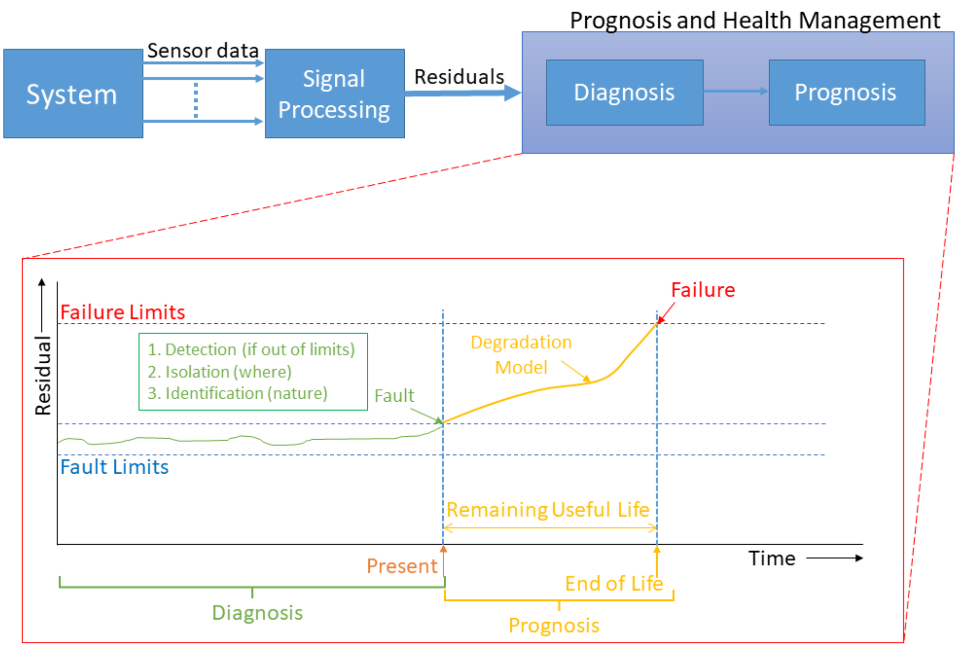

Figure 1.2: Schematic of Condition Based Maintenance.

Condition based Maintenance (CBM): Condition based maintenance can be described in short as 'maintenance according to requirement'. It is a maintenance strategy under which maintenance is scheduled by first analyzing the current state of system using system outputs and other sensor data and then using this information to calculate the time for maintenance and also the specific component that needs it.

Prognostics and Health management (PHM): Prognostics and health management (PHM) is an engineering approach which allows real-time health assessment and prediction of future state of a system while in operation. CBM is achieved using the concepts of PHM. PHM used the data collected by CBM system for appropriate maintenance decision.

Fault: According to ISO 10303-226, a fault is defined as an abnormal condition or defect at the component, equipment, or sub-system level which may lead to a failure. For this thesis a system component is considered faulty if the numerical value of it's corresponding physical parameter deviates from its intended value. For e.g. a spring considered as faulty if it's stiffness deviates from it's intended value.

It should be noted that a system under fault is not a system in failure.

Failure: A system succeeds if it able to fulfill it's desired functionality, similarly a system fails when it fails in it's functionality. Therefor, a system failure is the state of the under which it is unable to function according to it's intended requirements.

Diagnosis: The word 'Diagnosis' is derived from medical field meaning the identification of the nature of an illness or other problem by examination of the symptoms. In this thesis Diagnosis refers to Diagnosis of the system for faults. A fault diagnosis is achieved by three sequential steps:

1. Fault Detection
2. Fault Isolation
3. Fault Identification

As an example let's consider diagnosis of a simple motor driven wheel, *fault detection* tells us if there is any fault in the system. If there is a fault, *fault isolation* tells us the location of

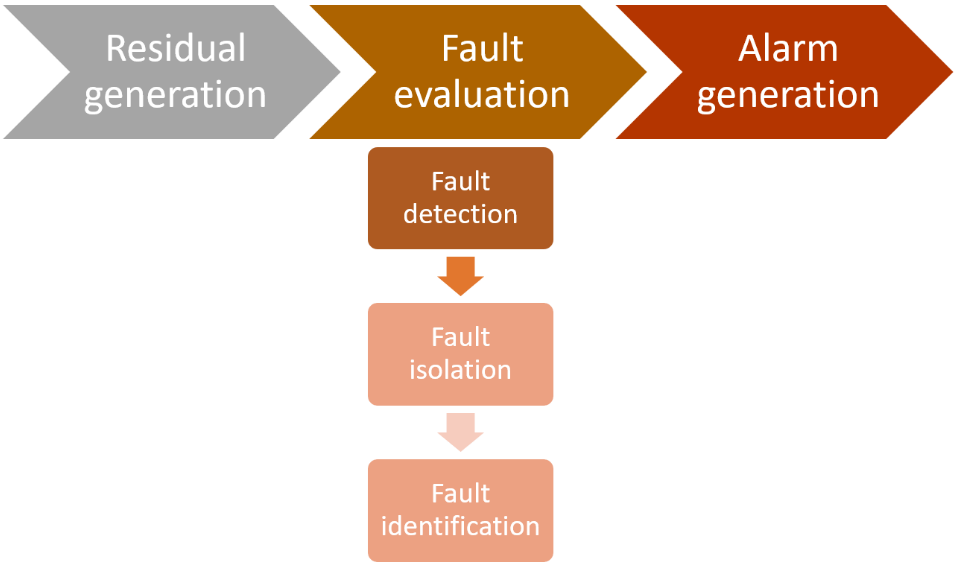

Figure 1.3: Overview of FDI process

the fault for e.g, if the fault is located in the motor or the bearing or the tyre. If the fault is isolated in the bearing, *Fault identification* tells us about the nature of the fault i.e. if there is a crack or if there a change in the rolling friction etc.

Prognosis: ISO13381-1 defines prognostics as: "the estimation of time to failure and risk for one or more existing and future failure modes". While diagnosis deals with the fault currently in the system, prognosis deals with prediction of the system behavior in future from its current faulty state till failure. Prognosis is generally used to calculate the remaining useful life of the system.

Degradation Model:Every component in any physical system continues to degrade continuously. However, a fault might accelerate this degradation. A degradation model is a mathematical tool to map the trend of degradation w.r.t time. A degradation model of any component can either be known beforehand or can be approximated on the go by PHM system. The current state of the system is extrapolated using the degradation model to calculate the end of life of the system.

End of Life (EOL): End of Life is the instant of time at which the system reaches failure.

Remaining Useful Life (RUL): At any instant after the detection of fault, remaining useful life of the system is defined as the time between that instant and EOL.

Residuals: Residuals are signals that carry fault information. These are calculated by observing the deviation between the actual signal generated from the system and the corresponding signal generated from simulation of fault free model.

1.3 Fault Detection and Identification

Fault detection and identification as the name suggests concerns with the accurate and timely detection of faults occurring in the system. The objective of FDI is to answer three basic questions:

1. Is the system under fault now?
2. If the system is under fault, where is the fault located i.e. which is the component under fault?

3. Once the location of the fault has been identified, what is the nature of the fault i.e. is it constant or increasing?

The above questions are answered by the following three activities of the FDI process [134]:

1. **Fault Detection:** This is the first activity of FDI. It answers the first question and informs if the system is currently under fault. Main performances at this step are false alarms and miss detection.

2. **Fault Isolation:** This activity starts after a fault has been detected in the system. It addresses the second question and informs about the location of fault i.e. the component responsible for the abnormal or sub-optimal system behavior. At this stage logic decision based on repertoried signatures are used

3. **Fault Identification:** This is the final activity of FDI and addresses the third question. This activity informs us about the nature of the fault.The previous steps are performed online while this stage is realized offline.

In general, the overall process for model based diagnosis consists of two steps before an alarm is generated (fig 1.3):

1. Residual generation: As discussed above, model based diagnosis based on the recreation of the known system information from the system outputs. The information recreated from the system outputs is compared to the known system information. The difference between the recreated system information and known system information is called residual. A near zero residual indicates a fault free system. However, if the residual deviates more than a pre-determined threshold, a fault is indicated.

2. Evaluation: The generated residual is examined to determine the presence or the location of the fault. Evaluation step incorporates also incorporates the various model uncertainties and measurement noise before coming up with a final decision on the fault.

1.4 Prognosis

By standard ISO13381-1, prognosis is defined as "the estimation of time to failure and risk for one or more existing and future failure modes". In essence, prognosis is the process predicting the time when the system will be unable to perform it's intended function with some required efficiency.

While utilizing prognosis as a part of a maintenance strategy, the purpose of prognosis is to find the condition of End of Life (EOL) and end of life time (t_{eol}). The end of life time should be calculated as soon as possible so that the remaining useful life is increased. This allows better decision on maintenance activity.

It must be realised that prognosis is much more complicated than FDI. This is primarily because in addition to the model and measurement uncertainties that are considered by FDI, prognosis should also include the effects of future uncertainties that have not yet been accounted for.

In addition to the above, a key element to prognosis process is the definition of the failure law undertaken by a failing component and definition of a failure limit in a manner that can be utilised by the prognosis process. The system performance is measured continuously using sensors placed on the system. The system performance measures and various definitions concerning the system failure are fed to a prognosis algorithm. The prognosis algorithm can

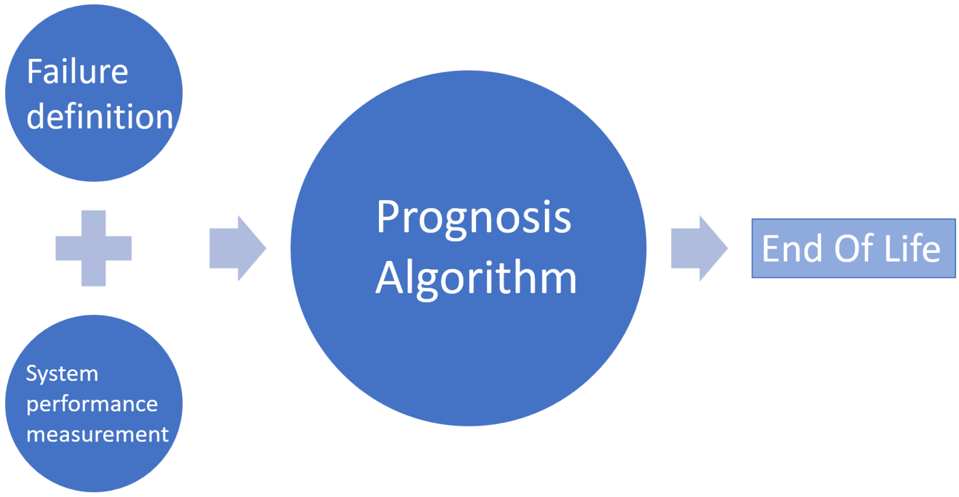

Figure 1.4: Overview of prognosis process

predicts the end of life of the system under the current working conditions. This process can be understood using fig 1.4.

However, prognosis has far reaching advantages (fig 1.5). The major advantages of prognosis are [130]:

1. Improved system design: Continuous monitoring of the system and prognosis can be used to redesign components to improve the overall system design, improve prediction model and preliminary logistics in the early phase of the system application.

2. Improved production: In manufacturing system the end product quality depends highly on the optimum working conditions of the system. Quality loss can accumulate quickly when the system works under sub-optimal condition. Prognosis of working conditions can be used to avoid this loss.

3. Benefits system operation: With continuous monitoring and good prognosis of the system the operation safety, reliability, availability, service life increases and system downtime, intermittent failures, false alarms decreases thereby improving the system operation.

4. Improved logistics: With a prognosis system in place CBM can be practiced. This saves a lot of logistic cost due to decrease in redundant inspections, unscheduled maintenance requirement etc.

5. Benefits in phase out and disposal: prognosis can be used to increase the working life of the system. Over time this reduces waste, improves system recovery and enables green manufacturing.

1.5 Prognosis and Health Management

Prognosis and health management (PHM) is the overall framework which allows for application of condition based maintenance.

A concise overview of the PHM process is given by fig 1.6. The main component of PHM are as follows:

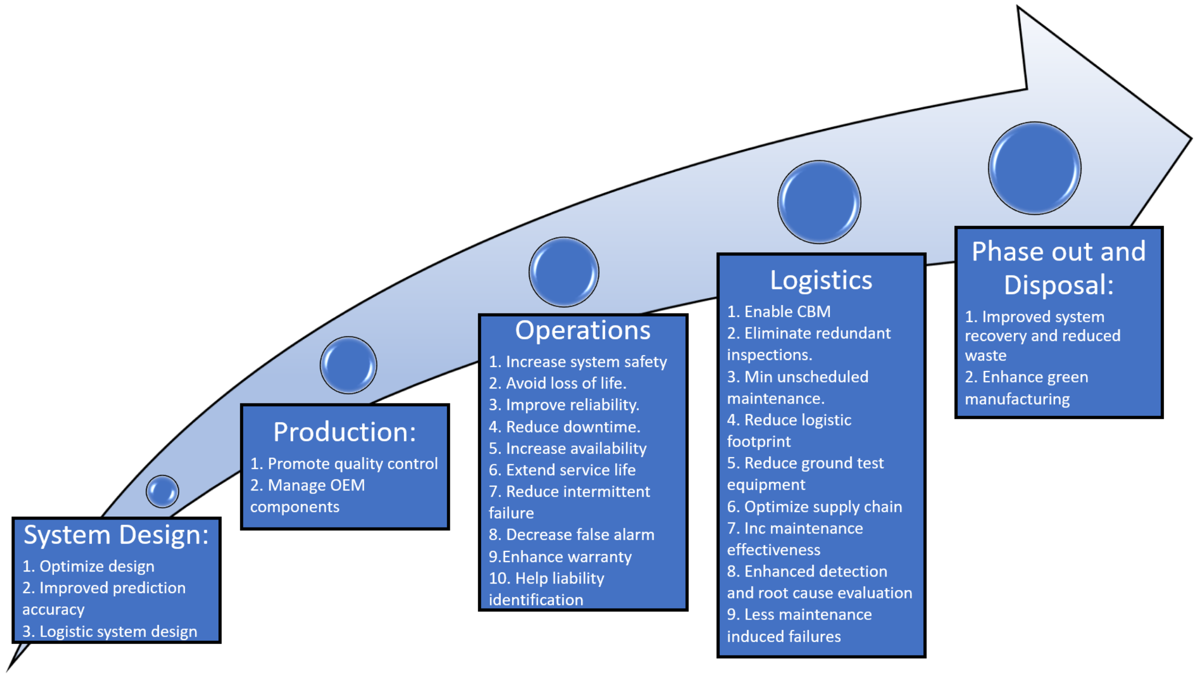

Figure 1.5: Advantages of prognosis in product life cycle [130]

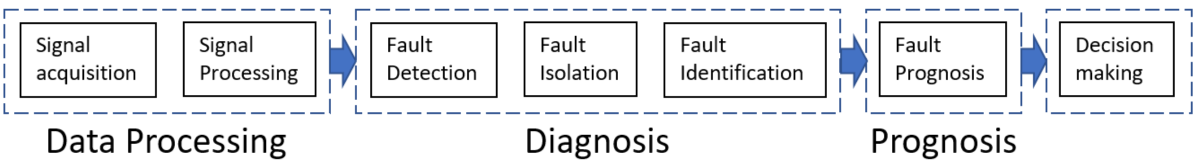

Figure 1.6: Overview of PHM

- *Data processing*: System is characterised by a set of physical values that have to follow predefined trajectories expressed by system input-output relations. Data processing extracts from the sensor signals the relevant information used for further analysis and system control.

- *Diagnosis*: System health estimation groups the FDI procedures allowing to estimate the health state of the system (faulty or non faulty). These procedures consist in three steps.

  - *Fault Detection*: Fault detection investigates the consistency between the actual values of the system outputs provided by the sensors and the predicted values of these outputs obtained from the reference system model.

    A fault is detected as soon as this consistency, expressed on the form of mathematical expressions called residuals, is not respected. Equation 1.1 gives the general form of a residual where $Y_{measured}$ is the actual value of the system output Y and $Y_{estimated}$ is its estimated value predicted by the model or other reference tables.

$$Residual = Y_{measured} - Y_{estimated} \tag{1.1}$$

  - *Fault Isolation*: Fault isolation consists in finding the faulty component using sensor information and, for examples, logic procedures, signal processing or reference tables.
  - *Fault Identification*: Fault identification gives an interpretation of the nature and the cause of the fault.

- *Prognosis*: Prognosis is a dynamic estimate of the degradation of the system. This deals with calculation of the End of Life of a system, a point in time at which the fault increases to its maximum limit resulting in system failure. Remaining Useful Life (RUL) of the system is expressed by equation 1.2 where $t_{failure}$ is the predicted time where the system cannot continue to operate due to complete failure and $t_{current}$ is the time at which the RUL is calculated.

$$RUL = t_{failure} - t_{current} \tag{1.2}$$

- *Decision making*: Detecting the occurring fault and estimating the RUL of the system can help in both protecting the system components, the system environment and/or ensuring the continuity of service when possible.

  Decision making can range from immediate human intervention to implementation of fault tolerant control by putting in priority users safety measures, system protection and continuity of service.

1.6 Thesis objective

Fault diagnosis and prognosis are the most fundamental building blocks of the PHM process. There are different schools of thought concerning relationship between diagnosis and prognosis [158] [64] [44]. The most widely accepted relationship assumes diagnosis as pre-requisite for prognosis and for most of PHM systems, prognosis follows diagnosis. However, despite this precedence constraint, diagnosis and prognosis are traditionally developed independently of each other, using well established but different techniques. So, merging both diagnosis and prognosis becomes then a real challenge, justifying the need of a common metric. Many attempts have been made to establish a common parameter for both diagnosis and prognosis. Integration of FDI and prognosis has been attempted using model based approaches [94] [59] [63] [111] which

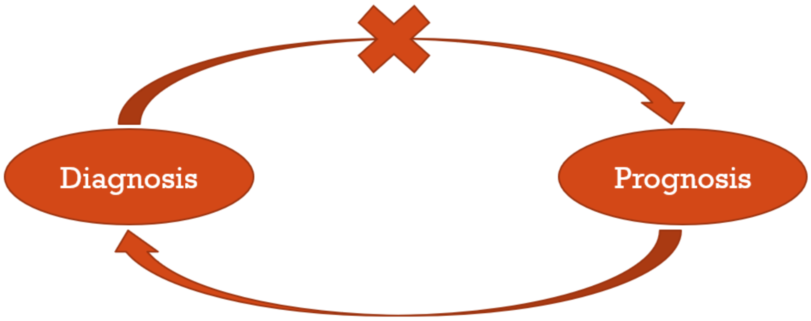

Figure 1.7: Proposed diagnosis-prognosis information exchange

utilise the mathematical description of the underlying physical phenomena in the system for FDI and prognosis, data based approaches [156] [139] [57] [79] which utilise data based techniques like fuzzy logic and neural networks without utilising the behavioral or physical models and hybrid approaches [141] which utilise a combination of both physics models and historical data.

In general but specifically in model based approaches, study of FDI being much more established has always pushed researchers to extend the use of a known fault diagnosis parameter for prognosis despite a fundamental difference between the two. Indeed, the study of FDI always assumes that the initial conditions of system are unknown. This is not the case for prognosis. For prognosis, initial conditions for the system are known fully or partially [94]. For FDI, the system analysis concerns detection of fault and the time of initiation of fault is not known, therefore, analytical redundancy FDI method uses dynamic equations in derivative causality while initial conditions are not known in real process. On the other hand, for prognosis the analysis concerns the prediction of the evolution of system from it's ideal state to failure state. Hence, the initial running condition, i.e. the ideal system conditions are known. This is the reason why, contrary to traditional approaches which consist in trying to extend the tools developed for fault diagnosis purpose, to prognosis, it is proposed to exploit the additional knowledge given by the system initial conditions by using the metrics suited for prognosis to fault diagnosis. This proposed knowledge exchange in an integrated diagnosis and prognosis framework is summarised in fig 1.7.

The main goal of the thesis therefore, is to find a suitable model based prognosis parameter which can be extended and developed to improve the fault diagnosis capability of a system. The processes can then be combined to create an integrated fault diagnosis and prognosis framework for PHM.

1.7 Contribution positioning in framework of group activities

MOCIS (Méthodes et Outils pour la Conception Intégrée de Systèmes) research group has a lot of experience in model based system engineering. The research group has contributed heavily in previous decades to the development of model based FDI. Since 2015, the focus of the research group on model based prognosis has increased. Model based prognosis algorithms for prognosis were developed using extended kalman filters and particle filters. With the recent restructuring of group from MOCIS to PERSI (PERennisation des Systèmes Industriels) the focus of the research group towards prognosis is bound to increase. This thesis is a an attempt to improve the PHM process by using a common metric from both diagnosis and prognosis.

1.8 Main contributions

The main contributions of this work are as follows:

- A hybrid framework using energy activity for integrated fault diagnosis and prognosis is introduced. The framework is composed of a model based fault detection, a data based fault isolation and a model based prognosis.

- The hybrid framework is improved so as to accommodate model and measurement uncertainties. This is a crucial task to have a robust framework for real applications.

- The most optimum form of energy activity for PHM is discussed.

- The traditionally used differential equations are often incapable for detection of minute and incipient faults under uncertain conditions. The advantage of using integral equations similar to energy activity for countering the misdirection problem of such faults is highlighted.

1.9 Manuscript organisation

This thesis is organised in the following chapters.

- The second chapter presents the general overview and state of art about the PHM process. A special focus is given on all the previously proposed techniques for diagnosis and prognosis stages of the PHM process. This chapter also allows for positioning the work compared to the existing framework of PHM.

- The third chapter focuses on the conceptual understanding of the concept of energy activity, which is the backbone of the integrated fault diagnosis and prognosis framework presented in this thesis. The chapter presents both the mathematical foundation and the physical interpretation of energy activity.

- The fourth chapter introduces to the integrated fault diagnosis and prognosis framework using energy activity. The various stages of the framework are discussed in detail. The proposed approach is simulated on a spring-mass-damper system.

- The fifth chapter expands on the methodology proposed in the previous chapter. The framework proposed in fourth chapter is improved so as to handle model and measurement uncertainties. Under the mentioned uncertainties the advantages of using energy activity for fault detection are highlighted and the optimum form of energy activity for the proposed framework is discussed. The modified framework is tested on a two-tank system.

- The sixth chapter summarises the conclusions, limitations and future prospects of the current work.

1.10 Disseminated Results

The results of the thesis were disseminated through the following publications:
International Journals

1. Manarshhjot Singh, Anne-Lise Gehin, Belkacem Ould-Bouamama. Fault diagnosis and prognosis in uncertain systems using Energy Activity. **in review process**, IEEE Transactions on Reliability.

2. Manarshhjot Singh, Anne-Lise Gehin, Belkacem Ould-Bouamama. Robust detection of minute faults in uncertains ystems using Energy Activity. **in review process**, IEEE Transactions on Mechatronics.

International Conferences

1. Manarshhjot Singh, Anne-Lise Gehin, Belkacem Ould-Bouamama. Prognosis and Health Management using Energy Activity. IFAC World Congress (2020), pp. 10445-10452.

2. Manarshhjot Singh, Belkacem Ould-Bouamama, Anne-Lise Gehin.Bond graph model for prognosis and health management of mechatronic systems based on energy activity. International Conference on Systems and Control. pp. 430-434.

Chapter 2

State of Art

Contents

This chapter explores in detail the overall PHM process. The various stages of the PHM process, their requirements and their relationship with the other processes is discussed.

2.1 Prognostics and Health Management (PHM)

The detailed PHM process is shown in figure 2.1. The PHM process consists of four major constituents:

1. **System**: This stage requires the understanding of the overall plant that is being analysed and some prior understanding about the nature, sources and consequences of faults that can occur in the system.

2. **Data Processing**: This stage deals with acquiring the relevant information from the system under consideration and processing it such that the information can be used for analysis.

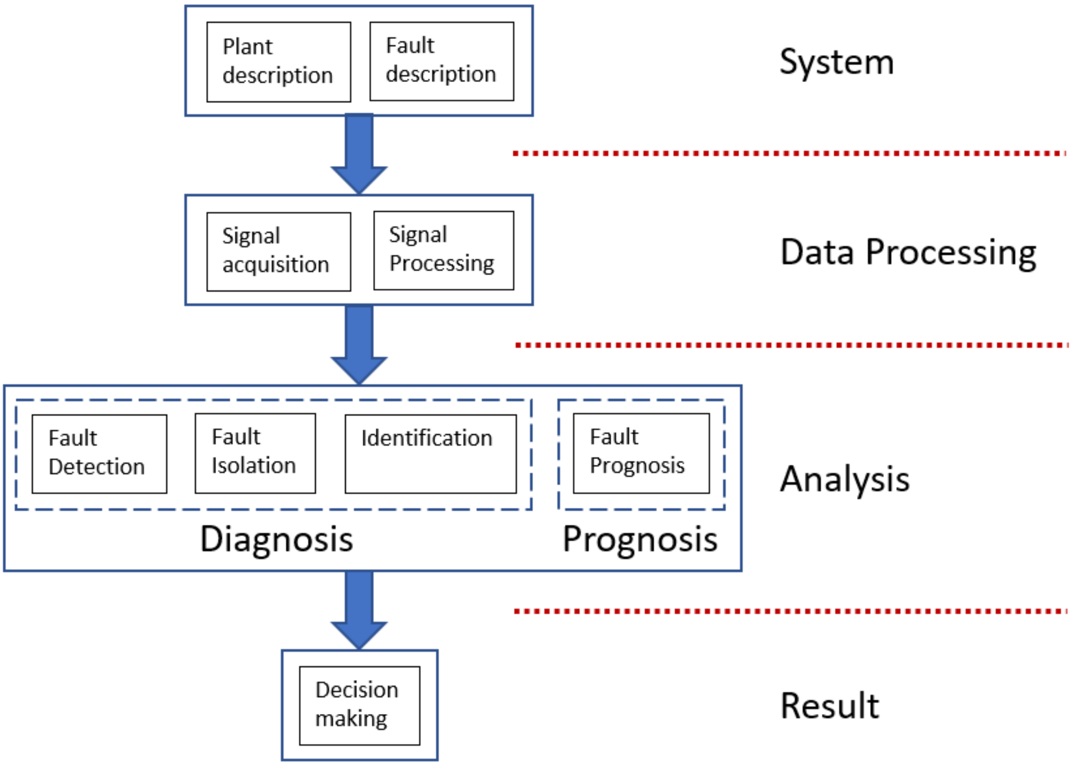

Figure 2.1: PHM Process

3. **Analysis**: This is the most fundamental and stage in the PHM process. Discussion on the various existing techniques for analysis forms the majority of this chapter. This stage consists of diagnosis and prognosis, the two main pillars for PHM however, they are fundamentally different from each other. While diagnosis is a static indicator of the system, prognosis is a dynamic indicator.

4. **Results**: The results of analysis do not conclude the PHM process. Based on the findings of the analysis an optimum decision must be proposed by the system. This constitutes the final step of PHM

2.2 System

As discussed in the previous section, Health Management (HM) and Prognosis are the two pillars of PHM architecture. Both HM and prognosis are fields of study on their own. Many techniques for HM and prognosis have been developed for both individual and combined application. A careful analysis of these techniques reveal that there is no single technique which is capable of performing a specific task for all system applications. Every technique has some advantages and limitations. Therefore, proper section of techniques for HM and prognosis is a critical decision. This decision depends highly on the system itself. So, an understanding of system description is crucial.

Two major ingredients required to describe the system are:

1. Plant Description: It groups a hierarchical and a behavioral description of the system.

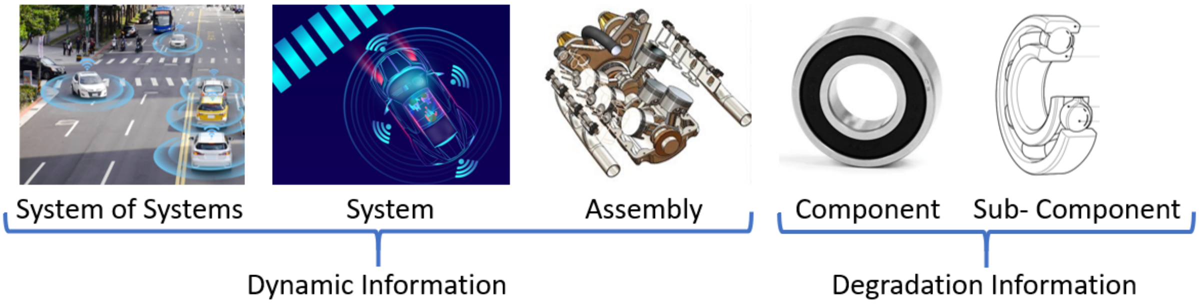

Figure 2.2: Plant description levels.

2. Fault Description: This deals with the faults in a plant, their propagation and conditions for system failure.

2.2.1 Plant Description

Plant description is crucial for PHM. The nature of the system that is under study gives an insight for the nature of faults it can undergo. Therefore, the study of plant is a crucial step. Two aspects which must be described about the plant are:

1. Description level
2. Description model

2.2.1.1 Description Level

Modern machines are complex integration of different components interacting with each other. Therefore, proper understanding of level of a component in a plant hierarchy can be very beneficial. Based on the complexity, the plant can have the following levels on which the individual units can interact.

1. Sub-component level
2. Component level
3. Assembly level
4. Machine/System level
5. System of Systems level

The above are ordered in increasing order in their hierarchy i.e. from the most fundamental level to the highest level. Components of lower level are assembled to form subsystems of higher level and so on. Components of lower level can themselves be seen as a group of sub-components. This can be understood using the fig 2.2. The ball/rollers, inner/outer race etc, are the sub components of a component i.e. bearing. The bearing is part of as assembly i.e. engine. The assemblies of the system i.e. transmission line, power system, steering line etc form a machine/system i.e. a car. A collection of cars can work interactively to form a system of systems. It is crucial to understand these hierarchical levels of plant so that different information about different levels could be incorporated while designing the PHM architecture.

The actual physical phenomena of degradation like crack initiation and propagation are applicable at the sub-component level (or component level if sub-components do not exist). However, the plant model might not be fully known at this level. As the level of hierarchy increases, so does our understanding of the dynamic models, in general. Therefore, a more accurate plant description is known at levels for which failure models are not applicable. Also, a failure at higher level might occur before the actual failure at the sub-component level, on account of a loss in minimum performance threshold. The failure model is usually needed to map the degradation of components lower in the hierarchy to loss in performance measured in upper hierarchy levels. Hence, taking into account the different levels in plant can have far reaching benefits for PHM.

2.2.1.2 Description Model

The description model of plant holds the mathematical description of the relationship between the system inputs and system outputs. Many methods for modelling the different aspects of a model have been developed over the years. These methods can be broadly classified into the following types:

1. Finite Element Models: The Finite Element (FE) is a very popular technique for modelling complicated systems. These models discretise the system domain into limited (finite) elements. The elements are connected to each other by nodes. Many different solving methods like Finite Element Method (FEM), Finite Volume Method (FVM), Finite Difference Method (FDM), Boundary Element Method (BEM) have been developed to model different domains. For eg, FEM has proven to be a very successful method for structural analysis and FVM has proven to be a very successful method for fluid flow analysis. The biggest advantages of these models if their ability to capture the smallest geometrical properties and ability to solve a wide variety of complicated physics equations, including the acutal equations of physics of failure defined at sub component level. The biggest limitation for this method lies in the model size. As numerous equations need to be solved for the simplest of systems, this makes the solution process slow therby limiting real time application. Upcoming solvers like Extended-FEM (xFEM) allow for quick and accurate solution of discontinuous functions, thereby allowing this modelling technique to capture crack propagation and fracture mechanics. This makes it suitable especially for prognosis. [132]

2. Quantitative Models: Quantitative models capture the plant behaviour by representing it's constituents at the same or different hierarchy levels using variables and thereby formulating a mathematical relationship between them. The number of equations in this model is equal to the order of the model. Hence, these are faster to obtain and to solve than the Finite Element models. Also, they are highly accurate is the physical behaviour of the different components is fully known. The major disadvantage of these models is that many times the values of the characteristic parameters of the components are not known accurately. The most popular techniques for development of quantitative models include state-sapce representation, Lagrangian [4] , Hamiltonian [137] and Bond Graph [97] technique.

3. Qualitative Models: Qualitative models do not capture the physical behaviour of the plant but just an empirical relation between the inputs and outputs of the

system is developed. Qualitative models can be developed using either statistical techniques like markov, semi-markov, hidden markov process or using AI techniques like Artificial Neural Networks. The biggest advantage is that the most complicated physical behavior of the plant can be captured easily. The biggest limitation is the requirement of large amount of performance data for accurate capture of plant behaviour. The qualitative models represent even the most complicated system in simple relations hence they have been used extensively for real time applications.

2.2.2 Fault Description

As the final objective of the PHM architecture is fault prognosis, which is a dynamic component, some information about the possible faults in system and their behaviour is a must. The fault information that can be categorised as follows:

1. Degradation model: This tells us how the fault progresses in a component.
2. Fault interaction model: This tells us how the a fault in one component affects the other components in the plant.
3. Failure criteria: This tells us the the fault should be considered a failure.

2.2.2.1 Degradation model

Degradation model deals with the increment in fault given that the operating conditions of the plant remain the same. This is a crucial information as it gives us the trend of fault magnitude development. There can be many causes of degradation like aging, corrosion, wear etc. Based on the cause of degradation, the fault increment rate is affected. Therefore, in general any degradation model can be categorised as linear or convex or concave [94]. Degradation models can be physics based or data based.

Physics based degradation models: Physics based model use the concepts of physics of failure like fracture mechanics for finding a description of fault development. Most of physics based degradation models assume crack as fault and crack propagation as failure [120]. Crack propagation can be considered a three phases process given in figure 2.3. The first phase is called initiation, followed by propagation phase and finally fast crack propagation phase.

Some common physics based degradation models are:

1. **Paris-Erdogan Law**[103]: It is the most common degradation equation expressed as:
$$\frac{\mathrm{d}a}{\mathrm{d}N} = C.(\Delta K)^n \tag{2.1}$$
a is the crack length, N is the number of cycles, ΔK is the stress intensity factor and C & m are the Paris' constants. The equation is valid in the propagation phase.
2. **Foreman equation**[40]: This is a modified form of Paris-Erdogan law which is applicable to both propagation and fast crack propagation phase.
$$\frac{\mathrm{d}a}{\mathrm{d}N} = \frac{B.(\Delta K)^m}{(1-R)(K_{lc} - \Delta K)} \tag{2.2}$$
here, R is the ratio of minimum to maximum stress in a load cycle, B is a parameter.

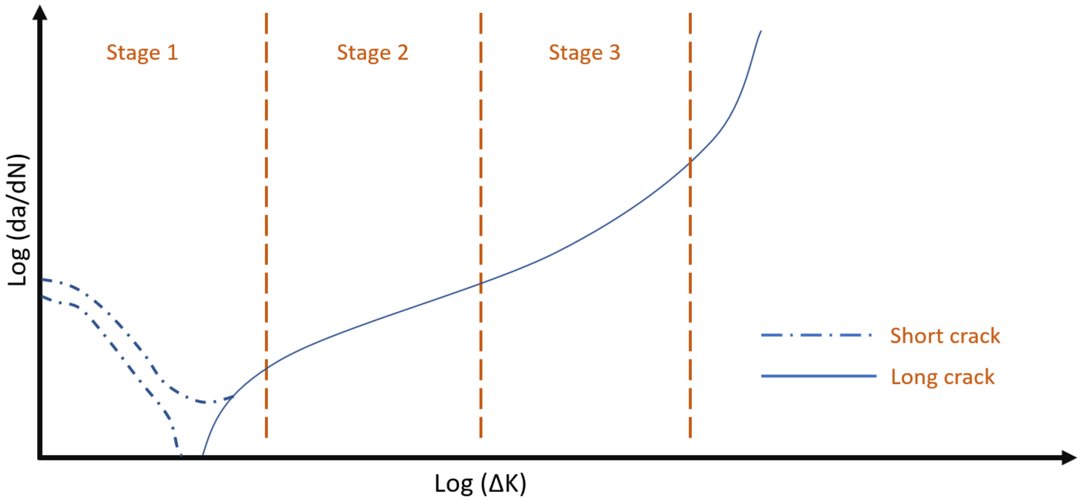

Figure 2.3: Fatigue crack graoth.

3. **McEvily Equation**[93]: This variation of Paris-Erdogan law incorporates degradation in the crack initiation phase. The equation had two to differentiate between short and long cracks. For short cracks the equation is given as:

$$\frac{\mathrm{d}a}{\mathrm{d}N} = D(K_{max} - K_o - \Delta K_{th})^2 \tag{2.3}$$

where, D is a material constant, K_{max} is the maximum load, K_o is the crack-tip open load, ΔK_{th} is the fatigue threshold. For long cracks, the equation is given as:

$$\frac{\mathrm{d}a}{\mathrm{d}N} = D[K_{max} - (1 - e^{-kl})K_{opmax} - \Delta K_{th}]^2 \tag{2.4}$$

where, k is a parameter, l is the length of parameter, K_{opmax} is the crack opening level for long cracks.

4. **Coffin-Manson model**[25]: This is used to model crack growth due to cyclic variation in temperature.

$$N = A \cdot f^{-a} \cdot \Delta T^{-b} \cdot exp(\frac{E_A}{k} \cdot \frac{1}{T_{max}}) \tag{2.5}$$

where, N is the number of cycles before failure, f is frequency of thermal loading, A is a coefficient, ΔT is the range of temperature in a cycle, b is temperature range of the component, E_A is the energy of activation, T_{max} is the highest temperature reached in cycle, k is the Boltzman's constant.

Data based degradation models: Many a times the degradation behaviour of the fault does not match the above mentioned models. In such a case, data is used to fit a failure model to the observations. Baysian statistical models are generally used for modelling the degradation from data. The commonly used statistical models are:

1. **Markov Chain**: The degradation can be modelled as a markov process if the system is fully observable, The underlying assumption for Markov process is that the probability distribution of state at any particular instant depends on the state at the previous instant.

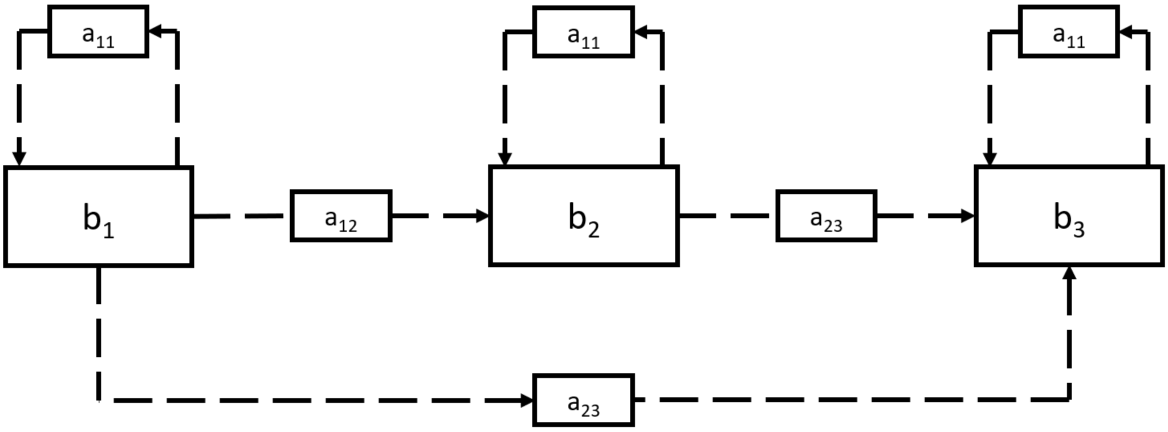

Figure 2.4: Schematic of hidden markov process with three states.

A Markov chain representing a sequence of states $w_1, w_2, ..w_n$ can be modelled as:

$$P(w_1, w_2, ...w_n) = \prod_{a=1}^{n} P(w_a|w_{a-1}) \tag{2.6}$$

assuming that

$$P(w_a|w_{a-1}, ...w_1) \approx \prod_{a=1}^{n} P(w_a|w_{a-1}) \tag{2.7}$$

2. **Hidden Markov model**[160][99]: A hidden markov model can be imagined as a Bayesian network with finite states, linked with a markov chain. This allows the user to model multiple stages of degradation. Hidden-Markov model can be used when states of the system are partially observable. Hidden markov models require a large amount of data for training. A hidden markov model is denoted by $\lambda(\pi, A, B)$ where π is the probability distribution of the initial state, A is the probability distribution among the states, B is the probability distribution of observations. A schematic concept of hidden markov process is shown in fig 2.4.

2.2.3 Failure criteria:

Defining a failure criteria (a.k.a End of Life definition) in measurable terms is one of the most difficult and one of the most crucial components of fault description. Failure criteria defines the point at which the system fails. The failure criteria can be defined in many ways based. Two of the most popular methods for defining failure criteria are [62]:

1. Threshold on mission conformity: This criteria assumes that a system fails when it fails to deliver the necessary threshold of performance parameter. This performance can be defined by the system manufacturer or the user based on parameters like running cost [17] or by industry standards [11]

2. Definitive EoL threshold: This criteria considers a system failure when the system fails to perform a task under safe conditions. This criteria is difficult to define as the safety conditions of similar systems may vary according to application conditions [108] and safety norms of where the system is located.

Once the failure criteria is selected, this criteria must be mapped to some index that is defined from the system measurements.

2.3 Data Processing

Data processing involves all the processes that may be required for gathering information from the system and providing it in a form that can be used for fault diagnosis and prognosis. Data processing in itself is a very vast study but for PHM data processing generally has two major functions:

- Data filtration
- Feature extraction

2.3.1 Data filtration

Data deals with reading the correct and relevant information from system. The irrelevant components of the signal are filtered out and the components of signal that are of interest are retained. Some common data filters used in PHM are:

- Low Pass Filter: The sensors for any measurement are selected considering the Shannon sampling theorem. According to this theorem, a continuous-time signal can be sampled and perfectly reconstructed if the waveform is sampled over twice as fast as it's highest frequency component. Therefore selected sensor operates at a frequency at least twice of the frequency of the signal that is being measured. Hence, the measurement noise, an inherent component of any sensor also has a high frequency. This noise can be removed from the signal using a low pass filter which allows low frequency components of the signal to pass.

- High Pass Filter: In addition to the measurement noise, the sensor may also undergo a bias or a drift. This slowly deviates the measured values from the real values of the outputs being measured. In such a situation, a high pass filter is used.

- Averaging Filter: The averaging filter is a smoothing filter used to smooth the signal obtained from the sensors. Average (or mean) filtering is a method of 'smoothing' the signal by reducing the amount of intensity variation between neighbouring measurements. The average filter works by moving through the signal measurement by measurement, replacing each value with the average value of neighbouring measurements, including itself.

- Median Filter: Median filter is very similar to averaging filter in operation and purpose i.e. smoothing. The difference is operation lies in the fact that median value of neighbouring measurements is performed instead of average value. The median filter is used to filter out sharp peaks from the signal.

2.3.2 Feature Extraction

Many time the measured outputs are not in a form that can be used directly for fault detection or prognosis. The specific information required for analysis must be extracted from the measurement. Some common feature extraction methods used in PHM are:

- Fourier Transformation: A lot of the mathematical tools used for signal analysis use trigonometric relations. If the output signal being measured does not follow the trend of one of the standard trigonometric functions then these mathematical tools can not be applied. Also, many time the analysis depends on the frequency information of the outputs, which can not be measured directly. In order to solve both above, fourier transformation of the output signal is performed. The fourier transformation provides the individual frequency components of the signal.

- Short Time Fourier Transformation: For output signal changing over time, the fourier transformation can not capture the change. For this, short time fourier transformation is used. The Short-time Fourier transform (STFT), is a Fourier-related transform used to determine the sinusoidal frequency and phase content of local sections of a signal as it changes over time. In practice, the procedure for computing STFTs is to divide a longer time signal into shorter segments of equal length and sunsequently compute the Fourier transform separately on each shorter segment.

- Wavelet Transformation: A wavelet is a mathematical function used to divide a given function or continuous-time signal into different scale components. Usually one can assign a frequency range to each scale component. Each scale component can then be studied with a resolution that matches its scale. The wavelet transform is useful in detection of abnormal operating conditions based on decomposition of the power signals into different ranges of frequencies. This usually provides us a time-frequency multi-resolution analysis that greatly useful for identifying any short of abrupt variations in measurement.

2.4 Analysis: Diagnostic-Prognostic Relation

As discussed earlier, diagnostic and prognostic are the pillars of PHM. Together, diagnosis and prognosis constitute the analysis part of the PHM process. Diagnosis is a static indicator of the system while prognosis is the dynamic indicator of the system. In other words, diagnosis informs us about the current state of the system including the presence and location of the fault. On the other hand, prognosis indicates the evolution of the system in time. The study of diagnosis is very well established and is independently called Fault Detection and Isolation (FDI) but the study of prognosis is relatively new and not as developed as diagnosis. Due to this difference in experience with diagnosis and prognosis a fixed consensus has not been developed on the relationship between diagnosis and prognosis, mainly because the prognosis process itself and it's role has not been clearly defined. Three schools of thought for the relationship between diagnosis and prognosis exist.

1. *Diagnosis precedes prognosis*: This is the most common and the most widely accepted relationship between diagnosis and prognosis. The purpose of prognosis is to predict the time of failure. According to this, initially ,the system must checked

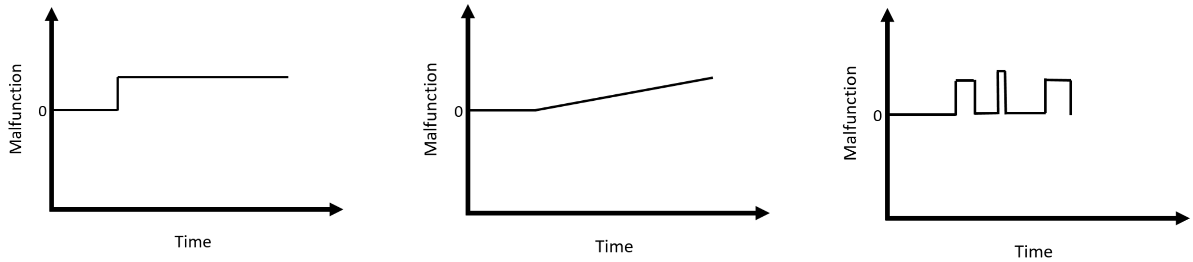

(a) Abrupt Fault (b) incipient Fault (c) Intermittent Fault

Figure 2.5: Types of malfunction

for faults with diagnosis techniques. Once the fault is detected, the function of prognosis is to study the evolution of the detected fault. Therefore, diagnosis is considered as a prerequisite for prognosis. [64]. This school of thought, being most widely accepted forms the basis of this thesis.

2. *Prognosis precedes diagnosis* : A common alternative to the above is the concept of performing prognosis before diagnosis. This thought is proposed because system can degrade without occurrence of fault. The purpose of prognosis is to predict the occurrence of fault. According to this, the object of prognosis is to study continuously the system and predict the potential faults. The purpose of fault diagnosis is to accurately detect and isolate the fault before any secondary damage or failure to the system. [158]

3. *Prognosis without diagnosis* : This is a rare thought and is can considered as a special case of prognosis preceding diagnosis. This is beneficial in special cases when the occurrence of a fault causes an immediate failure. Therefore, the diagnosis in such a case is of no use. [44]

2.5 Diagnosis

The diagnostic stage deals with the malfunctions in the system. The malfunction can manifest in the following forms (fig 5.7):

- Abrupt: the malfunction occurs step-wise. Discrete components usually undergo such malfunctions.
- Incipient: Such a malfunction gradually increases in magnitude over time. Such malfunctions usually occur in continuous systems undergoing degradation.
- Intermittent: Such malfunctions occur and resolve on their own. The extent and frequency of occurrence of a malfunction is not fixed. Such malfunctions usually occur due to changes in the working environment of the system.

Based on the part of the system where they occur, the malfunctions can be categorised as [18]:

- Actuator malfunction: A malfunction in the system inputs.
- Process malfunction: A malfunction in the system itself.

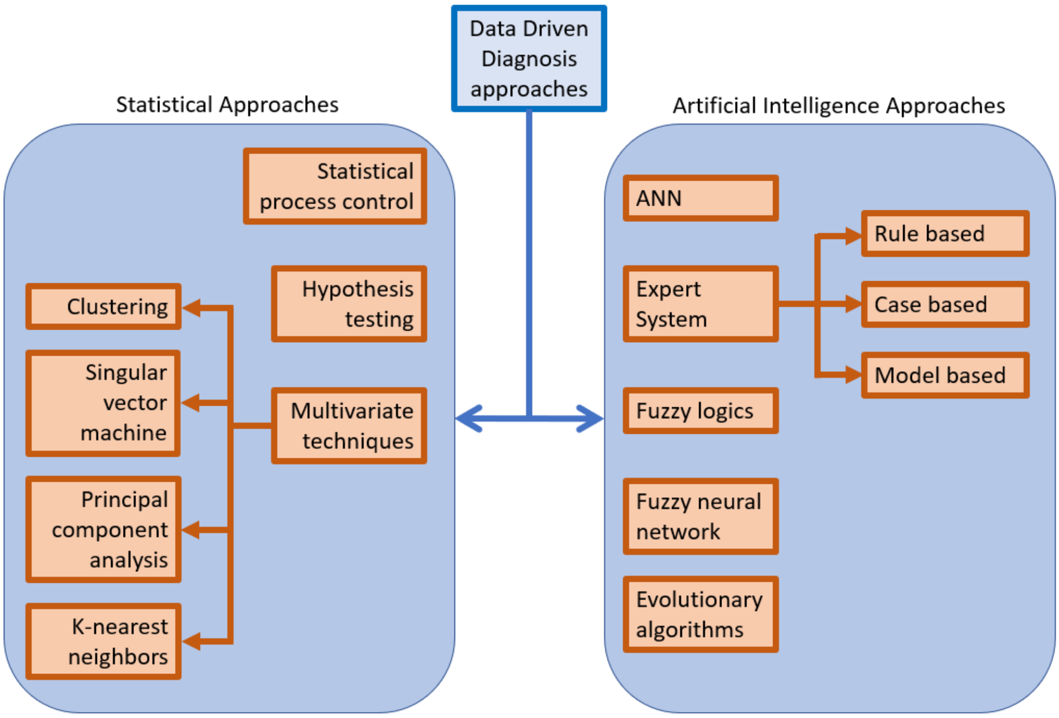

Figure 2.6: Data driven diagnosis approaches

- Sensor malfunction: A malfunction in output measurement.

Diagnostic approaches are categorised depending on the source of the rules that govern the diagnostic process.The approaches for diagnosis can be:

- Data-driven approaches: Utilizing the available data to develop rules governing the diagnosis system.
- Model based approaches: Utilizing the knowledge of system to develop the rules governing the diagnosis system.

2.5.1 Data driven diagnosis

For data driven approaches, based to method of handling the data, the approach can be sub-classified as statistical approach or artificial intelligence approach (see fig 2.6). Statistical approaches, use statistical tools on recorded data to map the fault conditions to the recorded data. These rules are used for subsequent diagnosis process.

Statistical techniques can be classified into three main groups:

- *Statistical Process Control*: In these techniques, deviations of a signal is measured from an ideal. If the signal deviates more than a pre-defined range, a fault is flagged. [118], [42]
- *Hypothesis Testing*: This is a very widely used technique in which a fault detection is proposed as a hypothesis testing problem. The presence of a fault is proposed as a null hypothesis H_0 and the absence of fault is proposed as hypothesis H_1. The null hypothesis is either accepted or rejected taking into account the various outputs from the system. [66] [125]

- *Multivariate techniques*: Multivariate techniques are useful when a large number of parameters are being measured in a system. Multivariate statistical techniques are usually applied in two methods i.e. reduction and classification. These methods can be used individually for diagnosis but are often joined in conjunction for rapid performance.

  The first method, reduction, transforms a high dimensional data set into a reduced size so as to make it more visual and manageable for the subsequent phase. The most widely used technique for order reduction is Principal Component Analysis (PCA). PCA is based on orthogonal decomposition of the co-variance matrix of variables along directions that exhibit maximum variation of data. The data set from PCA can be directly used for diagnosis by comparing the future observations to the created data set using various statistical measures such as T^2 and Q statistics [134]. Time varying (dynamic) processes can be captured using two-dimensional PCA [153].

  The second multivariate method is classification. Classification methods find distinct features in the signals so as to differentiate between non faulty state and the different types of faults. Clustering analysis, groups signals into different fault categories based on similarity of characteristics. This analysis results in several heterogeneous groups of homogeneous content. The clustering can be based on many possible metrics such as quotient distance [50], itakura distance [82], feature vector correlation coefficient [102] etc.

  Another classification method is Support Vector Machine (SVM). In SVM, the data is classified by optimizing the boundary that separates the data sets. The boundary is placed such that the distance of the point closet to the boundary is maximised. Standard SVM can be used directly [37], or by incorporating loss functions for improved accuracy [146]. Dual feature SVM can use the first and second derivative information of the degradation profile for early fault detection [104].

  After the classification is performed, the new measurement are categorised into one of the classified regions. This can be achieved using k-nearest neighbours technique [159].

Artificial Intelligence techniques make a relation (mathematical or not) between the inputs and the outputs. This relation can be used for fault diagnosis. Artificial intelligence methods have shown improved performance oven conventional approaches, however, a major challenge for using this approach is the lack of efficient procedure to create the training data set and lack of specific knowledge to train the model. Artificial intelligence techniques include, artificial neural networks (ANNs), expert systems, fuzzy logic systems, fuzzy-neural systems and evolutionary algorithms. For fault diagnosis, ANNs and expert systems are most commonly used techniques. Artificial neural networks mimic the learning behaviour of human brain. A neural network consists of simple processing elements connected in a layered structure. The processing elements consists of weights and biases. The numeric value of weights and biases is optimized so that the input-output relation is satisfied. ANNs have been used extensively for fault diagnosis [70], [127], [138], [161]. Expert systems [16] use expert knowledge about the system in form of a computer program. Three major reasoning methods employed for expert systems are rule based method [32], case based method [140], and model based method [69].

2.5.2 Model Based diagnosis

Model based diagnosis utilizes a description of the system, usually developed using the laws of physics, in order to perform diagnosis. The system description can include but not limited to structural, functional and behavioral information among the constituents of the system. The underlying assumption in model based diagnosis is that the rules defining the proper functioning of the system can be checked using the outputs from the system. In case of a discrepancy in recreation of these a fault is signalled. However, the full model of a system is rarely know in advance. This is especially true for complex systems. Hence, the system model must recognise and incorporate the unknown information about system as uncertainties. Incorporation of uncertainties exposes the diagnosis process to three types of errors as follows

1. Missed detection: These occur when the system is under fault but due to overestimation of uncertainty, the discrepancy in measurement is attributed to model uncertainty instead of the fault. Hence, an alarm is not raised even when the system is under fault. Therefore, missed detection can compromise the safe functioning of the system.

2. False detection: These are a complete opposite to missed detection. These occur when the system is not under fault but due to underestimation of uncertainty, the discrepancy in measurement is attributed to model fault instead of the uncertainty. Hence, an alarm is raised even when the system is not under fault. Therefore, false detection can increase the overall cost of the system due to frequent interventions.

3. Misdetection: This occurs when the presence of fault is accurately detected but the location or nature of fault is not identified correctly, thereby affecting the subsequent prognosis and decision making.

Model based diagnosis requires some a priori information about the system to generate and evaluate residuals. Based on how the type of information, model based diagnosis can be either qualitative or quantitative.

Qualitative models of system describe the system structure, causal relationship etc among the various components of the system. Qualitative models are used when numerical information about the system is unavailable. Many tools for qualitative analysis have been proposed like digraphs, signed digraphs, qualitative bond graphs, qualitative simulations using fuzzy logic etc. As the model does not incorporate the numerical values, the diagnosis system becomes less sensitive to measurement noise [45].

Quantitative models describe a numerical relation between system inputs, system parameters and system outputs. Generation of residuals using quantitative models is relatively easy and use of such residuals for fault diagnosis is well developed. Residual generation using observer quantitative models falls under one of the three approaches:

- Observer based approach: Observers are dynamic systems that reconstruct the states in the state space model of the system using the measured inputs and outputs. Using observers, the state of the system can be measured fully or partially. Observers can be used in deterministic or stochastic setting. [41]

- Parameter estimation approach: Parameter estimation approach assumes that faults in the system occur due to changes in system parameters. Therefore, continuous monitoring and estimation of system parameters allows the detection of faults as deviation of parameters from ideal. [56] [2]

- Analytical Redundancy Relations approach: Analytical Redundancy Relations are certain numeric constrains that are applied between the system inputs and outputs, owing to the structural of the dynamic model. The structural constrains follow some governing physical law like ohm's law, law of conservation of mass etc. [128] [6]

After the residuals are generated, these residuals are evaluated such that the various uncertainties and measurement noise are incorporated in the final decision. In other words, the fault detection should be robust. Two approaches are used for making the detection process robust i.e. Active approach and passive approach. Active approach is applied during the residual generation stage. In this approach, the generated residuals are sensitive to faults but insensitive to uncertainties. Passive approaches are applied in the evaluation stage. In this approach, the uncertainty is propagated to generated residual. The residual is allowed to deviate within thresholds calculated by incorporating the uncertainty in the model.

Other special methods of fault detection using finite element analysis [133], energy analysis [20], [92], eigenvalue/eigenvector analysis [110],[39] etc have been developed but their application remains very limited.

2.6 Prognosis

Prognosis is the most important and often the most difficult part of the PHM process. The objective of prognosis is to predict the remaining useful life of the system. A universally accepted consensus on classification of prognosis approaches has not been achieved but attempts have been made by [64]. In this section the prognosis techniques are also classified as:

1. Experience based approaches
2. Data driven approaches
3. Physics based approaches

The application of various prognosis techniques can be understood using the figure 2.7. Experience based approaches are applicable in a wide variety of applications but suffer on account of accuracy. Experience based approaches are followed by data driven approaches which is further followed by physics based approaches.

2.6.1 Experience based approaches

As the name suggests, these approaches try to correlate the expert knowledge to the actual observation, and thus, depend highly on the previous experiences with the system. Statistical information about failures frequency, collected over time forms the basis of this approach. Therefore, calculation of Mean Time between Failure (MTBF) is a very important aspect of this approach. Experience based approaches are generally categorised as follows:

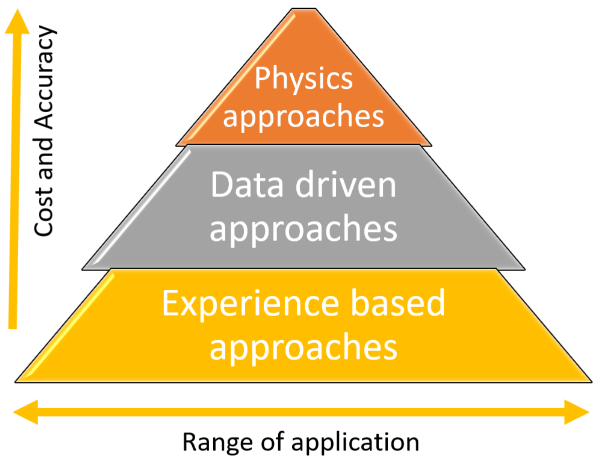

Figure 2.7: Classification of Prognosis approaches.

2.6.1.1 Expert Systems

Expert systems are based on the heuristic facts that the system experts have gained over years of experience. These are a often a complex web of if-then and if-then-else logic statements [5] but can also use fuzzy logic techniques [91]. Therefore, the generation of an accurate and extensive knowledge base is crucial. These approaches being combinatorial in nature, can get too large too fast. So, these approaches are usually limited by the number of inputs and outputs in the system. Another limitation of these approaches is the high dependence on occurrence and correct recording of as event in the past. A new type of fault can not be handled by these approaches easily.

2.6.1.2 Life Expectancy Modeling

Many times the system data collected over time fits very nicely in a statistical form. This is because even though the mathematical nature if the system is not fully known, it can be observed form the outputs. These observations can be assumed to replicate in similar types of failures thereby can be described using a probability density function [120]. This makes the prognosis process easier because most of the times the observations can be fitted easily using an linear, exponential, normal, gausian and weibull function. Also, there exist many techniques like least square methods, maximum likelihood method etc., that can be used for the recorded data on the selected curve.

Weibull function, also known as the bathtub curve, is often used as it can accommodate the chances of failure over the different phases of the product life as shown in fig 2.8. The First phase has very high chances of failure at the start but the chances of failure decrease sharply over time. This due to the wearing of the components when the system start. The next phase is indicated by very low chances of failure. The last phase is indicates by gradual increase in the chances of failure over time. This phase is due to the fatigue and degradation of components over time. As degradation keeps on increasing, so does the chances of failure.

2.6.2 Data driven approaches

Data driven approaches for fault prognosis are extensively explored. Data driven approaches usually follow one of the two following strategies. The first strategy is a two

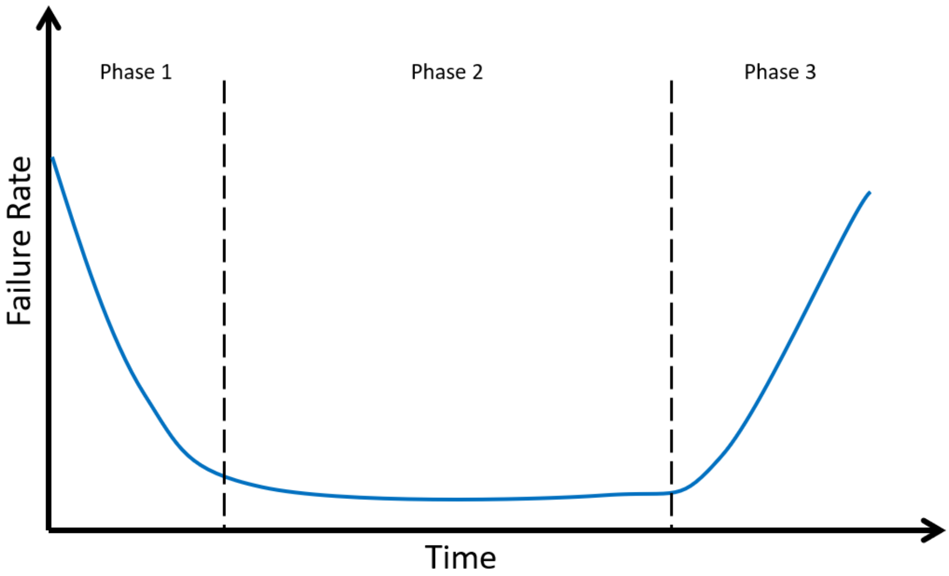

Figure 2.8: Weibull curve (bathtub curve) for failure rate over time.

step process. Firstly, the data is processed for appropriate dimension reduction algorithms and/or feature extraction to map the system outputs to degradation of the system. Secondly, the signals are extrapolated till they reach the pre-defined failure threshold.The second strategy comprises of direct mapping of system outputs to the degradation of the system. While the first strategy usually employs statistical techniques, the second strategy employs machine learning and artificial intelligence techniques.

A thorough survey of the different data driven approaches is provided in [158]. In the survey, the different data driven techniques, suitable to different types of systems are discussed (figure 2.9). The types of system discussed are as follows:

- *Dynamic system*: Most of data-driven prognosis methods either neglect the dynamic characteristics of the system or accommodate it by increasing the sampling interval. This leads to loss of partial dynamic fault information and an in effect the effect of noise on the data. This reduces the fault prognosis performance.

  State estimation methods can be used for such systems. These methods do not predict the health status directly but estimate the state variables which are used to estimate performance degradation. Common methods for state estimation include hidden markov model [126][80], particle filters [150], fuzzy logic [24] etc. Another method for prognosis of dynamic systems is regression analysis method. This method establishes a quantitative relationship between variables. Auto Regression (AR) was used for prognosis in [71] and [157].

- *Nonlinear systems*: Non linearity generally arises from linear combination or linear equations of system's dynamics. They are more difficult to predict that linear system. Most of the linear methods of prognosis assume a linear behavior of system within some range to perform prognosis but this affects the overall accuracy of the final results.

  Kernel based methods are widely used for prognosis of non-linear systems. A kernel function is mapped to the variable space and a higher-dimension kernel space.

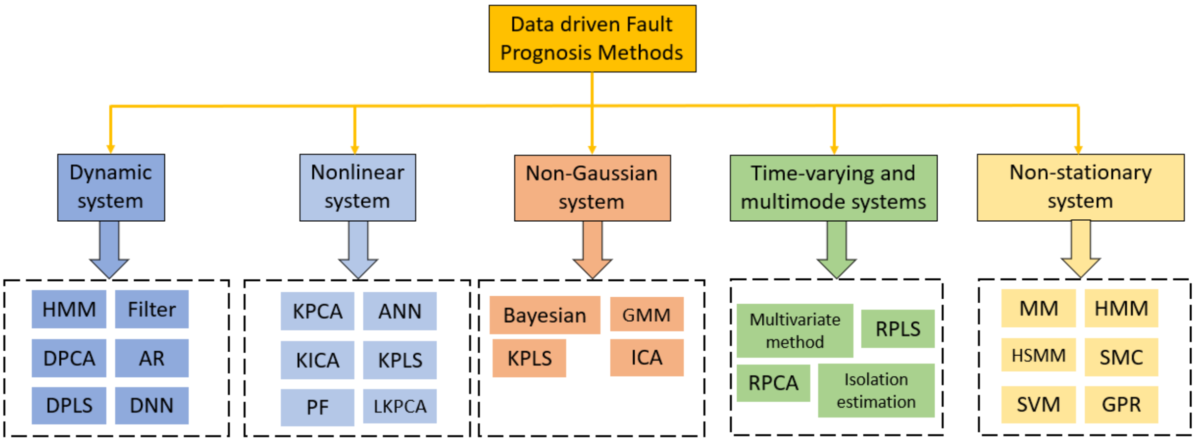

Figure 2.9: Classification of data driven prognosis methods. [158]

This allow the linear methods to be applicable to non-linear systems. Kernels can be combined with PAC (KPCA) [149], support vector machines [29] etc for fault prognosis. Particle filtering methods [155] and neural networks [120] have also been employed for prognosis of nonlinear systems .

- *Non-Gaussian system fault prognosis*: Most prognosis systems assumes that the system conforms to Gaussian distribution. Non-Gaussian systems are those whose outputs do not conform to the Gaussian distribution. Systems usually become non gaussian when they can not be completely isolated form the external environment factors.

  Independent Component Analysis (ICA) [90][89] and Gaussian Matrix Models [144] are usually used for prognosis of non-gaussian systems.

- *Time varying and multimode systems*: A majority of prognosis methods assume that fault occurs in a single component with a single fault mode. This means that the degradation phenomenon is stable. This is not applicable when the system running under varying change. Also, one fault can give rise to a subsequent fault. Therefore, stable degradation models are not applicable for modern systems.

  As a single fault mode can not achieve accurate prediction, simplest solution involves using multiple degradation models for prediction [135]. Switching kalman filters can also be used to handle mode changes [73]. For slow changing systems, adaptive and recursive method are more suitable [31][145][112]. Isolation estimation methods can achieve fault prognosis for multiple faults simultaneously [155].

- *Non-stationary systems*: Under perfect operating conditions the process variables of an industrial system should remain stationary at the point of best performance. However, the process variables can drift from their intended value due to a variety of reasons even when not under fault. Therefore, a prognosis algorithm that does not consider this variation is not reliable for prognosis of a non-stationary system.

  Successful prognosis of non-stationary systems was performed using hidden markov method [35] [107], support vector machine [142] [21], sequential monte carlo technique [98] and gaussian process regression [52] [51].

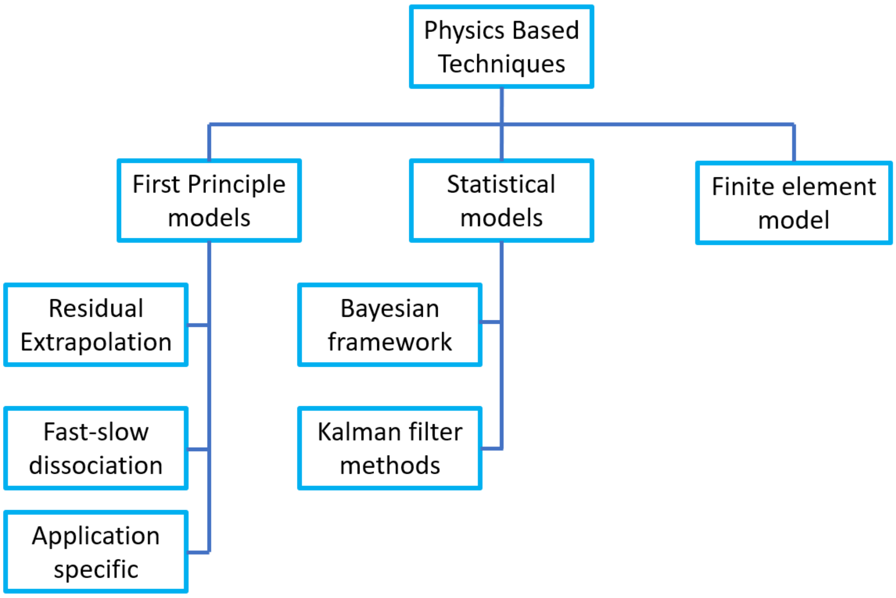

Figure 2.10: Physics based prognosis techniques

2.6.3 Physics based approaches

Physics based approaches uses the physical knowledge of the system and the process to perform prognosis. Prognosis through physics based approach are the most expected to be the most accurate. They also allow for a logical and deeper understanding of the prognosis process. However, there are many challenges to physics based approaches. In many cases, all the model parameters governing the underlying process are not recognised. To calculate the actual values of the model parameters that are used for creating the system model, specifically designed experimental and empirical data are required. In addition to the information of the system, failure modes under different faults are also required. This makes the physics based approaches very difficult and costly in implementation.

Classification of physics based methods is shown in figure 2.10. Based on the type of model used, physics based methods can by of two types i.e. methods based on first principles of physics and methods based of statistical models.

When available, physics-based models derived from first principles of physics and proper understanding of underlying mechanisms tend to significantly outperform other models [87]. In these methods, changes in model output is as described using residuals which have a direct physical meaning [120]. These residuals can be directly used and extrapolated in time to perform fault prognosis. A prognosis method based on extrapolation of analytical redundancy relations was proposed by [94] for a known fault trend evolution. The known system model can be dissociated into fast and slow component and extensive work has been done on such dissociation techniques [100][129]. The slow and gradual degradation of the system can be modeled as a 'slow-time' process which is coupled with the 'fast-time' system. In [12] and [27] battery degradation was monitored using this approach. Certain application specific methods can be used when the complete information about the system is available. In [88] stiffness based prognosis model of suspension system was developed and vibration response was analysed to perform prognosis. It should be noted that first principle models may not be available to complex systems. In addition, a physics-based model is often built case by case. Hence, it is not generally

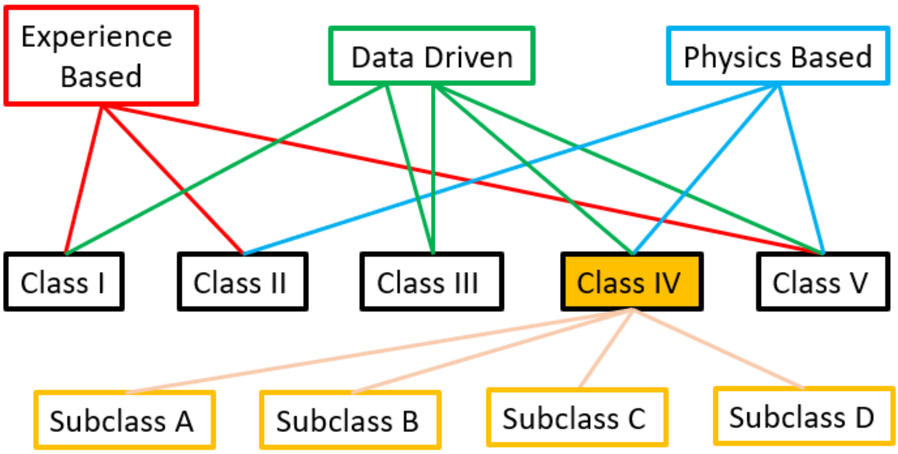

Figure 2.11: Classes of hybrid prognosis approach.

applicable to different systems easily.

Statistical models are usually applied when degradation model is available. Statistical models are exploited while continuous monitoring of the system. The system states are continuously monitored. Therefore, new data is added to the statistical model recursively. This can lead to increased accuracy of the prognosis process with time. Variants of kalman filters are like simple kalman filter [19], switching kalman filter [74] [26] , extended kalman filter[9][123] [67], particle filters [28] [61] [113] [141] have been used with high success.

Unlike the first principle models based prognosis approaches, the FEM approach acts on component level and not system level. New line finite element method is a very old and reliable method of simulating various phenomenons of physics. FEM is considered very reliable as it requires very basic equations for any physical phenomenon. For purpose of prognosis and RUL estimation extended finite element method (XFEM) can be used. This method utilises principles of fracture mechanics for simulating the growth of a crack from initiation to failure. The highly accepted paris crack growth model is usually used. XFEM was used for modelling the crack growth phenomenon directly [136] [65] [121] [22] [147]. XFEM models are highly dependent on the geometry of the component. Therefore, a manufacturing defect can lead to errors. Also, this method is demands an accurate estimation of crack initiation point which is very difficult. The biggest limitation of using XFEM approach lies in the fact that this approach has only been used for failures related to mechanical crack formation. Prognosis of other forms of degradation can not been studied.

2.6.4 Hybrid approaches

Many times, due to the limitations discussed, one particular approach can not be applicable with high accuracy. This is usually because a large amount of data is not available for experience based and data driven approaches, and incomplete knowledge of the underlying process does not allow the high accuracy prognosis using physics based approaches. In such a case, a combination of approaches is used for prognosis. This is called hybrid approach. Hybrid prognosis approaches have be classified into five classes by [72] as shown in figure 2.11.

1. *Class I - Experience based + Data driven*: Expert systems cannot directly deal with

Table 2.1: Subclasses of data-driven + physics based hybrid prognosis.

Subclass	Role of data-driven model	Role of physics based model
A	System model	RUL prediction
B	RUL prediction	System model
C	Future measurement	RUL prediction
D	RUL prediction	RUL prediction

continuous variables as the output of expert systems is usually a discrete event. This limits the application of expert systems for RUL estimation. Data-driven models can easily handle continuous data and learn to correlate and the underline structure only from data. Hence, this class of hybrid approach can provide the opportunity of integrating domain knowledge into data-driven models for system state or health level estimation, based on which RUL can be calculated. Such hybrid framework was used in [119].

2. *Class II - Experience based + Physics based*: Approaches in this class integrate both experience based models and physics-based models. In this prognosis set-up, the output of the experience-based model is often used as an auxiliary to improve the physics-based model. The experience-based model can also be used to estimate the system health state based on which RUL can be predicted. This hybrid approach was used in [10] and [131] for prognosis.

3. *Class III - Data driven + Data driven*: There are two approaches for this category of hybrid prognosis. In the first approach, a data-driven model is used to estimate the internal system state (e.g., crack growth rate) when it is not possible to measure it directly using sensors. The estimated system state can be used to extrapolate the future state of the system to predict RUL, which is calculated using another data-driven model. Data-driven health state estimation methods and prediction methods have been extensively studied in the past so this approach can be easily adopted, and sometimes without additional data requirements. This hybrid approach was used in [151] [54] and [81]

   In the second approach, different competing data-driven models can be developed for RUL prediction. The results of different models can be aggregated to improve the prediction performance by a carefully designed fusion mechanism. Many techniques have been used for fusion of results from multiple data driven methods like Kalman filter [106] [48], Weight Application to Failure Times (WAFT) method [43], majority voting[36] etc.

4. *Class IV - Data driven + Physics based*: This class of hybrid prognosis is extensively practiced and is much more developed than the others. Based on the roles played by the data driven model and physics based models, this class of hybrid prognosis is categorised further into the sub classes listed in Table 2.1.

   - **Subclass A: Use of data driven model as measurement model and physics based model for RUL calculation**: The internal state of the system might not be directly accessible for sensor measurements. In such a situation, these are inferred from measurements to estimate the internal system state indirectly. These predictions are used for RUL estimation using a physics-based model. The mapping from the measurement to the internal system state is also called the measurement equation in literature. Using a data-driven model to map from measurements to the internal state allows the use of a mathematically sound physics-based model to predict the RUL. The date-driven measurement model implicitly incorporates uncertainty into the physics-based model, but it also avoids error accumulation due to the formulations similar to Paris' Law [95]. This subclass is also used in [95] [115] [55].

- **Subclass B: Data driven model to replace physics based model for fault propagation**: This is similar to the previous sub-class, but instead to replacing the mathematical model for state estimation, the mathematical model for RUL calculation is replaced with a data driven model. This hybrid approach is used if the derivation of the physics-based model is complex or when it is prohibitive to estimate the parameters of a fault growth model or both. Limitations to this are in the availability of data. If the data is not sufficient, it introduces uncertainties in the prediction. This subclass is also used in [15] [13].
- **Subclass C: Use a Data-Driven Model to Predict future measurements and Use a physics based model to predict RUL**: This type of hybrid approach addresses the high dependency on availability of data when updating a physics-based prediction model during long-term prediction using a data-driven model to predict future measurement. If the future measurement can be accurately predicted by the data-driven model, it can correct the physics-based model in long-term prediction, especially when the degradation doesn't follow the fault growth model. However, if the data-driven prediction performs poorly, the prediction result are severely affected, and it could be worse than the physics-based model prediction. Therefore, the challenge is to ensure the accuracy of the data-driven model, and fusion mechanism that can be designed to balance the both types of prediction models. This subclass is used in [77]. This type of hybrid approach further addresses the issue of data availability when updating a physics-based prediction model during long-term prediction using a data-driven model to predict future measurement
- **Subclass D: Use of Data driven model and physics based model for prediction and subsequent fusion of results**: This hybrid approach calculates the RUL of the system simultaneously using two prognostics models, i.e., a physics based model and a data driven model. The final RUL is calculated by fusing the results of both prognostics models. This improve the accuracy of RUL prediction and narrow the confidence boundaries. This subclass is used in [46] [47].

5. *Class V - Experience based + Data Driven + Physics based*: This class of hybrid prognosis intends to utilize the strengths of all the basic prognosis approaches i.e. experience based, data driven and physics based approaches. Even though this class of hybrid prognosis is highly desirable, it is very rarely used. In [3], this class of hybrid prognosis was achieved using Dynamic Bayesian Networks. Dynamics Bayesian networks were used for fuse heterogeneous information like expert opinion, experimental data, operation data and mathematical model for detecting fault, whereas particle filter was for prognosis. Heterogeneous information was also fused using probabilistic update process in [101]. In [148], fusion of homogeneous information

was achieved. For prognosis, an optimal linear combination of RUL calculated from various individual algorithms for accurate prediction. The major challenge to this class of hybrid prognosis is the heterogeneous information fusion.

2.7 Decision Making

Decision making is the final step for the PHM process. Traditionally the use of PHM was limited to the application of CBM. However, overtime it's potential outside CBM has been realised. A big contribution to this change in perspective is attributed to developments in decision making process. For applications in CBM, the only possible decision is the scheduling of maintenance actions. With developments in decision making process other decisions like implementation of fault tolerant control, mission rescheduling etc can also be considered. The final decision is highly dependent on the RUL [62] [124]. The final decision that is taken can be categorised as follows [8]:

- **Maintenance Decision**: These are the decisions regarding intervention in the process for performing maintenance action. The intervention could be immediate or scheduled anytime before the end of life. These decision is not only very important but also application and industry specific as this is usually accompanied by a system shut down to perform maintenance. These decisions are wildly studied in several industrial domains like transport [114], manufacturing [34] [78].
- **Operation Decision**: Operation decisions concern with changing the operating conditions of the system so as to avoid failure. These can be sub-categorised as follows:
  - **Production and task assignment**: In this category of decision the system schedule of completion of the task is altered according to the recognised degradation and the RUL. This was considered the best decision in situations discussed in [124].
  - **Control decision**:In this category, the control law governing the system is modified and the degradation of the system is incorporated in the control law itself. This allows the system to function properly even under degrading conditions [109] [68].
  - **Logistics**:In this category of decision the systems supporting the degrading system such as raw material are rescheduled according to the new system dynamics of the degrading system. Logistic decisions take into consideration the health condition of the system, the lead time of ordering and the storage levels to optimize the cost [75].
- **Mixed decisions**: These decisions concern with the optimum combination of maintenance and operating decision.

The role of RUL is very crucial in the decision making process. The final decision applied depends almost entirely on RUL. The RUL can be used by the decision algorithms in the following ways:

- As a classification criteria between the selection of various applicable decisions.
- As a variable for defining the new control law if control decision is selected.

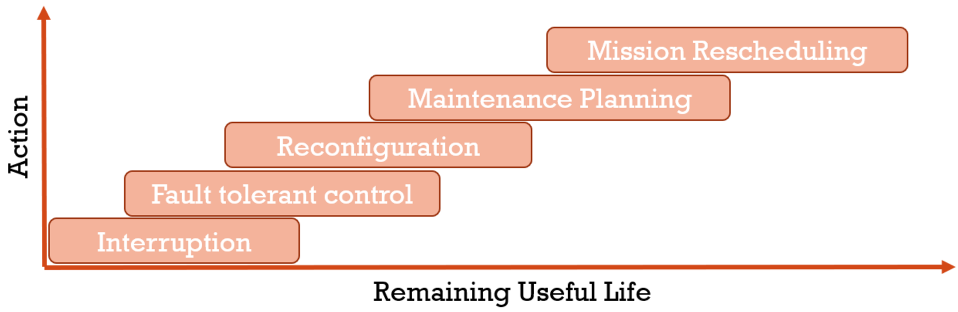

Figure 2.12: Decision making based on Remaining Useful Life.

- As a threshold of maintenance action.
- As a penalty in the objective function to reduce the lost remaining useful life due to early maintenance.

The most common decisions based on the RUL can be understood by fig 2.12.

For a very small RUL the where a critical failure can not be stopped the system functioning is interrupted immediately. Immediately stopping a system might be difficult and could bring about problems of it's own. Therefore, if the RUL is a little higher, a fault tolerant control is initiated to safely bring the system to stop.

For medium RUL where there is no immediate danger to the system or surrounding, maintenance must be initiated instead of stopping the system. Maintenance team might not be remotely available, so the system and it's associated components can be reconfigured to continue working in the faulty condition till the maintenance team arrives. If the RUL is longer, immediate maintenance is not required. Instead the maintenance is properly planned and the system continues to work in the current state.

For very long RUL, the maintenance is not required. Instead the system remains untouched and continues to work in the faulty state. The system mission time is updated for the faulty working conditions of the system.

2.8 Integrated diagnosis and prognosis

In most commonly used frameworks, prognosis immediately follows diagnosis. Prognosis depends on the results of diagnosis and the both are therefore highly co-relative.

In most of consulted literature, the diagnosis and prognosis techniques are selected independent of each other's consideration. Success has been achieved in many cases but an additional challenge in such a situation is the data fusion between the diagnosis and prognosis process. Therefore, a common technique for diagnosis and prognosis can help with the challenge of data fusion.

This fact has been realised and a few attempts have been made to use common techniques for both fault diagnosis and prognosis. Most of the techniques for integrated fault diagnosis and prognosis employ purely data driven techniques [156] [152] [143]. However, a challenge for purely data based techniques is that for a new system, failure data is not available.

Model information is therefore preferred for integrated fault diagnosis and prognosis. In [105] the FEM based vibration spectrum was generated and compared with the vibration spectrum of real system for fault diagnosis. Prognosis was performed using crack growth equation. In [14] particle-filters and bayesian estimation were used for both diagnosis and prognosis. In [141] diagnosis was performed using wavelet transformation and prognosis was performed using particle filters. In [111] bond graph model based techniques were used for diagnosis. Diagnosis was followed by parameter updating of system parameters and subsequent prognosis. In [154] bond graph based global analytical redundancy relations were used for fault diagnosis and prognosis of hybrid systems.

Independent study of fault diagnosis i.e. FDI is more developed than prognosis. This is probably the reason that the above mentioned works a particular technique of model based diagnosis was pushed to perform prognosis. However, the working conditions of FDI and prognosis are very different. For FDI, the system analysis concerns detection of fault and the time of initiation of fault is not known, therefore, analytical redundancy FDI method uses dynamic equation in derivative causality while initial conditions are not known in real process. On the other hand, for prognosis the analysis concerns the prediction of the evolution of system from it's ideal state to failure state. Hence, the initial running condition, i.e. the ideal system conditions are known. Hence, in the whole framework of PHM the initial conditions are known fully of partially in order to perform prognosis. This information of initial conditions is always negated when FDI techniques are used for diagnosis. Therefore, if fault diagnosis is performed incorporating the initial conditions, it can lead to improvements in the diagnosis process and therefore the overall PHM framework.

In this thesis a prognosis parameter which utilizes the initial condition information is pushed for diagnosis and an integrated PHM framework is developed.

2.9 Selection of prognosis parameter

The available literature, [62] suggests the following traits for a good and successful model based prognosis parameter:

1. Should be applicable in multiple domains like mechanical, chemical etc.

2. Should be a monotonic indicator making it easy to fix failure limit and extrapolation.

3. Should always increase with time.

For the above mentioned work, total energy in the system was selected as a prognosis parameter as total energy is a monotonic indicator, is applicable in multiple domains and always increases with time.

However, total energy is not a suitable parameter for the current work. The total energy can only be associated to whole system, it is difficult to apply it at component level in order to not only detect the fault, but to also isolate it. Therefore, another variant of energy must be selected.

In addition to the above mentioned traits, it is observed that parameter with component of time in it's mathematical definition will make it easier to extrapolate while finding the RUL.

The variants of energy and their suitability to be time-dependent and continuously increasing functions are given in Table 2.2. The variants of energy compared are Lagrangian (difference between generalised kinetic energy and potential energy), Hamiltonian (algebraic sum of generalised kinetic and potential energy), Power (rate of energy change) and Energy Activity (index of total energy interaction).

Table 2.2: Selection of prognosis parameter

	Lagrangian	Hamiltonian	Power	Energy Activity
Increases	-	-	-	+
Time	-	-	+	+

As Energy Activity (EA) seems to be the most suitable parameter to implement prognosis, it is used, in the presented work, to complete the two major steps of the PHM process, i.e. diagnosis and prognosis.

Calculation of EA depends on the calculation of power. As bond graph modelling tool is based on the analysis of power exchange dynamics in the system, bond graph is the most suited tool for using EA.

2.10 Conclusion to chapter

In this chapter a comprehensive details about the PHM process is provided. It is realised that fault diagnosis and prognosis are the pillars on which the entire PHM rests. In literature there are a number of approaches developed for both fault diagnosis and prognosis.

These approaches can be broadly categorised as model based, data based or hybrid approaches. All model based, data based and hybrid approaches offer some common advantages and suffer from some common disadvantages, weather they are applied for fault diagnosis or prognosis. Model based techniques offer high accuracy as they utilise the basic principles of physics for evaluation and do not need any experimental data neither in normal nor in failure mode.. The major limitation of model based approaches is the requirement of a complete and accurate model which is usually not available. Data based approaches are very successful because these approaches are based only on the real data representing the influence of all the unknown parameters that might not be considered using model based approaches. The biggest limitation for data based approaches is the requirement of large amount of data, Hence, this approach might not be suitable for a system under development for which data is not available. Hybrid approaches integrate the physics based information and data based information for analysis and are therefore very successful even with a small amount of available data. The hybrid approaches are limited by the fusion of physics based information and data information which is a very difficult task.

From literature a need for an integrated framework for fault diagnosis and prognosis using a common parameter is realised. Contrary to the traditional integration techniques of using diagnosis approaches for prognosis, it is realised that a prognosis approach should be used for diagnosis to create an integrated framework. The suitable traits of a model based prognosis parameter are observed from literature and Energy Activity is realised as a suitable parameter for integrated fault diagnosis and prognosis, and is therefore used for the work presented in this thesis.

Chapter 3
Energy Activity

Contents

This chapter provides a deeper insight to Energy Activity. The proper understanding of energy activity is crucial for proper understanding of this thesis. The basic concept, variations, applications and physical inferences of Energy Activity are discussed in detail.

3.1 Introduction Energy Activity

The word 'activity' in Energy Activity can be imagined as active participation during a fixed period. An element's energy activity can thus be inferred as a measure of participation of that particular element in the dynamics of the system during a fixed time period. Historically, the concept of energy activity has been used successfully for creation of reduced model while conserving the overall dynamics of the system [85]. The underlying concept was that components which are less active participate very less in the dynamics of the system. Therefore, these elements can be removed from the system in order to create a reduced order proper model.

3.2 Difference between Energy and Energy Activity

In any physical system, all the components, irrespective of their domain, interact among each other through energy exchange. This energy exchange is responsible for the overall dynamic behavior of the system. Energy is what enables a change in the system. Each domain of physics has it's own domain specific definition of energy change.

For eg. in electrical systems, energy change is defined using eq 3.1

$$Energy = I \times V \times t \tag{3.1}$$

where I is the current, V is the voltage and t is time.
Similarly, in linear mechanical systems, the total energy change is the sum of the kinetic energy change and potential energy change. Total is defined by eq 3.3.

$$Energy = KE + PE \tag{3.2}$$

$$Energy = \frac{1}{2}m\Delta V^2 + mg\Delta h \tag{3.3}$$

where m is the mass, $\Delta\vec{V}$ is the velocity and g is the acceleration due to gravity and Δh is the height of the mass.

However, the definition of energy change is always derived from work-energy principle, irrespective of the domain of application. The work-energy principle states that the change in energy is equal to the total work done by internal and external forces acting on the system, and is defined by equation 3.4. Under standard conventions, work done by the system decreases the stored energy and the work done on the system increases the stored energy.

$$\Delta Energy = \sum Work_{F_{ext}+F_{int}} \tag{3.4}$$

Also, power is defined as the rate of work done, hence, the rate of energy change in the system. Therefore, energy change can be expressed using power as given by eq 3.6

$$Power = \frac{\mathrm{d}E}{\mathrm{dt}} \tag{3.5}$$

$$\Delta Energy = \int_{a}^{a+\Delta t} (Power)dt \tag{3.6}$$

While energy is a physical phenomenon, energy activity on the other hand is a mathematical concept with a physical inference. As discussed, the work done on the system increases the energy and the work done by the system decreases the energy. This is not the case for energy activity. Energy activity is the total work interaction by the system. In other words, weather the work is done by the system or work in done on the system, it always adds to the energy activity. Hence, the energy activity will always increase. The above concept can be expressed mathematically using eq 3.7.

$$Energy\ Activity = \int_{a}^{a+\Delta t} |Power|\, dt \tag{3.7}$$

Energy Activity (EA) was introduced to achieve physical model reduction [84]. EA of a component is the total energy interaction (both storage and release) that the component has with the system over some defined time period. The fundamental difference between energy and energy activity is that, the energy activity of the component can only increase with time, whereas this is not always true for energy. The difference between the two can be understood using fig 3.1. Fig 3.1b and 3.1c show the energy and EA variation for any system component undergoing a variation of power shown in fig 3.1a.

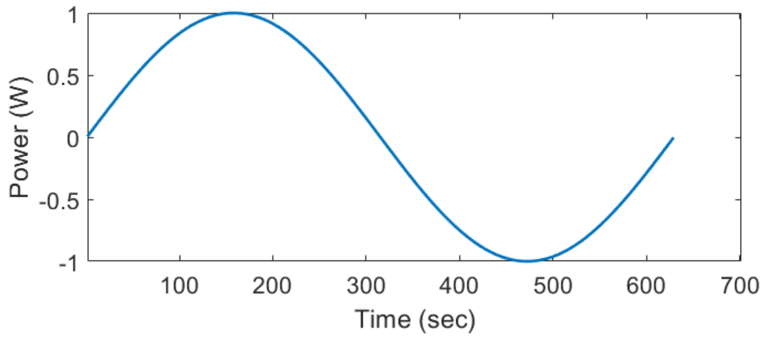

(a) Power variation in an element.

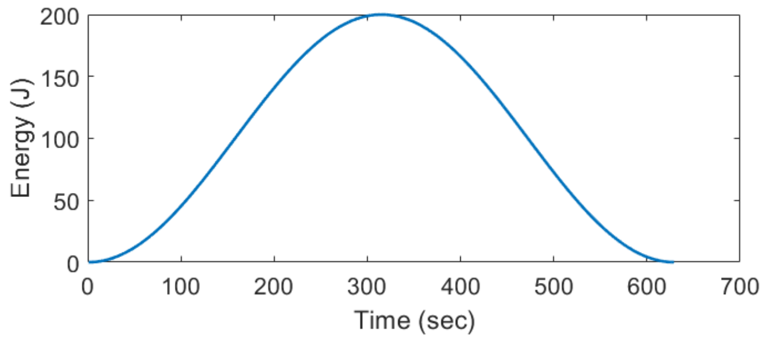

(b) Energy variation.

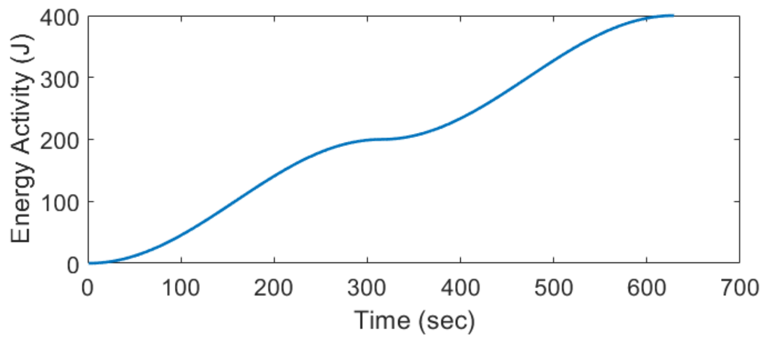

(c) Energy Activity variation.

Figure 3.1: Difference between energy and Energy Activity.

3.3 Indexes of Energy Activity in Bond Graph framework

The bond graph of a system (see Annex 1) is a graph, $G(N, B)$, with N nodes and B: bond. Nodes are associated with physical energy phenomena (dissipation, storage, transformation). Two power variables (generalised effort $e(t)$ and generalised flow $f(t)$) are associated with each a bond. Power in a bond is the product of it's corresponding generalised effort and flow . Energy activity is the time integral of the magnitude of power. As bond graph modelling is based on power, therefore bond graph is the most suitable tool for calculation of energy activity. It must however be noted that energy activity can also be evaluated using other modelling techniques but that might require additional mathematical operations [85].

3.3.1 Energy Activity

While using bond graph as modeling tool, power associated in any element in the system is defined as the product of the generalised flow and a generalised effort. EA can therefore be defined using equations 3.8 and 3.9.

In equation 3.8, f and e are the generalized flow and effort respectively. The relation between the generalised flow and effort for any element is defined by it's Constitutive Relationship (CR) which represents the physical law governing the component behavior.

In equation 3.9 S is the signal input from the system to the component. Based on the causality (derivative or integral) imposed on the component, S can represent either flow or effort signal. Function g is the Constitutive Relationship (CR) i.e. the equation 3.9 expresses the relation between the component input and output. It corresponds to the physical law applied by the component. It uses the numeric component value ϕ.

$$EA = \int_a^{a+\Delta t} |e(t).f(t)|\, dt \tag{3.8}$$

$$EA = \int_a^{a+\Delta t} |S.\phi g(S)|\, dt \tag{3.9}$$

For example, in a linear mechanical system, inertial element is used to model the mass. For inertial element in a linear mechanical system, in preferred integral causality, the signal input to the element is the resultant force acting on the mass and output is the velocity of the mass. The governing equation for inertial element in preferred integral causality is given as

$$f(t) = \frac{1}{\phi_I} \int_0^t e(t)dt$$

For linear mechanical system the generalised flow (f) is the velocity of the mass, generalised effort (e) is the resultant force acting on the mass and the numeric component value (ϕ_I) is the magnitude of the mass. The energy activity of an inertial element in preferred integral causality can therefore be calculated as:

$$EA = \int_a^{a+\Delta t} |e(t).f(t)|\, dt = \int_a^{a+\Delta t} \left| e(t).\frac{1}{m} \int_0^t e(t)dt \right| dt \tag{3.10}$$

Comparing eq 3.10 with eq 3.9, in the given condition the signal input S is the generalised effort (e), ϕ is $1/m$, and $g(S)$ is $\int_0^t edt$.

For energy storing elements (I and C), the function g can be either integral or differential in nature. The form used for calculation, depends on which power variable (e or f) is obtained using sensor information. The function g for C and I elements in both integral and differential form are given by equations 3.11 and 3.12 respectively. For the current work, equations in integral form are used.

$$\begin{aligned} e(t) &= \phi_C \int_0^t f(t)dt \\ f(t) &= \frac{\mathrm{d}}{\mathrm{d}t}(\phi_C^{-1} e(t)) \end{aligned} \tag{3.11}$$

Table 3.1: Element power calculation using bond graph.

Element	Known variable	Constitutive equation	Power
$\vert\!\!-\!\!\rightharpoonup$ R	$f(t)$	$e(t) = \phi_R(f(t))$	$f(t)\phi_R(f(t))$
$-\!\!\rightharpoonup\!\vert$ R	$e(t)$	$f(t) = \phi_R^{-1}(e(t))$	$e(t)\phi_R^{-1}(e(t))$
$\vert\!\!-\!\!\rightharpoonup$ C	$f(t)$	$e(t) = \phi_c \int f(t)dt$	$f(t)\phi_c \int f(t)dt$
$-\!\!\rightharpoonup\!\vert$ C	$e(t)$	$f(t) = \frac{\mathrm{d}}{\mathrm{d}t}(\phi_C^{-1}e(t))$	$e(t)\frac{\mathrm{d}}{\mathrm{d}t}(\phi_C^{-1}e(t))$
$-\!\!\rightharpoonup\!\vert$ I	$e(t)$	$f(t) = \phi_I \int e(t)dt$	$f(t)\phi_c \int f(t)dt$
$\vert\!\!-\!\!\rightharpoonup$ I	$f(t)$	$e(t) = \frac{\mathrm{d}}{\mathrm{d}t}(\phi_I^{-1}f(t))$	$f(t)\frac{\mathrm{d}}{\mathrm{d}t}(\phi_I^{-1}f(t))$

$$\begin{aligned} f(t) &= \phi_I \int_0^t e(t)dt \\ e(t) &= \frac{\mathrm{d}}{\mathrm{d}t}(\phi_I^{-1} f(t)) \end{aligned} \tag{3.12}$$

The function g for energy dissipating elements (R) is algebraic however the form used depends on the power variable known. The different forms are given in equation 3.13.

$$\begin{aligned} e(t) &= \phi_R f(t) \\ f(t) &= \phi_R^{-1} e(t) \end{aligned} \tag{3.13}$$

Table 3.1 denotes the constitutive relationship, power and energy activity expressions for I, C and R elements under different causality.

3.3.2 Energy Activity Index

Energy Activity Index (EAI) [85] of any component, calculated during a time interval, is the fraction of the energy activity of that component, in the total energy activity of the system during the same time. Hence, energy activity index analysis gives us the relative comparison of the activity of different components in the system. The expression used for the calculation of energy activity index of component i in a system containing n components is given by eq 3.14. EAI has been developed for model reduction [85], and fault detection [122] of systems.

$$EAI_i = \frac{EA_i}{\sum_{i=1}^{n} EA_i} \tag{3.14}$$

3.3.3 Junction Activity

While EA and EAI can be calculated using modeling techniques other than bond graph, Junction Activity (JA) and Junction Activity Index (JAI) are forms that are calculated specifically using bond graph. However, like EA and EAI, JA also has an associated physical meaning.

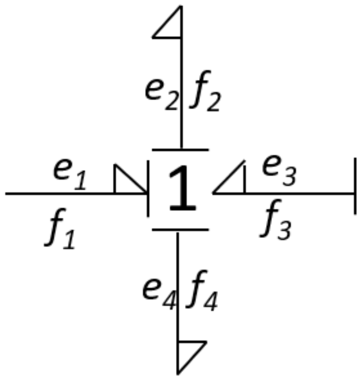

Figure 3.2: Junction activity calculation.

Junction activity [60] in bond graph is the total activity change at a junction due to all the components connected to the system through the same power conserving junction. there are two types of junctions used in bond graphs i.e. 1 junction and 0 junction. A 1 junction represents an equality of flow i.e. all the components connected to a common 1 junction receive equal generalised flow from the system. Similarly, 0 junction represents an equality of effort. So, all the components connected to a common 0 junction receive equal generalised effort from the system.

Hence, junction activity is the combined activity change brought about by all the components which receive similar information from the system. JA calculated at i^{th} junction, consisting of j elements is calculated using eq 3.15.

$$JA_i = \sum_{a=1}^{j} sign(a) EA_A = \sum_{a=1}^{j} sign(a) \int_a^{a+\Delta t} |e_a f_a| \, dt \tag{3.15}$$

For example, considering a bond graph as shown in fig 3.2 the JA for the 1-junction can be calculated as follows.

$$JA = \int_a^{a+\Delta t} |e_1 f_1| \, dt - \int_a^{a+\Delta t} |e_2 f_2| \, dt + \int_a^{a+\Delta t} |e_3 f_3| \, dt - \int_a^{a+\Delta t} |e_4 f_4| \, dt \tag{3.16}$$

3.3.4 Overall Junction Activity

The overall junction activity [60] is the total of all the junction activities in a bond graph model. The overall junction activity is different from the total EA of the system because JA is *"defined as the 'signed' algebraic sum of activities of all the elements connected to the power conserving junction of the bond graph model"*[60].

The overall junction activity of a system containing k junctions is given by eq 3.17.

$$Overall\ Junction\ Activity = \sum_{a=1}^{k} JA_a \tag{3.17}$$

3.3.5 Junction Activity Index

Junction Activity Index (JAI) [60] is similar to EAI in the context that both give a indicate a relative contribution and not absolute. While EAI indicates the relative contribution of one component in the overall activity of the system, JAI indicates the relative contribution of a junction in the overall junction activity in the system.

The overall junction activity indicates the total energy restituted to the system. Therefore, The JAI for any junction , represents the portion of the total restituted energy that is contributed through that junction. It is can be inferred that a low junction activity index indicates that the junction has smaller contribution to the overall restituted energy to the system. JAI of a junction i in a system with k junctions is indicated by eq 3.18

$$JAI_i = \frac{JA_i}{\sum_{a=1}^{k} JA_k} \tag{3.18}$$

3.3.6 Relative Activity at Junction

The Relative Activity at Junction(RAJ)[60] is the equivalent of EAI, defined in the sub environment of a particular junction of bond graph model rather than the whole system. Therefore, RAJ of an energy element is the ratio of its activity to the summation of the activities of all the energetic elements at that junction. The RAJ indicates the energetically active elements connected on a specific junction. The RAJ of an element i, connected to a junction with j elements is given by eq 3.19.

$$RAJ_i = \frac{EA_i}{\sum_{a=1}^{j} EA_a} \tag{3.19}$$

3.4 Energy Activity calculation

This depicts the procedure of calculation EA from a bond graph model of a system. This thesis uses only EA and EAI, therefore, only calculations of EA and EAI are discussed. The other variants of energy activity are not discussed as they are outside the scope of the current work.

The process of EA calculation can be understood by using a system as shown in fig 3.3. The bond graph of the system under consideration is shown in fig 3.4. The system consists of a voltage source (μ). An inductor I_1 and a resistance R_1 are connected in series. The circuit also consists of a capacitor C_2 and resistance R_2 connected in parallel. The numeric values of the system components are tabulated in table 3.2.

Fig 3.4 shows the bond graph model of the system using the preferred integral causality.

The structural properties of the system represented by the bond graph model using the 1 junction and 0 junction are given by eq 3.20.

$$\begin{aligned} 1 - junction &\begin{cases} e_1 - e_2 - e_3 - e_4 = 0 \\ f_2 = f_3 = f_4 \end{cases} \\ 0 - junction &\begin{cases} f_4 - f_5 - f_6 = 0 \\ e_4 = e_5 = e_6 \end{cases} \end{aligned} \tag{3.20}$$

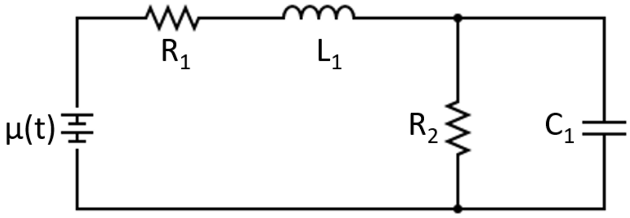

Figure 3.3: Simple electric circuit

Table 3.2: Numeric component values of circuit elements.

Component	Symbol	Value
Voltage	μ	$240 \cdot sin(377 \cdot t)$ V
Inductor	L_1	1.1 H
Resistance	R_1	5 Ω
Capacitor	C_1	2e-7 F
Resistance	R_2	35 Ω

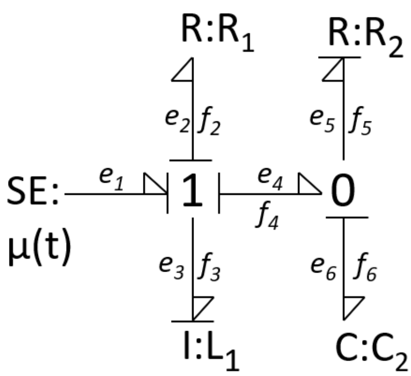

Figure 3.4: Bond graph model of electrical circuit.

Table 3.3: Energy activity calculation using bond graph.

	Effort	Flow	Power	EA
L_1	e_3	f_3	$e_3 \cdot f_3$	$\int_0^t \lvert e_3 \cdot f_3 \rvert \, dt$
R_1	e_2	f_2	$e_2 \cdot f_2$	$\int_0^t \lvert e_2 \cdot f_2 \rvert \, dt$
C_1	e_6	f_6	$e_6 \cdot f_6$	$\int_0^t \lvert e_6 \cdot f_6 \rvert \, dt$
R_2	e_5	f_5	$e_5 \cdot f_5$	$\int_0^t \lvert e_5 \cdot f_5 \rvert \, dt$

The constitutive relation for the components in integral causality are as follows:

$$
\begin{aligned}
f_3 &= \frac{1}{L_1} \int e_3 dt \\
e_2 &= R_1 \cdot f_2 \\
e_6 &= C_1 \int f_6 dt \\
f_5 &= R_2 \cdot e_5
\end{aligned}
\tag{3.21}
$$

Using equations 3.21 and 3.20 the generalised effort and generalised flow in all the elements can be calculated. The EA for all elements can then be calculated as shown in table 3.3.

For element component values given in table 3.2, EA is calculated upto 100s. The Energy activity for various element is shown in fig 3.5

Energy Activity Index The energy activity index of components can be found using the results of EA. EA for various components is found as follows

$$
\begin{aligned}
EAI_{L1} &= \frac{EA_{L1}}{EA_{L1} + EA_{R1} + EA_{C1} + EA_{R2}} \\
EAI_{R1} &= \frac{EA_{R1}}{EA_{L1} + EA_{R1} + EA_{C1} + EA_{R2}} \\
EAI_{C1} &= \frac{EA_{C1}}{EA_{L1} + EA_{R1} + EA_{C1} + EA_{R2}} \\
EAI_{R2} &= \frac{EA_{R2}}{EA_{L1} + EA_{R1} + EA_{C1} + EA_{R2}}
\end{aligned}
\tag{3.22}
$$

The evolution of energy activity index over 100s is show in fig 3.6. From fig 3.5 and 3.6 some aspects of the behavior of EA and EAI can be observed. The EA of components can not decrease. However, the EAI of the components can decrease but remains within a range of 0 and 1.

3.5 Model reduction using Energy Activity Index

Model reduction methods include all the techniques which allow for the generation of a reduced model of a system. A reduced model of a full model is any mathematical

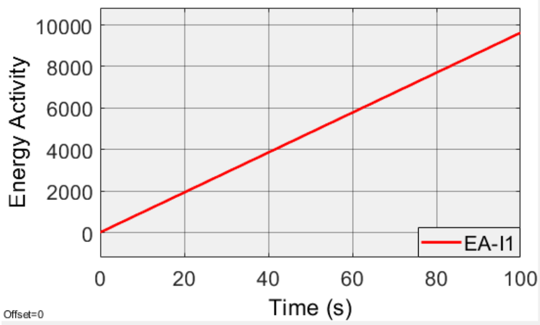

(a) Energy activity at I1.

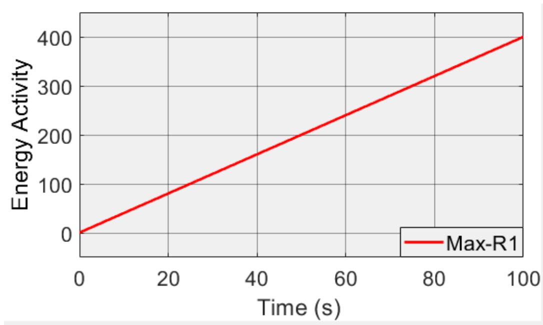

(b) Energy activity at R1.

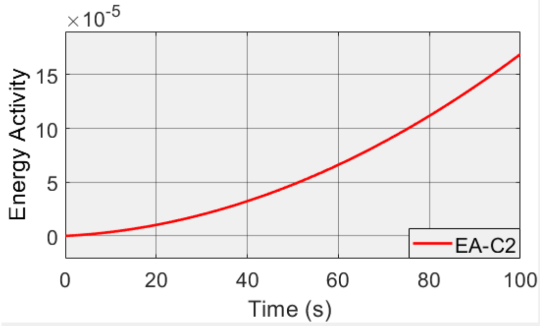

(c) Energy activity at C2.

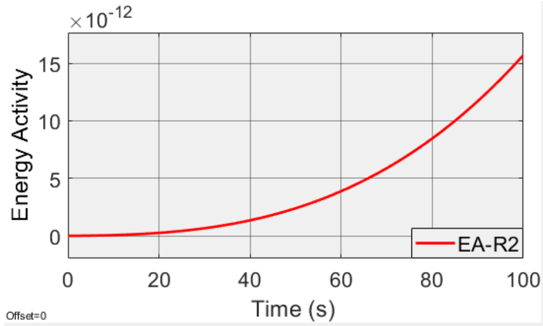

(d) Energy activity at R2.

Figure 3.5: Energy Activity of elements in circuit.

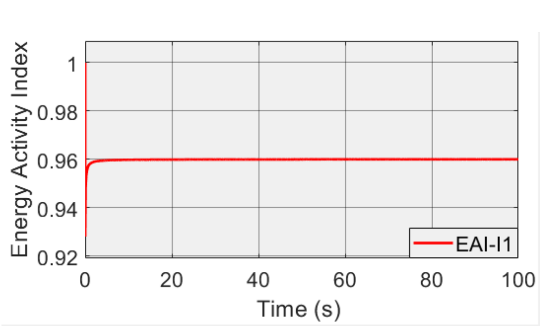

(a) Energy activity index at I1.

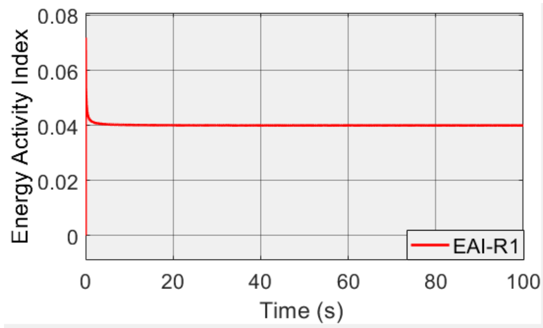

(b) Energy activity index at R1.

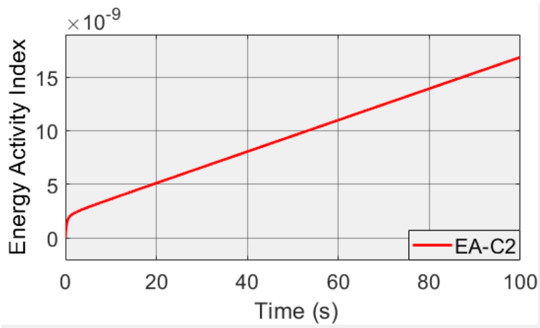

(c) Energy activity index at C2.

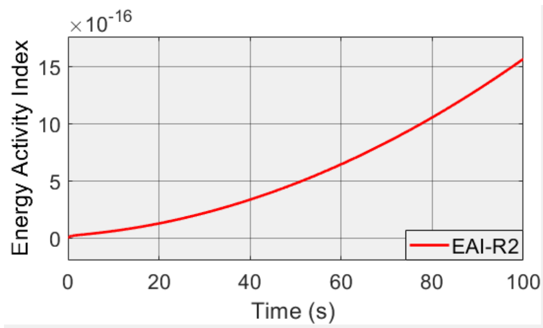

(d) Energy activity index at R2.

Figure 3.6: Energy Activity Index of elements in circuit.

description which provides nearly the same numerical results but with greatly reduced computation requirements. Most of the model reduction techniques involve mathematical reduction or truncation of governing equations [53][23]. However, when considering physical systems, the concept of reduced model is often replaced by the concept of Proper model. A proper model of a system is one that has the minimum complexity that is required for performance and control specifications. A proper model is obtained by selective inclusion of only the physically meaningful components in the system.

As discussed previously, the EAI is a relative measure of energy interaction of various components in the system. Therefore, EAI is used for deducing the components that can be neglected from the system in order to create a proper model. The basic steps for model reduction are as follows [85]:

1. Creation of the system bond graph model.

   Energy activity can be calculated using any technique of dynamic modelling. However, as bond graph provide a graphic of various elements involved in dynamic interaction, so bond graph is most suited tool for creating a proper model.

2. Simplification of bond graph model.

   The bond graph model created from the physical model might not be fully suitable for calculation of EA. This is because, in order to eliminate non performing elements and preserve the overall junction structure of the model, the energy elements must be directly connected to any of the junctions. So, the bond graph model is simplified such that all the energy elements are connected to the junctions directly.

3. Evaluation of EA and EAI of various elements.

   EA and EAI of all the elements in the system are calculated for a fixed time interval.

4. Removal of non significant elements.

   The elements with small EAI are considered as elements with non significant contribution to the system during the selected time period of simulation. These elements are removed from the system and the remaining system is the proper model.

3.5.1 Physical interpretation of Energy Activity

The physical interpretation of model reduction using EA is given by [86]. The first observation that must be made is that a low EA over some time corresponds to overall low power associated with the element during that time.

For any element with low EA, let the low EA be ε_{EA}. Since the argument of integration is always a positive quantity, a small value of integral indicates a small value of integration argument. This small integration argument can be assumed as ε_P.

$$EA = \int_0^T |P(t)|\, dt = \varepsilon_{EA} \Leftrightarrow |P(t)| = \varepsilon_P \tag{3.23}$$

The sign associated with power only indicates the direction of power transfer. As the direction of power has no effect on EA, it can be assumed that power always has a positive sign due to direction of transfer. Therefore 3.23 indicates that the power magnitude associated to the element is small.

$$P(t) = \varepsilon \tag{3.24}$$

The interaction of element with the system can occur in two ways i.e. either through a 1 junction or through a 0 junction. Therefore, these must be studied independently.

0 *Junction:* For an element placed on a zero junction, a low EA indicates low element power (eq 3.23 and 3.24). As power is product of generalised effort and flow, a low power indicates that either the generalised effort or flow is very low. For the purpose of understanding the physical implication of low activity, it is assumed that only the particular element in question has low EA. This condition assures that the generalised effort is not low, as this would render other elements connected at the junction as low activity elements. Therefore, a low activity element on a 0 junction indicates a low generalised flow and high generalised effort.

$$\begin{aligned} P &= ef = \varepsilon \\ e &>> \varepsilon \\ f &= \frac{\varepsilon}{e} = \varepsilon_f \end{aligned} \tag{3.25}$$

The influence of the above can now be studied on all three passive power elements i.e. I, C and R.

1. Generalised Inductance (I)

   The constitutive relationship is considered in integral form. This is because the real system behavior also follows integral causality. For constitutive relationship of generalised inductance in integral causality, the generalised component values (ϕ_I) is the reciprocal of the actual component parameter value(Z_i). For the element, CR is given as:

   $$f = \frac{1}{\phi_I}\int e(t)dt \tag{3.26}$$

   Therefore, substituting the expression of f from eq 3.25, and evaluating the expression for ϕ_I

   $$\phi_I = \frac{\int e(t)dt}{f} = \frac{e\int e(t)dt}{\varepsilon} \tag{3.27}$$

   As effort is assumed as not low, the integral of effort indicates that the ϕ_I is very high. Therefore, for an I element placed at a 0 junction to have low activity, it's component value should be very high.

2. Generalised Capacitance (C):

   Here also, the constitutive relationship is considered in integral form. For constitutive relationship of generalised capacitance in integral causality, the generalised component values (ϕ_C) is the reciprocal of the actual component parameter value(Z_C). For the element, CR is given as:

   $$e = \frac{1}{\phi_C}\int f(t)dt \tag{3.28}$$

Therefore, substituting the expression of f from eq 3.25, and evaluating the expression for ϕ_C

$$\phi_C = \frac{\int f(t)dt}{e} = \frac{1}{e} \int \frac{\varepsilon}{e} dt \tag{3.29}$$

As effort is assumed as not low, the integral of effort in denominator indicates that the ϕ_C is very low. Therefore, for a C element placed at a 0 junction to have low activity, it's component value should be very low.

3. Generalised Resistance (R):

The constitutive relationship for the element is algebraic.

$$f = \frac{1}{\phi_R} e \tag{3.30}$$

Therefore, substituting the expression of f from eq 3.25, and evaluating the expression for ϕ_R

$$\phi_R = \frac{e^2}{\varepsilon} \tag{3.31}$$

As effort is assumed as not low, the square of effort indicates that the ϕ_R is high. Therefore, for a R element placed at a 0 junction to have low activity, it's component value should be very high.

1 *Junction:* Similar to previous, for an element placed on a zero junction, a low EA indicates low element power (eq 3.23 and 3.24). As power is product of generalised effort and flow, a low power indicates that either the generalised effort or flow is very low. In this case under the same condition as the previous discussion, a low activity element on a 1 junction indicates a low generalised effort and high generalised flow.

$$\begin{aligned} P &= ef = \varepsilon \\ f &>> \varepsilon \\ e &= \frac{\varepsilon}{f} = \varepsilon_e \end{aligned} \tag{3.32}$$

The influence of the above can now be studied on all three passive power elements i.e. I, C and R.

1. Generalised Inductance (I)

The constitutive relationship for I element is given as

$$f = \frac{1}{\phi_I} \int e(t)dt \tag{3.33}$$

Therefore, substituting the expression of f from eq 3.32, and evaluating the expression for ϕ_I

$$\phi_I = \frac{\int e(t)dt}{f} = \frac{1}{f} \int \frac{\varepsilon}{f} dt \tag{3.34}$$

As flow is assumed as not low, the above expression indicates that the ϕ_I is very high. Therefore, for an I element placed at a 1 junction to have low activity, it's component value should be very low.

Table 3.4: Physical interpretation of low activity.

Element	Junction	Component value for low activity	Domain specific interpretation		
			Mechanical	Electrical	Hydraulic
I	0	High	Grounded body	Open circuit	Zero flow
	1	Low	Massless body	Short circuit	Zero pressure drop
C	0	Low	Rigid connection	Open circuit	Zero flow
	1	High	Broken connection	Short circuit	Zero pressure drop
R	0	High	Rigid connection	Open circuit	Zero flow
	1	Low	Broken connection	Short circuit	Zero pressure drop

2. Generalised Capacitance (C):

   Here also, the constitutive relationship is considered in integral form. For the element, CR is given as:

$$e = \frac{1}{\phi_C} \int f(t)dt \tag{3.35}$$

   Therefore, substituting the expression of f from eq 3.32, and evaluating the expression for ϕ_C

$$\phi_C = \frac{\int f(t)dt}{e} = \frac{f}{\varepsilon} \int f(t)dt \tag{3.36}$$

   Therefore, for a C element placed at a 1 junction to have low activity, it's component value should be very high.

3. Generalised Resistance (R):

   The constitutive relationship for the element is algebraic.

$$f = \frac{1}{\phi_R} e \tag{3.37}$$

   Therefore, substituting the expression of f from eq 3.32, and evaluating the expression for ϕ_R

$$_R = \frac{\varepsilon}{f^2} \tag{3.38}$$

   Therefore, for a R element placed at a 1 junction to have low activity, it's component value should be very low.

The condition for numeric value of a components corresponding to low EA for under different conditions are given in table 3.4. The table also has domain specif conditions which correspond to the corresponding condition of numeric component value.

3.6 Frequency domain formulation of Energy Activity Index

The frequency domain formulation of EA and EAI is explored in [83]. The frequency interpretation of EA and EAI can be calculated by considering a general dynamic system. Any dynamic system with states given by a vector x, input given by the vector u and outputs given by a vector y can be represented as:

$$\begin{aligned} \dot{x} &= Ax + Bu \\ y &= Cx + Du \end{aligned} \tag{3.39}$$

where A, B, C and D are the state space matrices representing the system. For bond graph models, the state space matrices can be calculated using the junction structure of the system model. The state space matrices can be calculated as given is eq 3.40, where J_{ij} represents kinematic interconnection between i and j multiports. The multiports can be of tree categories i.e. energy storage (S) corresponding to BG elements I and C, energy dissipator (L) corresponding to BG elements R or energy source (U) corresponding to BG elements SE and SF. The matrices S and L are diagonal matrices with numeric values of energy storage and energy dissipation parameters.

$$\begin{aligned} A &= (J_{SS} + J_{SL} \cdot L \cdot (I_{k_r \times k_r} - J_{LL} \cdot L)^{-1} \cdot J_{LS}) \cdot S \\ B &= J_{SU} + J_{SL} \cdot L \cdot (I - J_{LL}^{-1} \cdot J_{LU} \\ C &= \begin{bmatrix} I_{k_R \times k_R} \\ (I_{k_R \times k_R} - J_{LL} \cdot L)^{-1} \cdot J_{LU} \end{bmatrix} \cdot S \\ D &= \begin{bmatrix} 0_{n \times m} \\ (I_{k_R \times k_R} - J_{LL} \cdot L)^{-1} \cdot J_{LU} \end{bmatrix} \end{aligned} \tag{3.40}$$

As discusses previously, the constitutive relationship for energy storage elements (I and C) can be defined using differential or integral forms. Using the differential form, the power defined for various elements as follows.

$$\begin{aligned} P_I &= e_I \cdot f_I = \phi_I \cdot f_I \cdot \dot{f_I} \\ P_C &= e_C \cdot f_C = \phi_C \cdot e_C \cdot \dot{e_C} \\ P_R &= e_R \cdot f_R = \phi_R \cdot f_R^2 \end{aligned} \tag{3.41}$$

The above can be simplified when using output information conforming to the causal structure of various elements i.e. generalised flow as outputs from I elements and generalised effort as outputs from C elements.

$$y = \begin{Bmatrix} f_I \\ ... \\ e_C \\ ... \\ f_R \end{Bmatrix}$$

The power equations for energy storage and dissipation elements can be rewritten as eq 3.42

$$\begin{aligned} P_{I/C} &= \phi_{I/C} \cdot y_{I/C} \cdot \dot{y_{I/C}} \\ P_R &= \phi_R \cdot y_R^2 \end{aligned} \tag{3.42}$$

Using eq 3.42, the energy activity is defined as:

$$\begin{aligned} EA_{I/C} &= \int_{a}^{a+\Delta t} \left|P_{I/C}\right| dt = \phi_{I/C} \int_{a}^{a+\Delta t} \left|y_{I/C} \cdot \dot{y_{I/C}}\right| dt \\ EA_{R} &= \int_{a}^{a+\Delta t} \left|P_{R}\right| dt = \phi_{R} \int_{a}^{a+\Delta t} \left|y_{R} \cdot \dot{y_{R}}\right| dt \end{aligned} \tag{3.43}$$

Once the EA equation is defined, the inputs are considered. As superposition principle is applicable, the response from only one input is analysed. For the analysis the j^{th} system input is given by eq 3.44. A sinusoidal input is considered because any input response can be created using a combination of sinusoidal inputs using principle of superposition.

$$u_j(t) = U_j \cdot sin(\omega t) \tag{3.44}$$

where U_j is the amplitude and ω is the frequency of excitation. The output at the i^{th} sensor due to j^{th} can be expressed as

$$y_{ij}(t, \omega) = U_j \cdot Y_{ij} sin(\omega t + \theta_{ij}(\omega)) \tag{3.45}$$

where

$$\begin{aligned} Y_{ij} &= \left|G_{ij}(j \cdot \omega)\right| \\ G(s) &= C \cdot (A - sI)^{-1} \cdot B + D \\ \delta_{ij}(\omega) &= \angle G_{ij}(j \cdot \omega) \end{aligned} \tag{3.46}$$

Eq 3.46 can be substituted in eq 3.43. The integration window must also be decided. The integration window is set for one time period of the input. Therefore, the steady state EA can be calculated as shown below.

$$\begin{aligned} EA_{ij}^{ss}(\omega) &= \frac{\phi_i \cdot U_j^2 \cdot Y_{ij}^2(\omega) \cdot \omega}{2} \int_{a}^{a+\frac{2\pi}{\omega}} \left|sin(2(\omega t) + \delta_{ij}(\omega))\right| dt \\ EA_{ij}^{ss}(\omega) &= \phi_i \cdot U_j^2 \cdot Y_{ij}^2(\omega) \int_{a}^{a+\frac{2\pi}{\omega}} \left|sin(2(\omega t) + \delta_{ij}(\omega))\right| dt \end{aligned} \tag{3.47}$$

The definite integral is evaluated analytically. The definite integral for energy storage elements evaluates to $4/\omega$ and that for energy dissipators evaluates to π/ω. The EA expression for one input cycle then reduces to eq 3.48.

$$\begin{aligned} EA_{ij}^{ss}(\omega) &= 2 \cdot \phi_i \cdot U_j^2 \cdot Y_{ij}^2(\omega) \\ EA_{ij}^{ss}(\omega) &= \frac{\pi \cdot \phi_i \cdot U_j^2 \cdot Y_{ij}^2(\omega)}{2} \end{aligned} \tag{3.48}$$

Once the expressions for EA are calculated, the expressions for EAI under the same conditions, for energy storing and dissipating elements is shown given by eq 3.49

$$\begin{aligned} EAI_{ij}^{ss}(\omega) &= \frac{2 \cdot \phi_i \cdot Y_{ij}^2(\omega)}{2\sum_{a=1}^{k_I+k_C} \phi_i \cdot Y_{ij}^2(\omega) + \frac{\pi}{\omega}\sum_{a=1}^{k_R} \phi_i \cdot Y_{ij}^2(\omega)} \\ EAI_{ij}^{ss}(\omega) &= \frac{\frac{\pi}{\omega} \cdot \phi_i \cdot Y_{ij}^2(\omega)}{2\sum_{a=1}^{k_I+k_C} \phi_i \cdot Y_{ij}^2(\omega) + \frac{\pi}{\omega}\sum_{a=1}^{k_R} \phi_i \cdot Y_{ij}^2(\omega)} \end{aligned} \tag{3.49}$$

Eq 3.48 and eq 3.49 represents the steady state EA and EAI for i^{th} element due to j^{th} sinusoidal input. a general input response can be calculated by representing the input as addition of multiple sine waves. Similarly, multi input response can also be found using the principle of superposition.

3.7 Adaptive fault thresholds using RAJ

Previous work [60] used the concept of EA for reducing missed detection of system faults by generation of multiple thresholds for fault detection residual.

Fault in a system can be assumed as a deviation in numeric component value leading to non-optimal system behavior. However, the numeric component value can also deviate due to uncertainty in the component value. The uncertainties are incorporated by generating residual envelops instead of a single residual i.e. an upper and lower limit of residual is generated and a deviation outside these indicates a fault. A situation might occur that a fault might occur in a component but the fault is not detected because the residual do not deviate enough to overcome the bounds set due to uncertainty. This leads to faults being missed from detection.

Fault Detection and Isolation based on Bond Graph model has been widely developed [117] [7]. The methodology is based on structural and causal properties of bond graph model. Fault indicator (named Analytical Redundancy Relation ARR) which are relationships where all the variables are known, is systematically generated from the bond graph based on covering causal path for unknown variable elimination. The ARR candidate are associated with a junction (i.e. conservative law equation). To improve the robustness with respect to parameter uncertainties of the diagnosis algorithms, the bond graph LFT (Linear Fractional Transformation) has been developed further [33].

However, not all elements have same probability of deviation from it's ideal value. Therefore, multiple envelops should be generated according to the possibility of influence on the residuals. The sequence for which the element uncertainty should be included in the fault analysis is given by their relative contribution to the residual. Based on developed energy activity theory and LFT diagnosis bond graph, the Relative Activity Junction can be considered as the ARR candidate.

Instead of generating a single threshold as in case of LFT bond graphs, multiple thresholds are generated when generating ARRs with relative activity [60]. At first, relative activity of all the uncertain elements is calculated. In order to generate the multiple thresholds, the uncertainty of all the uncertain elements is not considered collectively. Instead, different elements uncertainties are considered to generate different thresholds. The inclusion of elements in a particular threshold depends on it's relative activity. For eg, in an ARR with n uncertain elements, n thresholds are generated. The i^{th} threshold is generating by considering the first i elements with least relative activity. Generation of multiple thresholds reduces instances on missed detection.

3.8 Pseudo Energy Activity

It must be noted that when a system undergoes a fault, the fault itself can be attributed to the change in the intended component value ϕ of the system. Therefore, for a system under fault, the EA of a component calculated using eq 3.9 might not represent the actual EA of the component. This is because, for the faulty component the actual component value drifts from nominal one (ie. energy activity inhealthy mode). Therefore, for the current work, *pseudo* EA is used. Pseudo EA is calculated as shown in eq 3.50. For the calculation, the component value is assumed to be constant even after detection of fault. The fault information relayed through S (always from sensor) is used for fault detection and prognosis. Hereafter, for the context of this work, EA always refers to pseudo-EA and EAI is calculated using pseudo-EA.

$$EA_{pseudo} = \phi_{ideal} \int_{a}^{a+\Delta t} |S.g(S)|\, dt \tag{3.50}$$

3.9 Conclusion of the chapter

The chapter introduces to the concept of Energy Activity. The physical and mathematical interpretation of various variants of energy activity are introduced and explained. The interpretation of energy activity in both time and frequency domain are explained. The time domain interpretation of energy activity is the the basis of the current thesis.

Chapter 4

PHM process using Energy Activity

Contents

In this chapter a general overview of the proposed integrated framework for fault diagnosis and prognosis using energy activity is proposed. The proposed framework consists of an offline phase for generation of a fault signature database, and an online phase for continuous fault diagnosis and prognosis. The proposed framework is discussed in detail and is simulated on a spring-mass-damper system.

4.1 Offline Phase: Fault Signature Database

A fault in the system is attributed to the change in the numeric value of one of a parameter of a component of the system but the system structure remains the same. Therefore, the magnitude and frequency of energy exchange and hence the EA among the various components change. The change depends on the both the location and intensity of fault. It must be noted that the magnitude of change is also dependent on the energy input. For eg, for a linear system, a fault that changes the component value by 1%, changes the EA of the component by 5J in 10 sec. For the same system, if the energy input is doubled, a fault equivalent to component value change of 0.5% will also bring a change of 5J in 10 sec. Therefore, a reliable fault signature can not use EA. This is due to the fact that EA presents an absolute picture of the system. Hence, to make the fault signature independent of the energy input to the system, EAI as it is a relative index and is independent of the input.

A residual based on the EAI is used for generating the fault signature database that is used for fault isolation. This residual is the difference between the EAI for a faulty system and an ideal fault free-system. As discussed above the frequency and magnitude of energy exchange changes with fault location. In order to utilise the frequency component of the residual properly, fourier analysis of the residual is performed.

The database is generated by simulations itself. A fault is simulated by changing the value of a component parameter. Therefore to have an exhaustive database, a range of fault for every component is decided. A fault-free system is simulated in parallel with the faulty system. The location of the peaks is recorded in the frequency domain. The noise peaks due to numerical errors i.e. peaks at high frequency and low amplitude can be removed directly using a thresholding filter. Fig 4.1 shows the procedure of generating the fault database.

The fault database is created under the following conditions:

- At a time only one component can have fault.
- Fault is introduced at the start of the simulation.
- For every iteration the fault magnitude remains the same.

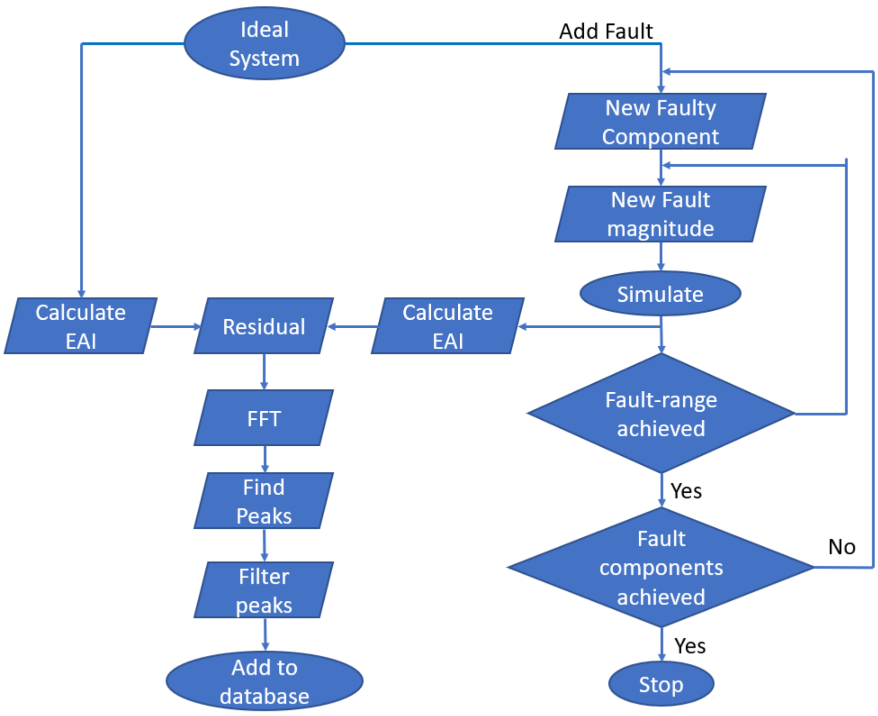

Figure 4.1: Generation of fault signature database.

4.2 Online Phase

The general overview of the online PHM process using Energy Activity is shown in figure 4.2. The overall online process is divided into three steps i.e. fault detection, fault isolation, prognosis.

4.2.1 Fault Detection

The process starts by generating a virtual system which is simulated continuously in parallel with the real system. The virtual system remains in fault-free conditions. The measured outputs from the real system are fixed by design. Therefore, similar outputs from the virtual system are used for the remainder of the process. Energy Activity from both the real and virtual system must be calculated using similar system outputs. These

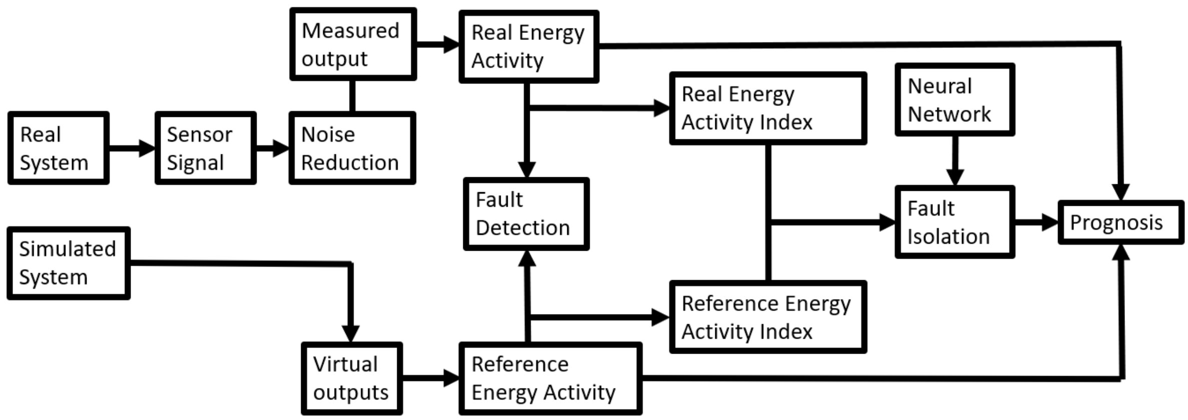

Figure 4.2: General overview of the online PHM process.

energy activities are compared against each other to detect the occurrence of fault. The EA calculated from outputs of the virtual system is called 'reference' EA. The reference EA can be calculated directly as discussed in the previous chapter. The EA calculated using the outputs from the real system are called 'real' EA. For calculation of the Energy Activities associated with real components, the output signals must be de-noised. The energy activity of various components corresponding are calculated and subsequently compared to generate the residuals. This residual is used for detection of the presence of a fault. A non-zero residual indicates a deviation of performance of real system from virtual (ideal) system. Therefore, a non zero residual indicates a fault.

The residual for fault detection is given by:

$$Residual = EA_{real} - EA_{virtual} = \int_0^t |S_{real}.g(S_{real})|\, dt - \int_0^t |S_{virtual}.g(S_{virtual})|\, dt \quad (4.1)$$

where S is the component input signal measured from real and virtual sensors to measure the real EA and virtual EA respectively. For integrated diagnosis and prognosis, information about the system initial state available for prognosis should be used for diagnosis. Therefore, for diagnosis the EA should be calculated from start to the current time. Hence, the integration limits change from 0 to t. A non-zero residual indicates a fault in the system.

4.2.2 Fault Isolation

Once fault is detected, fault isolation must be performed so as to identify the faulty component. For fault isolation, the fault database generated by the offline phase is used. As already discussed, the fault database consists of the fourier transformation of the EAI residuals. Therefore, once the fault is detected, EAI for various components is calculated. A residual of EAI is then calculated similar to residual based on EA used for fault detection, i.e., the residual of EAI is the difference of EAI of a real system and EAI of a faulty system.

Fourier transformation of this residual is then performed in order to use fault signature database. In a real system, fault can occur after some period of fault-free operation. Hence, the residuals change from zero to non-zero after some time. In such a case, a direct fourier transformation does not properly capture the change in behavior of residuals. In order to apply fourier transform continuously, Short Time Fourier Transformation(STFT) is used. In short time fourier transformation [76], the residual signal is divided into small windows of equal duration, and subsequently fourier transformation is applied on it. Using the short time fourier transformation, a time frequency map is obtained for the residual signals. The time step window for performing the STFT is equal to that used for generating the fault database. This assures that the neural network is able to recognise the pattern properly. The time window of short time fourier transformation should also be more than the time period over which the energy activity is calculated. Also, the window for short time fourier transformation should be equal in the offline and online phase.

Fault isolation is performed using classification. The fault signatures generated using STFT are compared against the fault database and the system condition is classified. Any classification algorithm can be used but for this thesis, neural networks are used. The main motivation for choosing neural network lies in the process of database generation. As discussed previously, the process database is generated offline by simulation. Therefore, for application to a real system with many uncertainties a robust classification algorithm is required. Hence, neural network are chosen for the current work. However, other robust algorithms for classification can also be explored.

4.2.3 Fault Prognosis

After fault isolation is complete, the prognosis of the system is performed in order to find the RUL. RUL is the time remaining before the system fails. Hence, a crucial task for prognosis is the setting of failure criteria. For the current work, the failure criteria is defined as the allowable deviation in numeric component value of a system component. For fault prognosis using EA, the rate of change of this numeric value of component is calculated and extrapolated using a known degradation law.

The fault prognosis using EA is entirely model based and the mathematical form of EA can be used to calculate the variation in the numeric value of faulty component, assuming that the allowable limits of a parameter and the degradation law are known.

In order to estimate the dynamics of the degradation (i.e. the time variation in the value of parameter), the time derivative of the EA is required. The EA of a component over time is a function of time and the component input signal which itself is a function of the numeric values of of the signals associated with the different components with which it is connected. Therefore, eq 4.2 is used to calculate the EA evolution under faulty condition. It must be noted that the EA under consideration can be of a component other than that undergoing a fault. This is because a fault can only redistribute the energy in components. Therefore, an element that handles a lesser amount of energy due to fault is accompanied by one or more components which handle a larger amount of energy (or vice versa) due to the same fault. Hence, fault is visible. However, for the purpose of prognosis the EA under analysis must be defined at an R-element. This is because it is easier to handle the absolute function while analysing the R-element.

$$EA = f(S(\phi), t) = \int_a^t |S(\phi).\theta_R \cdot g(S(\phi))| \, dt \tag{4.2}$$

where S is the component input signal obtained using sensor information, θ_R is the ideal value of the element, ϕ is the actual numeric value of the component degrading under fault, g is the constitutive relationship of the component, a is the time at which fault is isolated and prognosis begins, t is the current time.

From equation 4.2 the following can be calculated

$$\mathrm{d}EA = \frac{\partial EA}{\partial S}\frac{\partial S}{\partial \phi}\mathrm{d}\phi + \frac{\partial EA}{\partial t}\mathrm{dt} \tag{4.3}$$

$$\frac{\mathrm{d}EA}{\mathrm{d}t} = \frac{\partial EA}{\partial S}\frac{\partial S}{\partial \phi}\frac{\mathrm{d}\phi}{\mathrm{dt}} + \frac{\partial EA}{\partial t} \tag{4.4}$$

$$\frac{\partial \phi}{\partial t} = \frac{\frac{\mathrm{d}EA}{\mathrm{d}t} - \frac{\partial EA}{\partial t}}{\frac{\partial S}{\partial \phi}\cdot\frac{\partial EA}{\partial S}} \tag{4.5}$$

- $\frac{\mathrm{d}EA}{\mathrm{d}t}$ is the time derivative of the Energy Activity calculated from the real system.
- $\frac{\partial EA}{\partial t}$ represents the variation of the Energy Activity only in time, i.e. due to no change in ϕ. This term can be calculated as the time derivative of the Energy Activity of the fault free system.
- $\frac{\partial S}{\partial \phi}$ represents the variation of the input signal of the component due to the modification of component parameter value. As the dynamic model of the component is known as a pre-requisite this value can be calculated easily.
- $\frac{\partial EA}{\partial S}$ depends on the nature of relation g explained in the previous chapter.

For any R-element, constitutive relationship g is always algebraic and from equation 4.2

$$EA_R = \int_a^t |S\cdot\theta_R S| = \theta_R\int_a^t S^2 dt \tag{4.6}$$

where θ_R is the numeric component value of the R element.

Therefore sensitivity of EA to component input signal is given by,

$$\frac{\partial EA}{\partial S} = \theta_R\int_a^t \frac{\partial S^2}{\partial S}dt = 2\theta\int_a^t Sdt \tag{4.7}$$

Hence, for an R-element, eq 4.5 can be written as

$$\frac{\partial \phi}{\partial t} = \frac{\frac{\mathrm{d}EA}{\mathrm{d}t} - \frac{\partial EA}{\partial t}}{2\theta\int_a^b Sdt\cdot\frac{\partial EA}{\partial S}} \tag{4.8}$$

Equation 4.8 can now be integrated as shown in equation 4.9 to have an estimation of fault parameter from sensor data.

$$\phi = \int\frac{\mathrm{d}\phi}{\mathrm{d}t}\mathrm{dt} + \phi_{ideal} \tag{4.9}$$

The continuous calculation can then be extrapolated according to a known degradation trend. If a degradation trend is unknown, then a polynomial equation can be used to extrapolate the component value. The Remaining Useful Life can be easily calculated if the safe limits of the component values are known beforehand The trend of component degradation is extrapolated to find the point in time when the component value reaches the allowable limit. This point is called the End of Life. The time difference between present and end of life is the Remaining Useful Life.

Table 4.1: Ideal value of system components.

Element	Value in SI
Force (F)	10
Spring stiffness (k)	100
Mass (M)	10
Damping coefficient (b)	0.5

4.3 Application

The PHM process discussed in the previous section is simulated on a simple system in order to understand the process and checking the working of the process under ideal conditions.

4.3.1 System

In order to check the proposed methodology, a simulation is performed using a simple spring-mass-damper system. The system is shown in figure 4.3. The pre-requisites i.e. the dynamic model using bond graph, the ideal component values and component safe working limits are given by figure 4.4, table 4.1 and table 4.2 respectively.

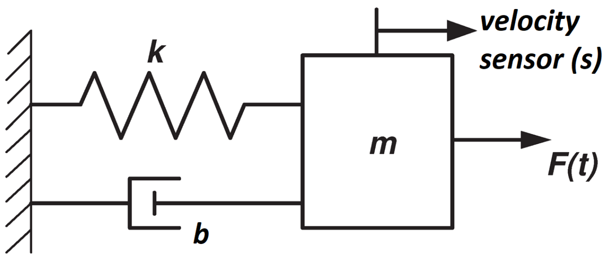

Figure 4.3: Spring Mass Damper System.

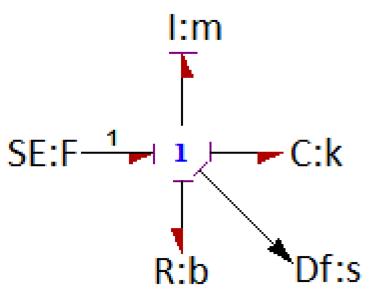

Figure 4.4: Bond Graph of Spring Mass Damper System.

4.3.2 Simulated Fault

During the simulation, a fault condition is indicated by deviation in one of the component value from ideal. For the purpose of the simulation, the fault magnitude is modelled as

Table 4.2: Value limits of system components.

Element	Lower safe limit	Upper safe limit
Spring	85	105
Mass	9	11
Damper	0.4	0.6

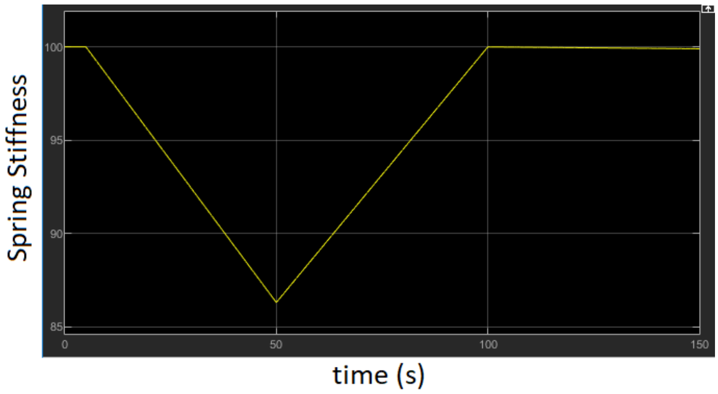

Figure 4.5: Fault as a variation in spring stiffness.

change in component value. Fault is introduced in the spring. The variation in spring stiffness is shown in figure 4.5. A fault is introduced at 5 seconds which continues to decrease the spring stiffness. At 50s from the start of simulation, a corrective action is simulated and spring stiffness starts to increase to recover its initial value at 100s.

4.3.3 Offline Phase: Fault Database generation and Neural Network Training

The first step is to pre-train a neural network. The procedure explained in figure 4.1 is used to train the neural network. The fault range for training the neural network are those given in table 4.2. For creating the fault signature database for and subsequent training of the neural network, the fault range of every component is divided into 20 equal intervals. The residual base on difference of EAI in real and virtual system are calculated and fourier transformation of the residuals is performed.

The frequency maps of residuals calculated at spring, due to faults in various components are shown in fig 4.6. The $\times$ marks represent the peaks of the residuals fourier transformation. The different colors of the marks indicate the different fault intensities. The following can be observed:

- For a faulty component, the frequency peaks fall at nearly the same frequency, irrespective of the fault magnitude. This indicates that the change in energy exchange rate among components under faulty conditions is almost the same in the given fault range i.e. the residual frequency components change very little due to the magnitude of fault.

- The frequency at which the peaks occur is different for different faulty components. This indicates that different component faults generate residuals of different component frequencies.

From the above it can be concluded that the proposed method of fault isolation by classification based on frequency map is valid.

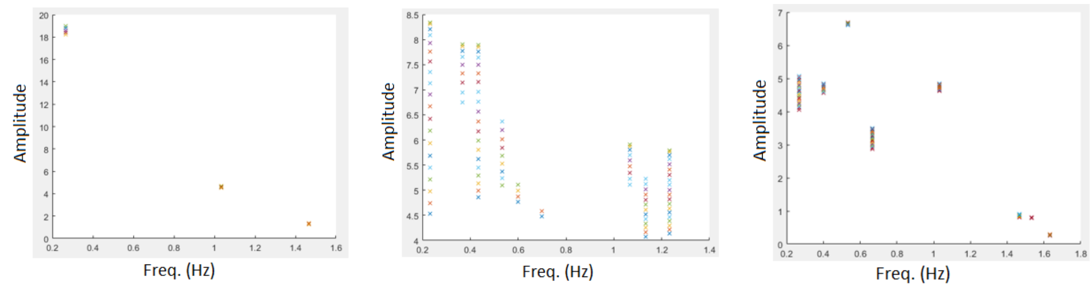

(a) Fault in Spring (b) Fault in Mass (c) Fault in Damper

Figure 4.6: Frequency map of residual at spring under various faulty components.

Table 4.3: Flow and effort calculation using sensor information.

Element	Generalised flow	Generalised effort
Spring	s	$k\int s.dt$
Mass	s	$m\frac{ds}{dt}$
Damper	s	$b.s$

The residual based on difference of EAI in real and virtual system is calculated at all possible locations for which calculation of EA is possible with the received sensor information. For the system under consideration, residuals at all the elements i.e. mass, spring and damper are calculated. A neural network for classification is trained on MATLAB. The neural network structure is optimised using trial and error. A network of 5 hidden layers is selected. 70% of the available database is used for training while 15% of database is used for validation and testing each.

4.3.4 Online Phase

The online phase includes fault detection, fault isolation and prognosis.

4.3.4.1 Fault Detection

Fault detection is based on the residuals generated using eq 4.1. In this system there is only one measured quantity i.e. the velocity of the mass. According to the BG presented by fig 4.4 the component signal input for the R and C element is generalised flow. Therefore, the generalised flow for R and C is given using the sensor information, and the generalised effort is given by the constitutive relationship in integral and algebraic form. However, for the I element, the signal input (generalised effort) is not known using sensors. Therefore for calculation of EA in this case, generalised flow is obtained by sensor information and generalised effort is obtained by expressing the constitutive relationship in differential form. The effort and flow used for calculation of EA in various components is given in table 4.3.

The fault is introduced after 5 sec from the start of the simulation. The residuals generated for fault detection for the first 10 sec are shown in fig 4.7. It can be observed that fault are detected using all three indicators very quickly.

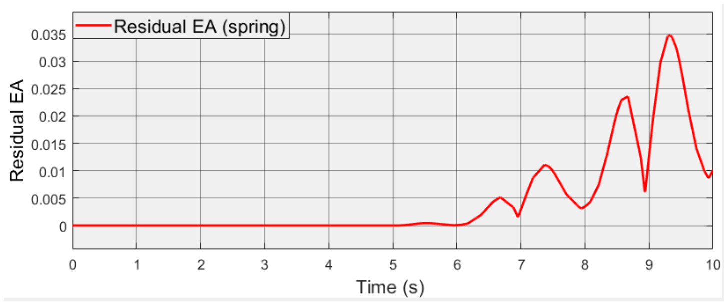

(a) Fault detection using EA at spring

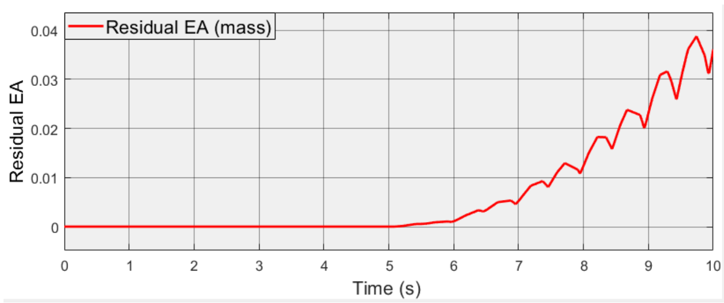

(b) Fault detection using EA at mass

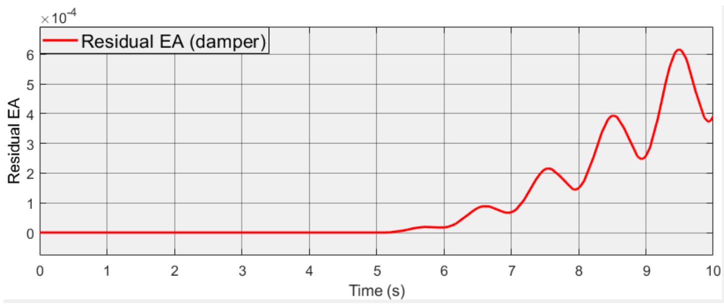

(c) Fault detection using EA at damper

Figure 4.7: Fault detection using residuals based on EA.

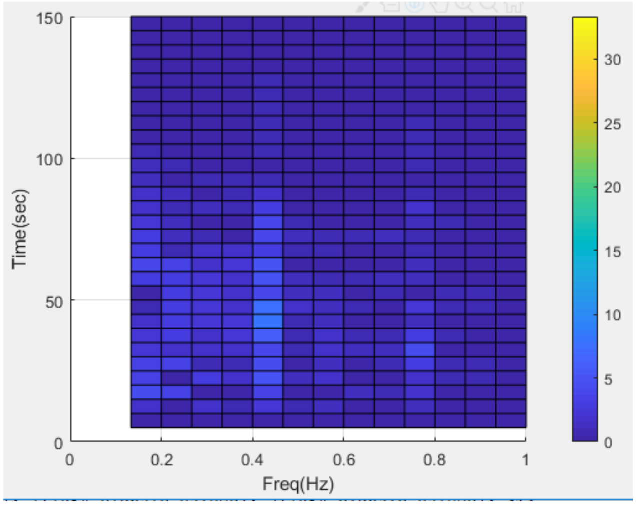

Figure 4.8: Time-Frequency map of Short Time Fourier Transformation.

4.3.4.2 Fault Isolation

The Time-Frequency map obtained from the Short Time Fourier Transformation is applied on the obtained residual. The Time-Frequency map is shown in figure 4.8. The data entries corresponding to each time interval are given as input to the neural network trained in the previous step. The neural network is able to correctly predict the fault location as spring.

4.3.4.3 Fault Prognosis

The change in spring stiffness ϕ introduces a change in the component input S, which affects the Energy Activity. The equation 4.8 is used for evaluating the spring stiffness change rate. The calculated stiffness change rate is passed through a median filter in order to remove sharp peaks due to numerical anomalies. The stiffness change rate after filtering is shown in fig 4.9. This change rate is integrated over time to find the actual spring stiffness. The calculated variation of spring stiffness is shown in figure 4.10. The error in the calculated spring stiffness is shown in fig 4.11. From the figure it is evident that the spring stiffness is calculated with good accuracy.

At any time when the fault is observed the trend of the parameter variation can be extrapolated using a polynomial equation. For the current example a first order polynomial is used. The point of failure i.e. End of Life is reached when the extrapolation trend reaches the allowed limit of the component value. The Remaining Useful Life is continuously monitored. Once the corrective action is applied the calculation of Remaining Useful Life is continued. This represents the amount of time for which the corrective action can be applied before the component value overshoots the allowable limits. Calculation of End of Life is shown in figure 4.10.

Table 4.4: Calculated End of Life

Cause of variation	End of Life Time (from starting time)
Fault	55s
Corrective action	113s

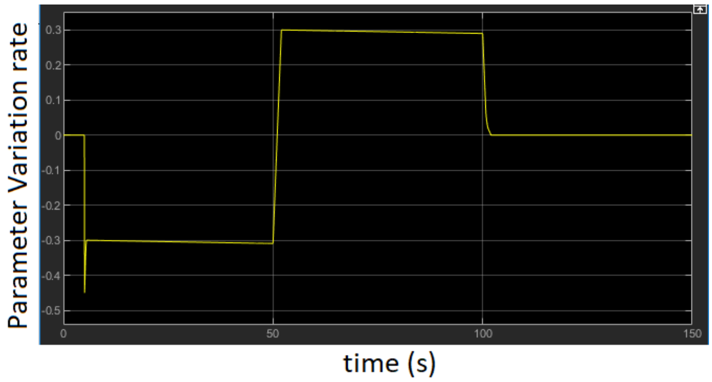

Figure 4.9: Calculated Parameter variation Rate.

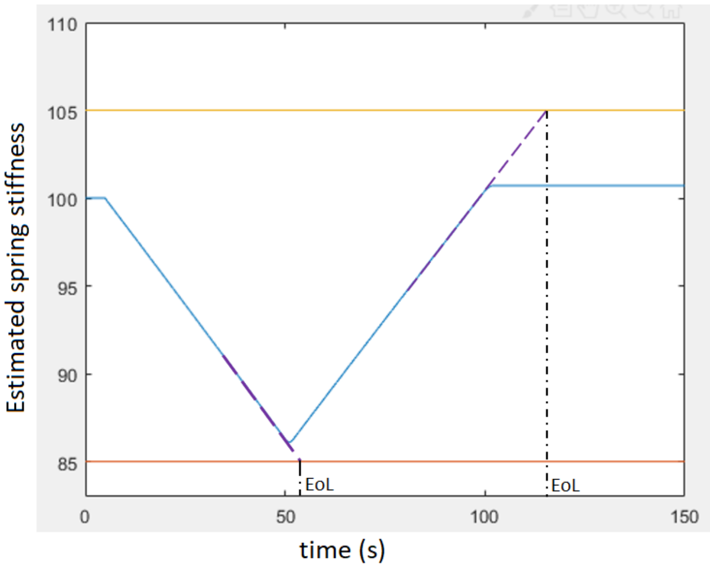

Figure 4.10: Calculation of End of Life.

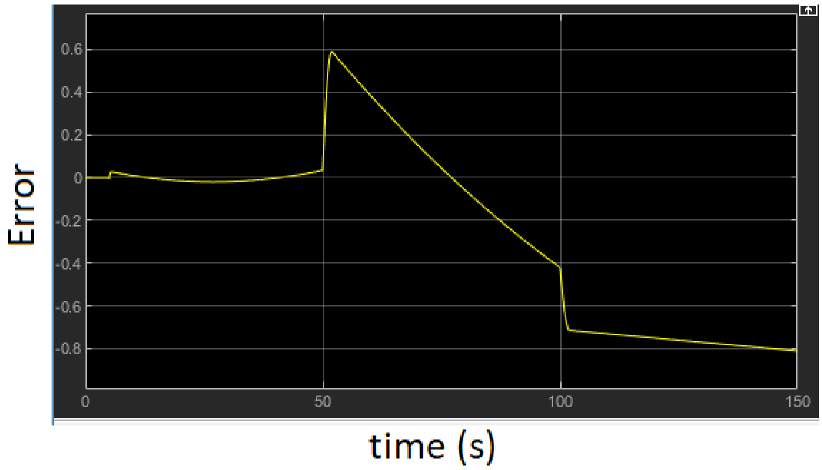

Figure 4.11: Error in calculated spring stiffness.

4.4 Conclusion of the chapter

In this paper a model based method for Prognosis and Health Management is proposed using Energy Activity. Both the diagnosis and prognosis processes are completed using variants of Energy Activity as a metric. Diagnosis is achieved by using a combination of Neural Network and Short Time Fourier Transformation. Given that the dynamic model of the system is known, the neural network is trained using fault simulations and does not require failure data. The prognosis process is completed using the mathematical nature of Energy Activity for energy dissipators. This can also be a limitation for the proposed process as the prognosis process can not utilize the energy storing elements. The proposed method is simulated for finding the end of life of a spring mass damper system undergoing a fault. The method is able to predict the fault location correctly and recreate the parameter values of the component under fault with good accuracy.

Chapter 5

PHM of uncertain system: Application to two tank system.

Contents

In the previous chapter the basic framework for using EA as a common metric for PHM is proposed. The discussion in the previous chapter was limited for ideal system. A detailed analysis for implementing the proposed framework in real system with various uncertainties is presented in this chapter.

In any model based PHM system, there can be the following uncertainties:

- *Model Uncertainty*: For any real system all the model parameters are not known with high accuracy. Therefore, a big source of uncertainty lies in the model information.

- *Measurement Uncertainties*: Another source of uncertainty lies in the measurement. Any sensor placed on any real system provides output with some inherent noise. Therefore, there is an uncertainty associated with the measured signal itself.

- *Process Uncertainties*: Once the fault is detected in the system, the prognosis is performed for find the end of life. This calculation always assumes the current approximated degradation to continue. However, it is possible that an unknown and unpredictable event occurs between the point of calculation and end of life. This event can alter the degradation rate thereby changing the remaining useful life.

In this thesis only model uncertainties and measurement uncertainties are addressed. The uncertainty analysis focuses on two aspects of the framework:

1. Accommodating the model and measurement uncertainties in the whole PHM process.
2. A detailed study of fault detection under uncertain conditions is also used to:
   (a) Establish the advantage of using EA for fault detection over existing model based FDI methods.
   (b) Select the preferred constitutive relationship for calculation of EA for PHM.

In this chapter the above are discussed in detail and applied to real a two tank system test-bench for validation.

5.1 Introduction

As discussed in the previous chapter, the proposed framework consists of parallel calculation of EA and EAI for generating residuals used at the various stages of PHM. The framework proposed previously needs to be modified to accommodate the model and measurement uncertainties before it can be applied to any real system. For handling uncertainties, the following are assumed for proper implementation of the framework.

Offline phase

1. Only one component can undergo a fault at a time.
2. Fault is introduced at the start of the simulation.
3. For every iteration the fault magnitude remains the same.

Online Phase

1. The noise to signal ratio low and noise characteristics are known [58].
2. Fault occurs in the system components or inputs but not in the detectors.
3. The degradation law for different components is known.
4. The component value be uncertain within a known range.
5. A drift in the component values after the beginning of the process, even within the limits of uncertainty, indicates fault/degradation.

5.2 Robust PHM using Energy Activity

5.2.1 Offline Phase

The offline phase includes the generation of a fault signature database and training of a neural network in order to achieve fault isolation using classification. The offline phase is unaffected by uncertainties. This is because the offline phase does not use any previous failure data but requires simulations based on the ideal system component values. Therefore, the offline phase remains unchanged.

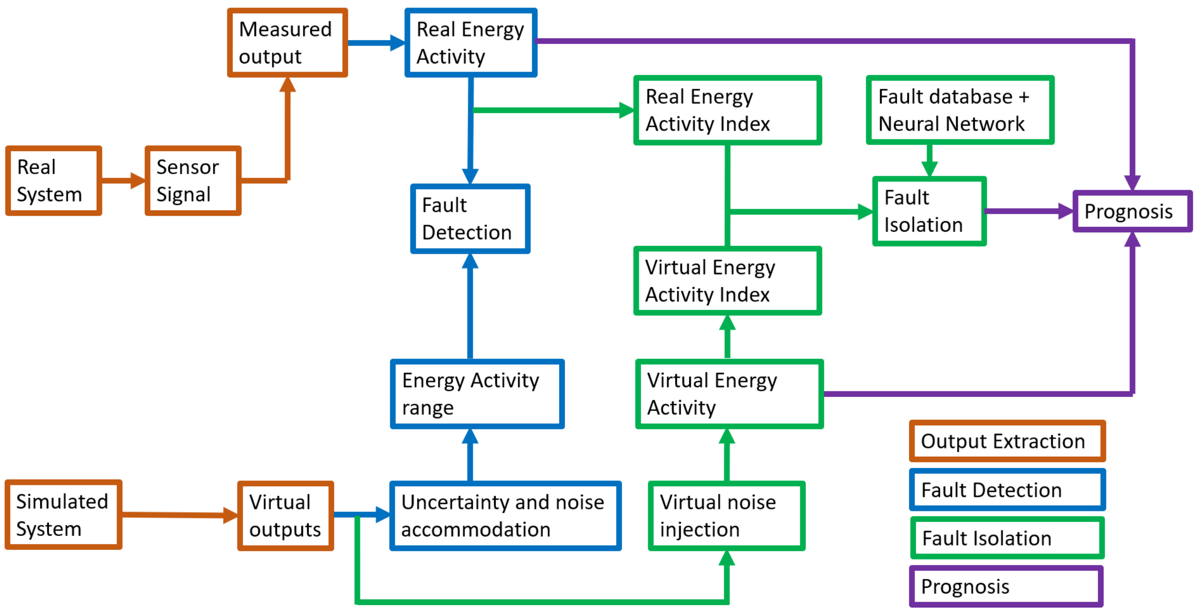

Figure 5.1: PHM using Energy Activity

5.2.2 Online Phase

The online phase deals with the real system. Hence, the online phase must be able to accommodate the model and measurement uncertainties. These uncertainties should be accommodated for fault detection, fault isolation and prognosis processes. It should be noted that the above mentioned are achieved by comparing the residuals from the real system to the corresponding residuals from the virtual systems. In this thesis, the model and measurement uncertainty are handled by accommodating components of the residuals from the virtual system. The signals and components of the residuals from the real system remain unaffected.

5.2.2.1 Fault Detection

Quick and accurate fault detection is one of the most important requirements of PHM. For detecting fault in any real system, the detection method must be able to handle system uncertainties and sensor noise.

5.2.2.1.1 Model uncertainty accommodation

While using Energy Activity for PHM, the measured EA must be compared to that calculated from an ideal system simulation. The deviation of calculated EA from simulated EA indicates a fault. Therefore, it is very important that the simulated model must accommodate the uncertainty in the component values of various elements of the system. In model based analysis, the uncertainty usually occurs because the numeric component values of the system is not known with full accuracy. However, a range of possible deviation of these component values from ideal are often known. Hence, under fault free conditions, the numeric component values can only deviate unto a certain range from ideal. This known range should be accommodated when generating the virtual components for fault detection.

The simulated system should thus provide a range of EA instead of a single value. The deviation of real EA outside this renage indicates a fault. This range of EA is calculated using Interval Extension Function (IEF) as discussed in chapter 1. Under nominal behavior, an envelop around a calculated quantity can be defined by the range of the quantity calculated using IEF [60]. The bounds are therefore generated by solving the system under IEF.

For IEFs, the uncertain variables (various component values in this case) in the equation are replaced be an interval range. Therefore, the result is a range instead of a single fixed quantity. This accommodates the model uncertainty in PHM analysis [1], [116]. The equations are then solved using the basic principles of interval arithmetic [49]. An uncertain variable x with minimum possible value x_{min} and maximum possible value x_{max} is represented as:

$$[x] = [x_{min}, x_{max}] \tag{5.1}$$

Therefore, the simulated EA for any component ϕ can be solved as

$$|EA_{virtual}| = [\phi] \int_{a}^{a+\Delta t} |S([\Phi]).g(S([\Phi]))| \, dt \tag{5.2}$$

Φ is the set of component values of all the components in the system and ϕ is the component value of the component for which EA is being calculated.

A detailed analysis of the methods and advantages of using EA for fault detection under uncertain conditions is provided in the next section.

5.2.2.1.2 Measurement uncertainty accommodation

Fault Detection is performed by continuous evaluation of EA in time domain. Therefore, measurement uncertainty (noise) is adjusted in the calculation of EA.

$$EA = \int_{a}^{a+\Delta t} |e(t).f(t)| \, dt \tag{5.3}$$

$$EA = \int_{a}^{a+\Delta t} |S(t).\phi.g(S(t))| \, dt \tag{5.4}$$

where S power variable input to the component. S is always obtained from a measured quantity, therefore, for noise accommodation, S is replaced with $S + \Delta S$, where ΔS is the noise component of the measurement.

$$EA = \phi \int_{a}^{a+\Delta t} |[S(t) + \Delta S(t)].[g(S(t) + \Delta S(t))]| \, dt \tag{5.5}$$

Assuming an LTI behavior of the system for the duration of calculation of Energy Activity, the eq 5.5 can be expanded as shown in eq 5.6,

$$\begin{aligned} EA = \phi \int_{a}^{a+\Delta t} & \mid S(t).g(S(t)) + \Delta S(t).g(S(t)) \\ & + S(t).g(\Delta S(t)) \\ & + \Delta S(t).g(\Delta S(t)) \mid dt \end{aligned} \tag{5.6}$$

For measurements with high signal to noise ratio, $\Delta S(t).g(\Delta S(t))$ can be neglected from eq 5.6. So, EA can be calculated using eq 5.7.

$$EA = \phi \int_{a}^{a+\Delta t} \mid S(t).g(S(t)) + \Delta S(t).g(S(t)) + S(t).g(\Delta S(t)) \mid dt \tag{5.7}$$

Comparing the above equation with

$$|a| - |b| \leq |a + b| \leq |a| + |b|$$

where

$$\begin{aligned} a &= S(t).g(S(t)) \\ b &= \Delta S(t).g(S(t)) + S(t).g(\Delta S(t)) \end{aligned}$$

It is noted that the integral of $|a|$ is the EA of system without measurement uncertainties as given in eq 5.4. Therefore, inequality relation can be applied to eq 5.7 in the form shown by eq 5.8.

$$EA_L < EA < EA_U \tag{5.8}$$

where

$$\begin{aligned} EA_L = EA_{min} - \phi \int_{a}^{a+\Delta t} & |\Delta S(t).S(s(t))| - \\ & |S(t).g(\Delta S(t))| \, dt \end{aligned} \tag{5.9}$$

$$\begin{aligned} EA_U = EA_{max} + \phi \int_{a}^{a+\Delta t} & |\Delta S(t).g(S(t))| + \\ & |S(t).g(\Delta S(t))| \, dt \end{aligned} \tag{5.10}$$

EA_{max} and EA_{min} are the maximum and minimum allowed Energy activity after accommodating the uncertainty in the system component values using IEF.

ΔS is the error in the component input due to noise. As noise can be either positive or negative, the r.m.s. value of error is noise is used for calculation. EA_L and EA_U are the final lower and upper thresholds for fault detection after accommodating both model and measurement uncertainty.

5.2.2.2 Fault Isolation

Fault isolation is initiated after a fault is detected. Fault isolation depends on the STFT of residuals based on EAI. Even under faulty conditions the EAI of an element varies slower than EA for the corresponding element. This makes the EAI less sensitive to model uncertainty than EA. Also, as isolation requires STFT of the residuals, so the high frequency measurement noise must be handled. Therefore, for fault isolation measurement uncertainty is accommodated.

The measurement uncertainty is accommodated by injecting the noise virtually in the virtual outputs. As it is assumed that certain characteristics of noise are known, a Gaussian noise of similar traits is added to virtual output. These noisy virtual outputs are used for calculation of virtual EA and virtual EAI. It is possible that occasionally, the sensor noise in the real system deviates from it's characteristics for some time. This has minuscule effect on the final calculations because, EA and EAI are calculated over a range of time and not instantaneously. The effect of such local deviations has minuscule effect when considering a larger time window.

The virtual EA is calculated using injected noise (Δs) as follows:

$$EA_{virtual} = \phi_{ideal} \int_{a}^{a+\Delta t} |(S + \Delta s).g(S + \Delta s)|\, dt \tag{5.11}$$

5.2.2.3 Prognosis

Once fault isolation is achieved, the mathematical form of EA can be used to calculate the real variation in the fault parameter, and furthermore the remaining useful life, assuming that the allowable limits of a parameter and degradation law are known for the recognised failure mode.

In order to estimate the dynamics of the degradation (i.e. the time variation in the value of parameter), the time derivative of the EA is required. Therefore, the prognosis is dependent on the rate of change of EA and not the actual value of EA.

$$\frac{\partial \phi}{\partial t} = \frac{\frac{\mathrm{d}EA}{\mathrm{d}t} - \frac{\partial EA}{\partial t}}{\frac{\partial S}{\partial \phi} \cdot \frac{\partial EA}{\partial S}} \tag{5.12}$$

This is captured using eq 5.12, as discussed in the previous chapter. This equation must now be modified to accommodate model and measurement uncertainties. In this equation there are three sources of information.

1. From real system: The component $\frac{dEA}{dt}$ is calculated using the real EA. As discussed earlier, the components from real system remain unaffected.

$$EA_{real} = f(S, t) \tag{5.13}$$

2. From virtual system: The component $\frac{\partial EA}{\partial t}$ is calculated using the virtual EA. As for prognosis, the measurement uncertainties are accommodated to virtual EA by virtual noise injection.

$$EA_{virtual} = f(S(\phi) + \Delta s, t) \tag{5.14}$$

3. From physical model: The denominator of the equation is entirely obtained using the information of the dynamic model. Therefore, model uncertainties are accommodated in this component using IEFs.

The final prognosis equation is given by eq 5.15

$$\left[\frac{\partial \phi}{\partial t}\right] = \frac{\frac{\mathrm{d}EA}{\mathrm{d}t} - \frac{\partial EA}{\partial t}}{\left[\frac{\partial S}{\partial \phi}\right] \cdot \left[\frac{\partial EA}{\partial S}\right]} \tag{5.15}$$

- $\frac{\mathrm{d}EA}{\mathrm{d}t}$ is the time derivative of the Energy Activity calculated from the real system.
- $\frac{\partial EA}{\partial t}$ represents the variation of the Energy Activity only in time, i.e. due to no change in ϕ. This term can be calculated as the time derivative of the Energy Activity of the fault free system.

- $\left[\frac{\partial S}{\partial \phi}\right]$ represents the IEF of variation of the input signal of the component due to the modification of component parameter value. As the dynamic model of the component is known as a pre-requisite this value can be calculated easily.
- $\left[\frac{\partial EA}{\partial S}\right]$ is and IEF that depends on the nature of relation g in the equation 3.9.

For an R-element in LTI system, g is algebraic and from equation 3.13

$$EA = \theta_R \int_a^b S^2 dt \tag{5.16}$$

Therefore,

$$\left[\frac{\partial EA}{\partial S}\right] = [\theta_R] \int_a^b \frac{\partial S^2}{\partial S} dt = 2\,[\theta_R] \int_a^b S dt \tag{5.17}$$

5.3 Fault Detection analysis

Accurate and timely detection of fault (i.e. a deviation of the system from it's desired operating conditions) is the one of the key objectives of any Fault Diagnosis and Isolation (FDI) system. The FDI framework should be able to detect the fault at the earliest. An early detection of fault enables a wider variety of response actions for the fault. The post fault detection decision depends on the Remaining Useful Life of the system [62]. Therefore, an early detection of faults can give more options for response for e.g. implementing fault tolerant control or scheduling maintenance or immediate intervention. This can be a of great advantage if the system under consideration is critical to safety.

Model based approaches [96] [38] use mathematical models derived from governing laws of physics. These approaches are preferred because they give a basic understanding about the functioning of the system and hence can be used with accuracy in any working conditions. The model can either be qualitative or quantitative [134]. Based on the the model, certain equations called residuals are generated which can capture the operating state of various components of the system. One of the major limitation for model based approach is that many times all the system component values are not known with high accuracy which is a necessity for proper detection and decision.

EA, a model based metric, can be used for faster fault detection. The proposed metric has the following properties which make it a better choice for fault detection:

1. **History:** Most of the residuals used for fault detection are found using Analytical Redundancy Relations (ARR) and observers. These methods only use the instantaneous information about the system to detect fault. It is proposed that development of metric which can use both the current and previous information about the state of the system can be a better solution to reduce missed alarms.

   Instantaneous nature of existing model based FDI techniques is attributed to the conditions in which FDI is assumed to function. For FDI the initial condition is assumed to be unknown as FDI is only concerned with detection of faults at the current moment. Therefore, the absence of initial conditions compels the use of differential equations for FDI. However, the initial conditions are known fully or partially for prognosis. This knowledge allow the utilisation of integral constitutive relationship for fault detection leading to more influence of history in fault detection.

2. **Energy Based:** The proposed metric is a parameter based on energy and has a physical significance. Therefore, it is easier to understand and better suited to multi-domain systems.

3. **Isolation from uncertain components:** The proposed metric depends only on various values detected using sensors and the component value of only the component for which it is calculated. Whereas, traditional methods use equations that depend on sensor values in conjunction with the component values of various components, including uncertain ones. The isolation of the metric from multiple uncertain component values reduces the propagated uncertainty.

As discussed previously, fault in a bond graph is represented as a deviation from nominal value (nominal operating mode) of its parameter represented by bond graph element (R,C, I, TF and GY). Depending upon their nature, the faults can be categorised in three types [59].

- **Abrupt Fault:** This fault occurs in a step-wise fashion and stays present. This fault is usually observed in components which can not vary continuously but in discrete steps.
- **Intermittent Fault:** This fault occurs and disappears suddenly. The fault magnitude and duration do not have a fixed pattern and vary randomly. This type of fault is usually caused due to environmental interference.
- **Incipient Fault:** This fault causes a gradual drift in the component value. This fault occurs due to gradual degradation of the system over time.

In this section, fault detection method using Energy Activity (EA) is developed, evaluated and compared against the ARR method. The proposed method is implemented on a real system. Before the actual implementation of the various proposed methods, system simulation is performed for comparison among themselves and with existing technique i.e. ARR. The major advantage of performing a simulation is that, it allows us to have a clear insight about the underlying methods without any external influence of the noise and other environmental factors. The best performing method in simulation is then further developed for practical implementation in order to accommodate noise from the sensors.

5.3.1 Energy Activities for fault detection

EA is calculated using the constitutive relationship (CR) between the component input signal and component output signal. For energy storing elements CR can be either in the differential or integral form. Energy activity calculated using CR in differential form captures the history of how fast the component signal has changed. On the other hand, EA calculated using integral form captures the history total change in the component signal. This situation is analogous to control systems which use PD controllers which are based on rate of error to generate the control signal and PI controllers which are based on total error to generate the control signal. In control systems, PI and PD controllers led to the development of PID controllers. Similarly the logical step in fault detection should also be to develop an EA metric which has both differential and integral components. This is achieved adding both the differential and integral forms of EA. From here on, the EA metric containing both the differential and integral form will be referred as dual-EA.

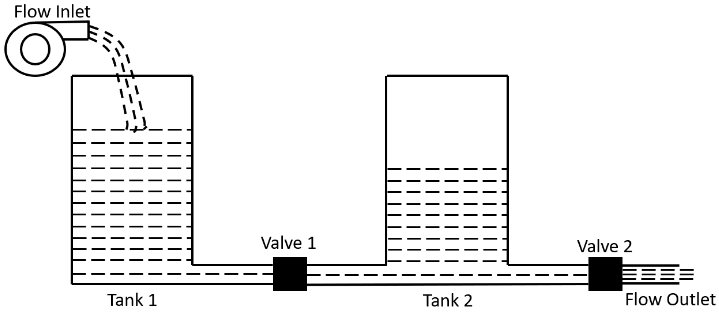

Figure 5.2: Schematic diagram of a two tank system.

The equations representing the differential, integral and dual-EA are given by eq 5.18, 5.19 and 5.20 respectively. The variables k_i and k_d in eq. 5.20 are the gains associated with integral and differential component of the equation.

$$EA_{diff} = \phi^{-1} \int_a^{a+\Delta t} \left| S.\frac{\mathrm{d}S}{\mathrm{d}t} \right| dt \tag{5.18}$$

$$EA_{integ} = \phi \int_a^{a+\Delta t} \left| S. \int_0^t S dt \right| dt \tag{5.19}$$

$$\begin{aligned} EA_{dual} =& k_i \phi \int_a^{a+\Delta t} \left| S. \int_0^t S dt \right| dt + \\ & k_d \phi^{-1} \int_a^{a+\Delta t} \left| S.\frac{\mathrm{d}S}{\mathrm{d}t} \right| dt \end{aligned} \tag{5.20}$$

5.3.2 System Simulation

The Energy Activity forms discussed are simulated on a two-tank hydraulic test benchmark system. The fault detection performance of the proposed methods are also compared with each other and with residuals generated using ARRs. The schematic diagram of the system is represented by fig 5.2. The system consists of two tanks joined to each other through a valve 1. Valve 2 is placed between tank 2 and outlet. Continuous and constant fluid input is maintained using a fluid inlet pump (Q_P). The flow rate through valve 1 (Qv_1), flow rate through valve 2 (Qv_2) is measured using sensors. The diameter of tanks are known, hence, compliance of tank 1 (C_{T1}) and tank 2 (C_{T2}) is known.

As discussed earlier, any physical system has certain components whose physical parameters are not known with high accuracy. However, the uncertainty related to these components can be approximated. In the current system, the flow coefficient for valves 1 and 2, are not known with high accuracy. However, the flow coefficients have an assumed value of 3.85×10^{-6} and 2.85×10^{-6} respectively with an uncertainty of $\pm 5\%$ each. The parameters for the remaining components of the system are known with accuracy. The system parameters used for simulation are given in table 5.3

The system bond graphs in integral and differential form, for the simulated system is shown in fig 5.4a and fig 5.4b respectively. Recall that in diagnosis bond graph (fig. 5.4b, devoted for FDI) sensors (detectors) are dualized into SS Source of signal while they become source of information for ARR generation using covering causal path. The generalised flow in hydraulic system represents the volume flow rate of the fluid and the

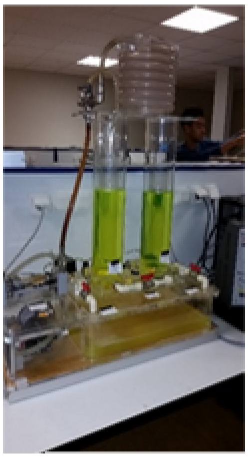

Figure 5.3: Two tank system

generalised effort represents pressure. For system in integral form, the system equations are solved in the integral form, hence, flow is imposed on the tanks and effort is calculated. On the contrary, for system in differential form, the system equations are generated in the differential form, therefore, effort is imposed and flow is calculated.

ARRs in bond graphs are calculated by creating the system in preferred differential causality. The system measurements from the real system are imposed (called duality of sensors). The structural relationship at the junction is then monitored. The equation for checking the structure is called an ARR. To accommodate known uncertainty in the model, LFT-bond graph is usually used [33]. The known uncertainty is added to the component input using a virtual detector. This allows the calculation of the bounds of ARR due to uncertainty. The LFT bond graph used for calculation of ARRs and the corresponding residual bounds is shown in fig 5.5.

There are two types of detectors attached to the system. Efforts associated with the fluid level in tank 1 and 2 are measured using detectors De_1 and De_2 respectively. The volume flow rate of fluid through valve 1 and valve 2 are measured using virtual detectors Df_1 and Df_2. The ARRs require the system in differential causality and dualised sensors. Therefore, for the current system, ARRs are evaluated using De_1 and De_2.

The generated ARRs are as follows:

$$\begin{aligned} ARR1 :& Q_P - C_{T1}\frac{\mathrm{d}}{\mathrm{d}t}De_1 - \\ & Cv_1 sign(De_1 - De_2)\sqrt{|De_1 - De_2|} = 0 \end{aligned} \tag{5.21}$$

$$\begin{aligned} ARR2 :& Cv_1 sign(De_1 - De_2)\sqrt{|De_1 - De_2|} - \\ & C_{T2}\frac{\mathrm{d}}{\mathrm{d}t}De_2 - Cv_2\sqrt{De_2} = 0 \end{aligned} \tag{5.22}$$

For evaluation of EA, the choice of measured quantity and hence the selection of sensors depends on the form of EA (differential, integral or dual). EA in differential forms requires the measurement of the power variable which is independent when the constitutive relationship is in the differential form. For e.g. EA in differential form for

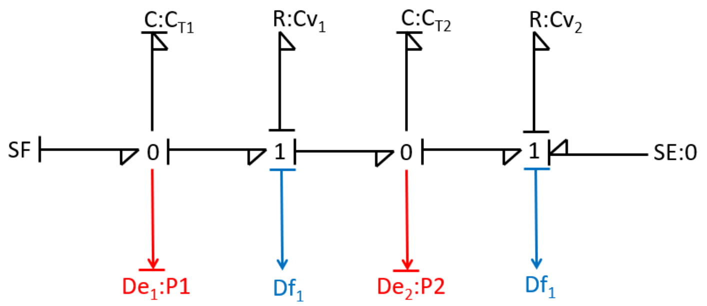

(a) Integral form

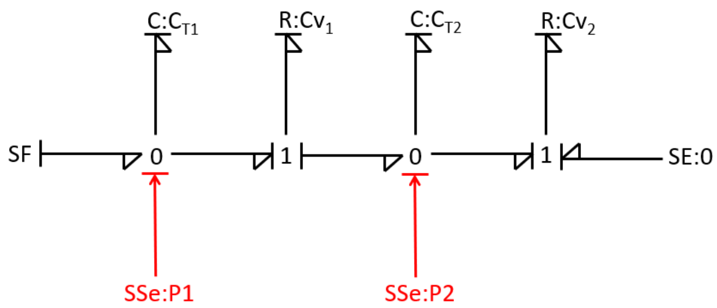

(b) Differential form

Figure 5.4: Bond graph models of two-tank system.

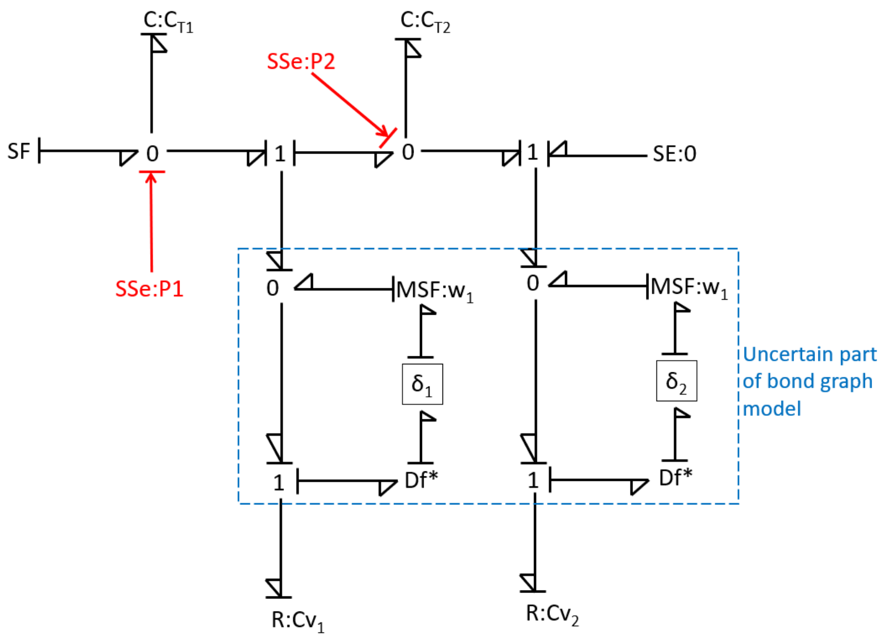

Figure 5.5: LFT-Bond Graph model of 2 tank system.

tank 1 is calculated as follows:

$$\begin{aligned} e &= De_1 \\ f &= C_{T1}\frac{\mathrm{d}}{\mathrm{d}t}De_1 \\ EA &= C_{T1}\int_a^{a+\Delta t}\left|De_1.\frac{\mathrm{d}De_1}{\mathrm{d}t}\right|dt \end{aligned} \tag{5.23}$$

The flow and efforts calculated using constitutive relationship in differential form for all the elements in the system is given in table 5.1. It is noted that in this form, only sensors De_1 and De_1 are required.

Table 5.1: Effort and flow expressions for calculation of Energy Activity in differential form.

	Flow	**Effort**
Tank 1	$C_{T1}\frac{\mathrm{d}}{\mathrm{d}t}De_1$	De_1
Valve 1	$Cv_1 sign(De_1 - De_2)\sqrt{\lvert De_1 - De_2\rvert}$	$De_1 - De_2$
Tank 2	$C_{T2}\frac{\mathrm{d}}{\mathrm{d}t}De_2$	De_2
Valve 2	$Cv_2\sqrt{De2}$	De_2

Similarly, EA in differential forms requires the measurement of the power variable which is independent when the constitutive relationship is in the differential form. For e.g. EA in differential form for tank 1 is calculated as follows:

$$\begin{aligned} f &= Q_P - Df_1 \\ e &= \frac{1}{C_{T1}}\int(Q_P - Df_1)dt \\ EA &= \frac{1}{C_{T1}}\int_a^{a+\Delta t}\left|(Q_P - Df_1).\int_0^t(Q_P - Df_1)dt\right|dt \end{aligned} \tag{5.24}$$

The flow and efforts calculated using constitutive relationship in integral form for all the elements in the system is given in table 5.2. It is noted that in this form only sensors Df_1 and Df_2 are required.

The EA in dual form is the summation of the previously discussed forms on EA i.e. differential and integral. Therefore, for evaluation of EA in dual form all the sensors i.e. De_1, De_2, Df_1 and Df_2 are required.

The system is simulated under the under validated system parameter values. The system parameters are validated using a real system and are given in table 5.3.

The system is simulated to under go a leakage in Tank 1. A leak in the tank corresponds to a reduction in the nominal flow delivered by the pump. This reduction is expressed as a percentage of total volume delivered. The amount of leakage i.e. the magnitude of fault is considered very small. The fault magnitude variation over time under the different types of faults (abrupt, intermittent and incipient) is shown in fig 5.7. Fig 5.7a represents the abrupt fault in the system. To simulate this condition, the flow is decreased by 2% after 50s from start and this change is maintained throughout

Table 5.2: Effort and flow expressions for calculation of Energy Activity in integral form.

	Flow	**Effort**
Tank 1	$Q_P - Df_1$	$\frac{1}{C_{T1}} \int (Q_P - Df_1)dt$
Valve 1	Df_1	$\frac{Df_1^2}{Cv_1^2}$
Tank 2	$Df_1 - Df_2$	$\frac{1}{C_{T2}} \int (Df_1 - Df_2)dt$
Valve 2	Df_2	$\frac{Df_2^2}{Cv_2^2}$

Table 5.3: System Parameters

System Component	**Parameter**	**Value (SI)**
Pump	Flow rate (Q_P)	0.0001
Tank1	Area (C_{T1})	0.0076
Valve 1	Flow coefficient (Cv_1)	$3.85 \times 10^{-6} \pm 5\%$
Tank 2	Area (C_{T2})	0.0079
Valve 2	Flow coefficient (Cv_2)	$2.85 \times 10^{-6} \pm 5\%$

the remaining time. Fig 5.7b represents the intermittent fault in the system. The fault occurs randomly and vanishes after some time. The magnitude and duration for any fault step are not fixed. Fig 5.7c represents an incipient fault in the system. The fault starts at 75s from the start of simulation and gradually increases to 2% at 1000s.

Also, it is discussed in the previous section that Energy Activity for the most active component should be used for fault detection. For the parameters given in Table 5.3, the Energy Activity Index for an ideal system is measured for 1000s. The variation of EAI of various components in the system is shown in fig 5.6. From the figure it is evident that tank 1 is the most active in the system. Therefore, Energy Activity evaluated at tank 1 is used for fault detection. Equations used for fault detection using differential, integral and dual form are eq 5.18, 5.19 and 5.20. For the purpose of current simulation k_i and k_d in eq 5.20 are both set to 1, thereby giving equal weights to both differential and integral components.

For the simulation using LFT-bond graph, it is noted that ARR1 (eq 5.22) is sensitive to the flow inlet to the system. ARR1 is used for the simulation.

5.3.3 Simulation Results and Discussion

The system undergoes 3 types of faults i.e. abrupt, intermittent and incipient. For each fault the system is simulated for 1000s. The residual trends for fault detection using ARR method, Energy Activity in differential form, Energy Activity in integral form and Energy Activity in dual form are given by fig 5.8, 5.9, 5.10 and 5.11 respectively. For each of these figures, sub-figure a, b and c show the generated residual for abrupt, intermittent and incipient respectively. The time taken for detection on various faults using the above mention methods is tabulated in table 5.4.

From table 5.4, it is observed that the residuals generated using ARR are unable to generate an alarm during the first 1000s of simulation. From fig 5.8, it can be observed that, the residuals do conform to the fault signal for all the three types of faults. However, an alarm is not generated because the residuals are not high enough to overcome the bounds due to uncertainty. Fig 5.8c shows a continuous drift in the generated residual so the method will be able to detect the fault but the fault magnitude will increase by that time which is not desirable.

From table 5.4, it is observed that the differential form of Energy Activity is able to detect intermittent faults during the stipulated time. However, the other faults are not detected in time. This is attributed to the fact that the change in EA depends on the rate of change of detected values. Therefore, as long as the system is not in a steady state, the calculated EA changes and it stabilises when equilibrium is reached under faulty conditions. For intermittent faults (fig 5.9b), due to numerous changes brought about by reoccurring faults, the total change in EA is big enough for detecting the fault. When system is under an abrupt fault (fig 5.9a), change is sensor values i.e. energy distribution occurs only once. Therefore, if the change brought about during the fault is not big enough, the fault is not detected. Fig 5.9c shows the EA under incipient fault. A drift in calculated EA is observed but is very small owing to the small rate of parameter degradation.

From table 5.4, it is observed that the Energy Activity in integral form is able to detect all three types of faults successfully, within the stipulated time. This is because in it's integral form EA captures the total energy change in a component. Therefore, the generated residual continues to deviate even when the system is stable. The amount of

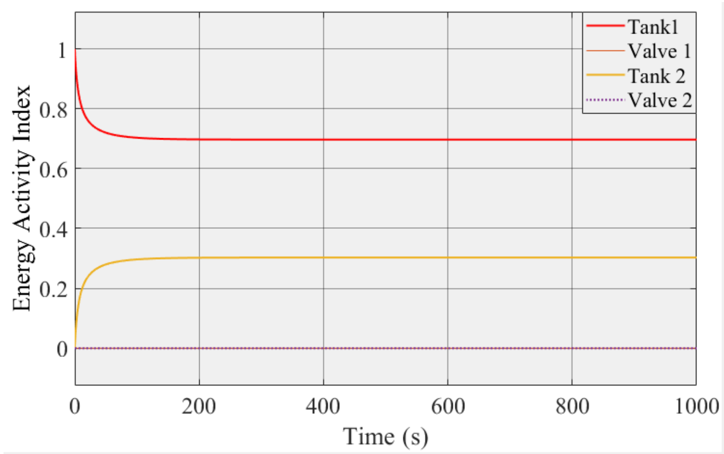

Figure 5.6: Energy Activity Index for various components in ideal condition.

deviation caused is also proportional the amount of error. Therefore, abrupt fault with a higher magnitude is captured in lesser time than the gradually increasing incipient fault.

From table 5.4, it is observed that the dual-Energy Activity is also able to successfully detect all the three types of faults within the stipulated time. However, compared to EA in integral form, the dual form is faster to detect the abrupt fault but slower to detect intermittent and incipient faults. A possible reason can be that for incipient and intermittent faults the differential increase in residuals due to summation of differential and integral components is slower than the increase in the detection range. On the other hand, a fast change due to high magnitude jump and retention of the fault causes a faster change in the differential component for the abrupt fault. This fast change, added to the integral component propels the net residual beyond the allowed limits quickly to generate the alarm.

Table 5.4: Fault detection time.

	Detection time for fault (sec)		
	Abrupt fault	**Intermittent fault**	**Incipient fault**
ARR	>1000	>1000	>1000
EA_differential	>1000	912	>1000
EA_integral	141	547	521
EA_dual	122	696	691

5.3.4 Implementation on a two tank system

The proposed fault detection method is implemented on a two tank system (fig 5.3) for checking the accuracy in working conditions. From the various simulations performed, Integral form of EA is used for the final application. As the real system measurements are never noise free, the calculation of Energy Activity are made robust as discussed

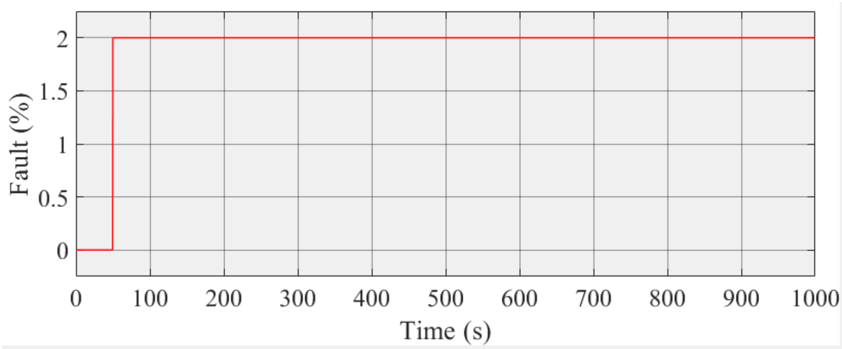

(a) Abrupt Fault

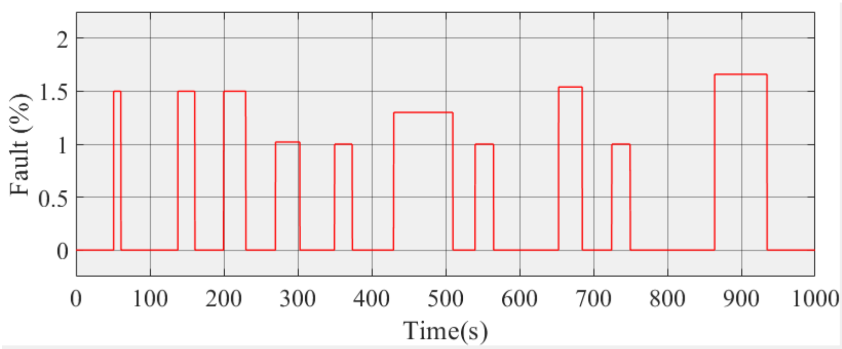

(b) Intermittent Fault

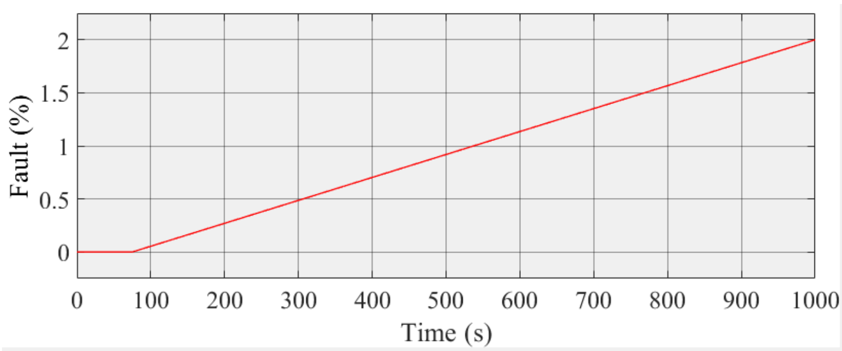

(c) Incipient Fault

Figure 5.7: Various types of faults measured as percentage change in ideal flow.

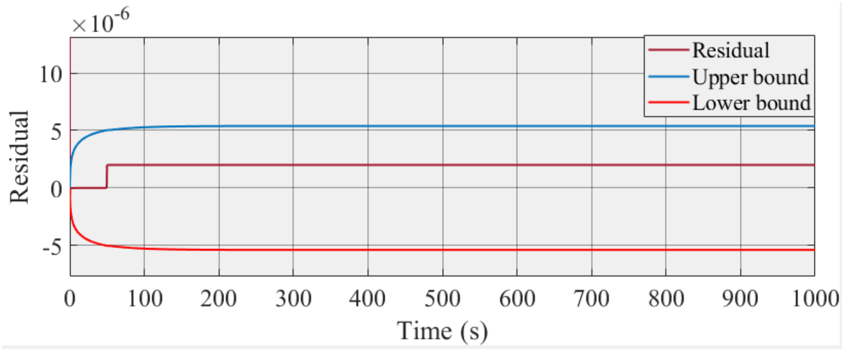

(a) Abrupt Fault

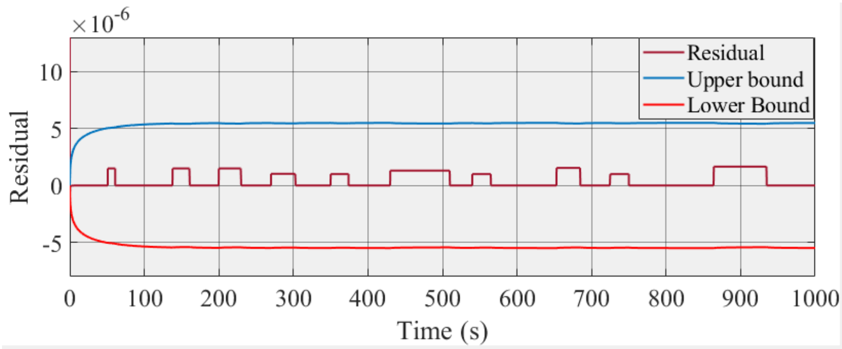

(b) Intermittent Fault

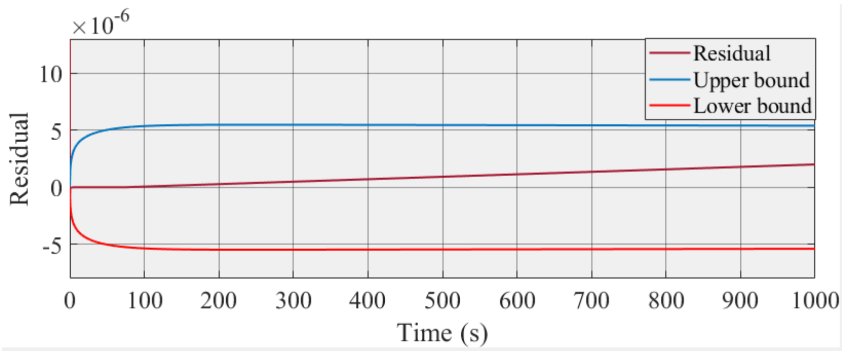

(c) Incipient Fault

Figure 5.8: Residuals generated for different types of faults using ARRs from LFT-Bond Graph.

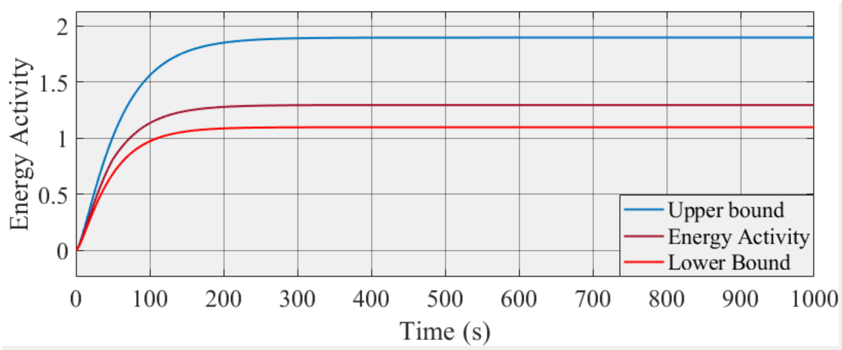

(a) Abrupt Fault

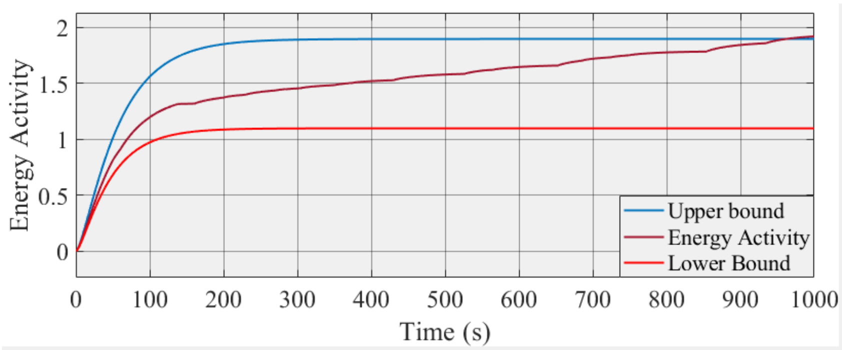

(b) Intermittent Fault

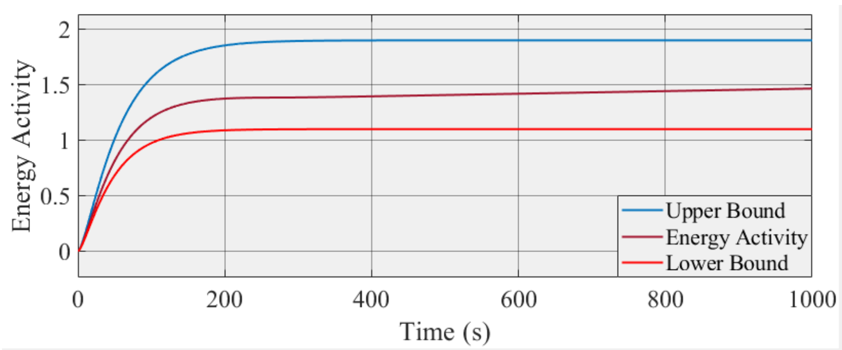

(c) Incipient Fault

Figure 5.9: Detection of different types of faults using Energy Activity in differential form.

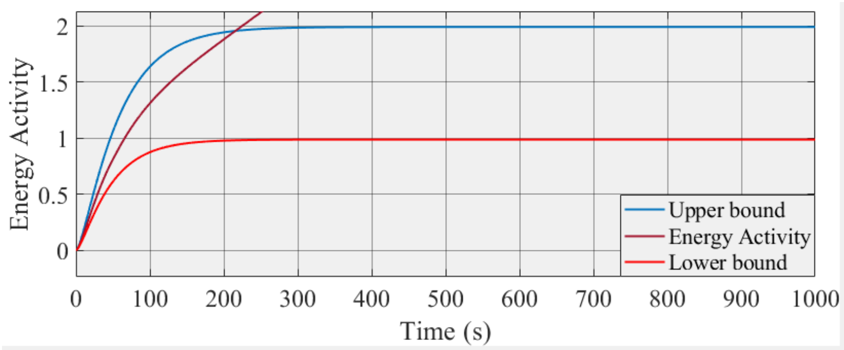

(a) Abrupt Fault

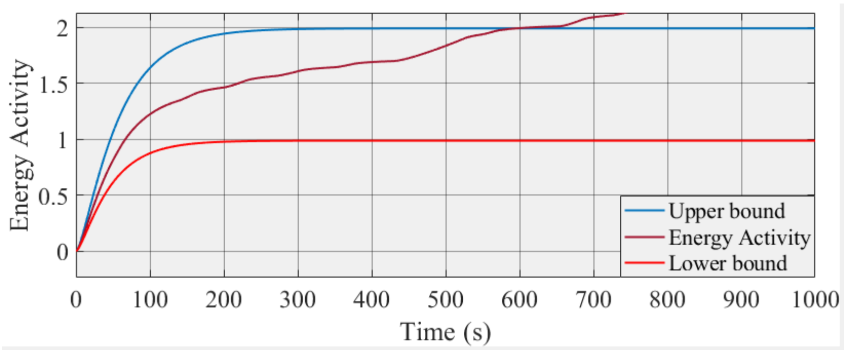

(b) Intermittent Fault

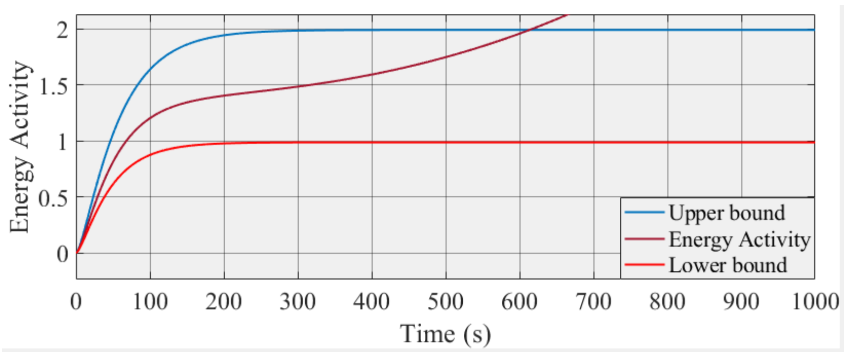

(c) Incipient Fault

Figure 5.10: Detection of different types of faults using Energy Activity in integral form.

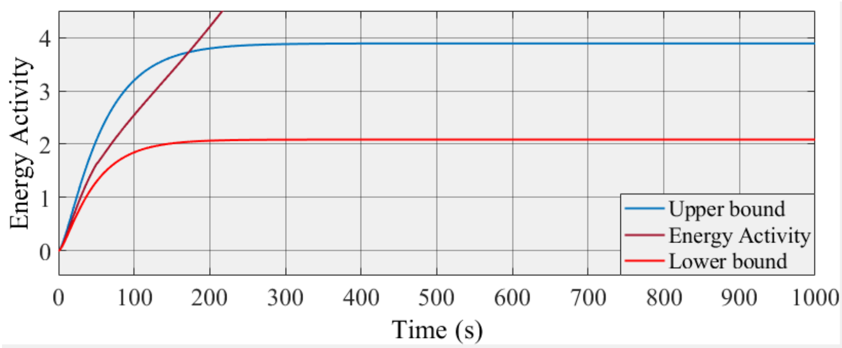

(a) Abrupt Fault

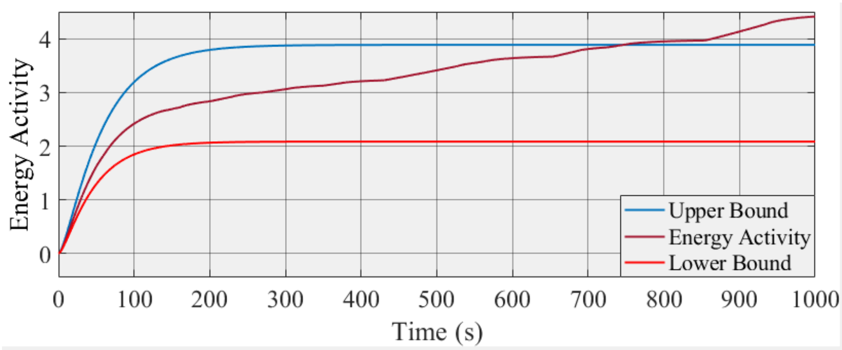

(b) Intermittent Fault

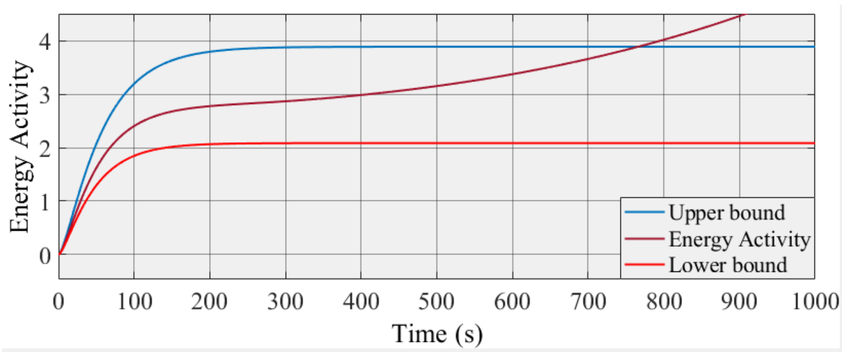

(c) Incipient Fault

Figure 5.11: Detection of different types of faults using Energy Activity in dual (differential + integral) form.

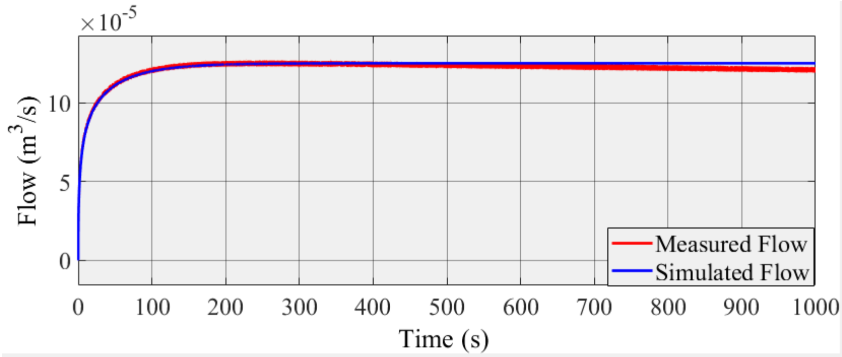

(a) Measured and Simulated flow through valve 1.

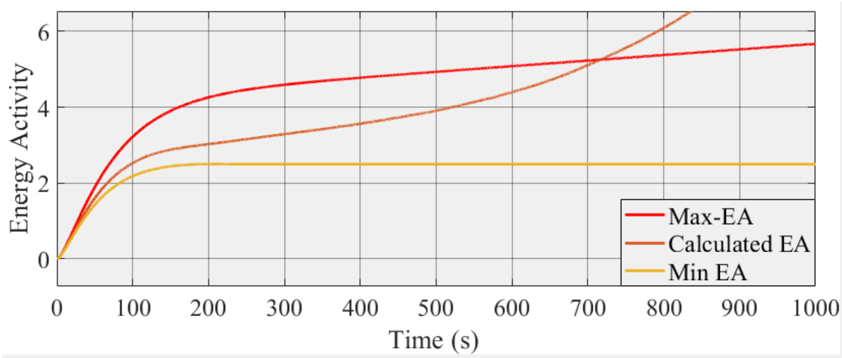

(b) Calculated Energy Activity

Figure 5.12: Flow through valve 1 and Energy Activity for two tank system undergoing leakage in tank 1.

previously.

The method is checked for two types of faults i.e. an actuator fault and a system fault. The actuator fault is introduced by changing the flow input to the system and system fault is introduced by opening the leakage valve in the tank 1. For both the above, small incipient faults are introduced. The system is considered immune from intermittent faults from the environment. The r.m.s error for measurement is known ($4.48 * 10^{-7}\ m^3/s$).

Measured flow through valve 1 (fig 5.12a) and Energy Activity calculated at tank 1 (fig 5.12b) for a two tank system undergoing leakage in tank 1 is shown in fig 5.12. A leakage in tank represents a system fault. Similarly, for a system with actuator fault i.e. faulty pump is shown in fig 5.13. From the above figures, it is evident that minute incipient faults that are missed in traditional FDI processes like ARRs are detected successfully using EA in integral form.

5.4 PHM of two tank system using Energy Activity

The leakage and actuator faults discussed in the previous section are genuine problems however, prognosis, which differentiates PHM from FDI is more suited for degradation. As discussed earlier, degradation corresponds to incipient faults. Therefore, once the form most suited form for EA is established, PHM is performed for the system under valve degradation. Also, a pre-requisite for PHM is the definition of failure, which is also performed.

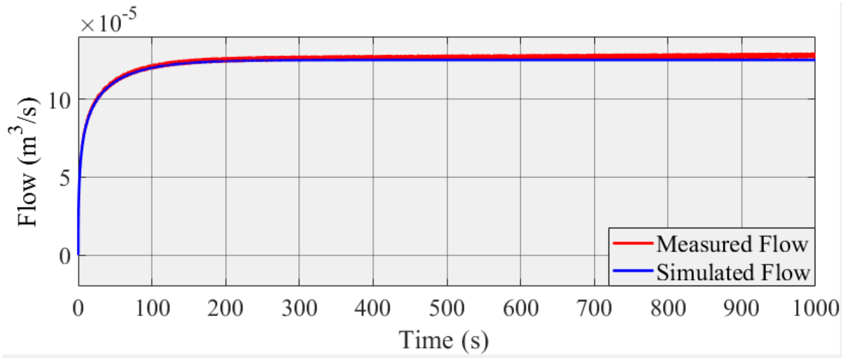

(a) Measured and Simulated flow through valve 1.

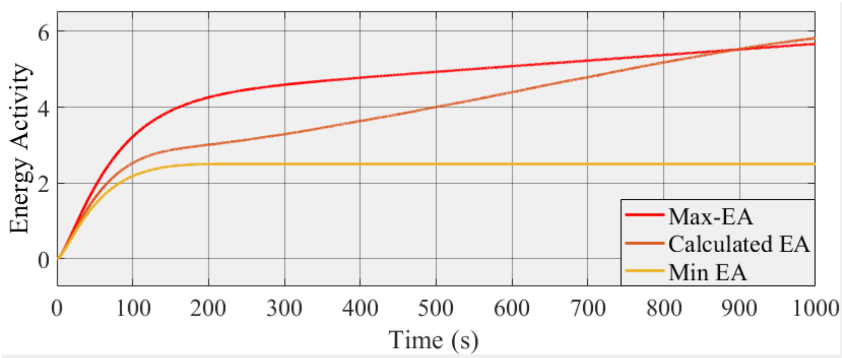

(b) Calculated Energy Activity

Figure 5.13: Flow through valve 1 and Energy Activity for two tank system with faulty pump.

5.4.1 Failure Definition

At first, the point of failure for the system is fixed. The system is assumed to fail when the height of fluid in tank 1 rises more than an allowed upper threshold or dips below an allowed lower threshold. Under ideal conditions the tank is assumed to have a fluid height of 30.5 cm. The system fails when the fluid height increases more than 35 cm or reduces below 25 cm.

Once the failure is defined, the modes of failure for the system are recognised. The first mode of failure is due to an actuator fault i.e. change in volume flow rate of pump. The second mode of failure is valve degradation i.e. loosening or blockage in valve leading to change in flow coefficient for any of the valve. The third possible mode of failure is a leakage in tank. The leakage in tank 1 can be modelled as a reduction in flow from inlet pump and a leakage in tank 2 can be modelled as undesired opening of valve 2.

The failure criteria is then mapped to all the component values of the system. For eg, to model actuator failure limit, the fluid inlet corresponding to the upper and lower allowed threshold is calculated. These limits are calculated assuming the ideal component values of the system. As the dynamic model is available for the system, this model can be used to find the failure limits under ideal working conditions. The calculated failure criteria for various components are given in table 5.5.

The system undergoes gradual degradation inciting the loosening of valve 1.

The equations used for evaluation of Energy activity are given in table 5.2.

Table 5.5: System parameters at failure limits.

	Ideal Value	Upper Limit	Lower Limit
Pump	1.25×10^{-4}	1.3439×10^{-4}	1.1338×10^{-4}
Valve 1	3.85×10^{-6}	5.3319×10^{-6}	3.2069×10^{-6}
Valve 2	2.85×10^{-6}	3.3060×10^{-6}	2.565×10^{-06}

5.4.2 Offline Phase

The modes of failure are recognised. The various failures can be modelled as a fault in either the inlet pump or valve 1 or valve 2, hence, the leakages in tanks are also attributed to change in valve coefficients during prognosis. However, the degradation law and residual evolution in these components might be different, therefore, the simulation for all the components under fault needs to be performed to create a fault database.

The leakage in tank 1 is simulated by considering a leakage valve in parallel with valve 1. Similarly, leakage in tank 2 is simulated by considering a leakage valve in parallel with valve 2. Therefore, the total flow coefficient is the sum of flow coefficient of the actual valve and the leakage valve in parallel to it. For simulation of actual valve degradation, the flow coefficients for valve 1 and valve 2 are changed from their respective lower limits to upper limits. However, for simulation of leakage, the flow coefficients for the leakage valve is varied from 0 to the range of allowed flow coefficients for the real valve parallel to it.

5.4.3 Fault Detection

As discussed in previous section, for fault detection of uncertain systems with noisy signals, the uncertainty in system parameters and noise characteristics should be known. For the current system, the parameter uncertainties are given in table 5.3 and the r.m.s. value of noise of flow sensors is $4.48 \times 10^{-7}\ m^3/s$.

The time period for which the EA is calculated is very important. A larger time window allows smaller faults to be detected as it allows for concatenation of small variations over time in order to overcome limits. However, a longer proportion of fault free operation in the time window also depreciates the effect fault in EA thereby making fault detection difficult. Therefore, for fault detection, the integration window was limited to 100 sec. Hence, the equation used for calculation of EA is given by eq 5.25.

$$EA = [\phi] \int_{t-100}^{t} |S.g(S)|\, dt \tag{5.25}$$

The fastest detection is done by the EA calculated at tank 1. The EA calculated and fault detection is given in fig 5.14. The fault is successfully detected at 335 sec after the start.

5.4.4 Fault Isolation

For the current system, in ideal situation fault can be isolated by simple comparison of flow rate measured at the valves. For eg, an unequal flow measurement in valve 1

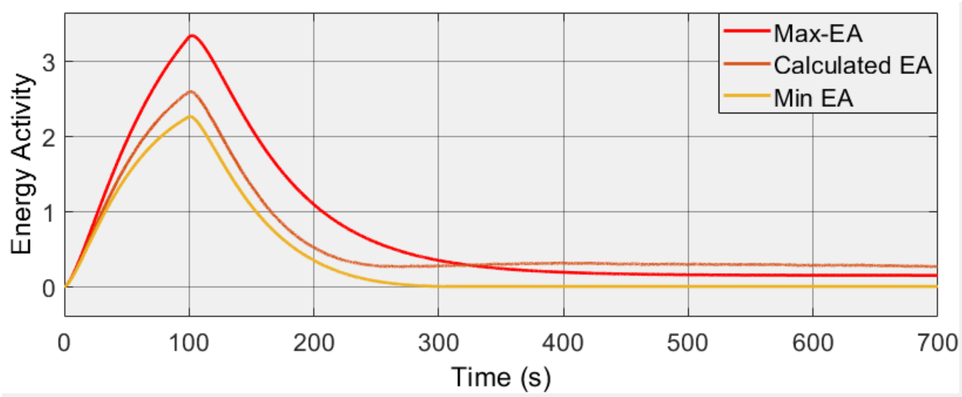

Figure 5.14: Calculated EA for fault detection.

and valve 2 indicates a leakage in tank 2. However, under slow degradation, the actual changes in flow are masked by sensor noise. Therefore, fault can not be isolated directly.

For fault isolation, before the start of experiment, a fault database of residuals (using EAI) is created using simulated system. STFT is performed on the residuals and neural network is trained for classification of faults. The STFT is performed over a time window of 50 sec. Therefore, once the fault is detected the equation for calculation of real EA changes to:

$$EA = [\phi] \int_{t-50}^{t} |S.g(S)|\, dt \tag{5.26}$$

The fault is isolated to occur in the valve 1 of the system. The fault is isolated at 485 sec (i.e. after 3 cycles of STFT). The STFT for residuals calculated at tank 1 are shown in fig ??. STFT for residuals generated at all the components is used for fault isolation.

5.4.5 Prognosis

It is noted that constitutive relationship for R element is not linear.

$$f = C_V.sign(\Delta e)\sqrt{\Delta e} \tag{5.27}$$

However, the $sign(\Delta e)$ term in the equation just assures the proper direction of flow. Assuming that there is no reversal of flow, eq 5.28 can be used instead of eq 5.27.

$$f = C_V\sqrt{\Delta e} \tag{5.28}$$

Therefore, eq 5.17 is not applicable. However, eq 5.15 is always applicable. Therefore both $\frac{\partial EA}{\partial S}$ and $\frac{\partial S}{\partial \phi}$ must be calculated.

For valve 1:

$$S = e_1 - e_2 \therefore \frac{\partial S}{\partial C_{V1}} = \frac{\partial e_1}{\partial C_{V1}} - \frac{\partial e_2}{\partial C_{V1}} \tag{5.29}$$

where

$$e_1 = C_{T1}\int_0^t f_p dt - C_{T1}C_{V1}\int_0^t \sqrt{e_1 - e_2} dt$$

and

$$e_2 = C_{T2}C_{V1}\int_0^t \sqrt{e_1 - e_2}dt - C_{T2}C_{V2}\int_0^t \sqrt{e_2}dt$$

Hence,

$$\frac{\partial e_1}{\partial C_{V1}} = -1(C_{T1}\int_0^t \sqrt{S}dt + C_{T1}C_{V1}\int_0^t \frac{1}{2\sqrt{S}}\frac{\partial S}{\partial CV1}dt) \tag{5.30}$$

and

$$\begin{aligned} \frac{\partial e_2}{\partial C_{V1}} =& C_{T2}\int_0^t \sqrt{S} + C_{T2}C_{V1}\int_0^t \frac{1}{2\sqrt{S}}\frac{\partial S}{\partial CV1}dt \\ &- C_{T2}C_{V2}\int_0^t \frac{1}{2\sqrt{e_2}}\frac{\partial e_2}{\partial CV1}dt) \end{aligned} \tag{5.31}$$

$\frac{\partial S}{\partial C_{V1}}$ can be calculated by substituting eq 5.30 and eq 5.31 in eq 5.29.
$\frac{\partial EA}{\partial S}$ can be calculated as follows:

$$EA = \int_{t-50}^{t} |e.f|\,dt = \int_{t-50}^{t} \left|S.C_{V1}\sqrt{S}\right| dt \tag{5.32}$$

As it is assumed that there no reversal of flow. This is possible when fluid level in tank 1 remains higher than that of tank 2. In this situation, $e_1 - e_2 > 0$ always holds. Hence, both generalised effort and generalised flow associated with valve 1 are positive. Therefore, the absolute sign in eq 5.32 can be removed without affecting it's value.

$$EA = \int_{t-50}^{t} S.C_{V1}\sqrt{S}dt \tag{5.33}$$

Therefore,

$$\frac{\partial EA}{\partial S} = \frac{3}{2}C_{V1}\int_{t-50}^{t} \frac{1}{\sqrt{S}}dt \tag{5.34}$$

It must be noted that similar to fault detection, in order to accommodate model uncertainty, IEF are used to calculate an upper and lower limit of a range of possible degradation rates. The effects of noise are minimised using a median filter. The degradation rate of is then fitted. From literature it is a common practice to use a linear degradation for faults in valves [94]. This corresponds to a constant degradation rate. The prognosis is run for some more duration till the a constant degradation rate trend is visualised. The calculated upper and lower degradation rates are 6.737×10^{-10} and 3.527×10^{-10} (fig 5.15) respectively.

The range of end of life according to the prognosis are as follows:

$$t_{eol}^{min} = \frac{C_{V1}^{fail} - C_{V1}^{max}}{\frac{\partial C_{V1}}{\partial t}^{max}} + time_{detection}$$

$$t_{eol}^{max} = \frac{C_{V1}^{fail} - C_{V1}^{min}}{\frac{\partial C_{V1}}{\partial t}^{min}} + time_{detection}$$

The minimum and maximum end of life time are estimated as 2177 sec and 4994 sec respectively. The system is allowed to run till failure to validate the range. The measured

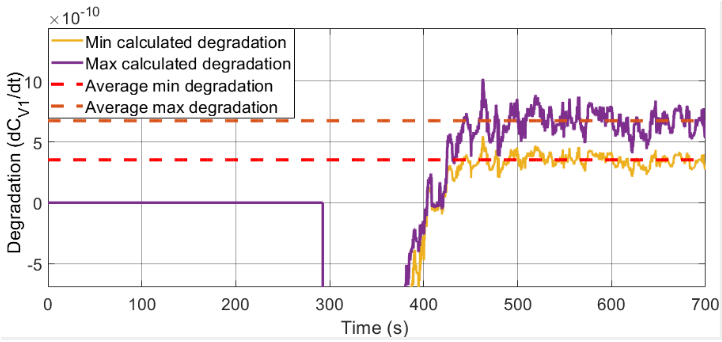

Figure 5.15: Valve degradation from prognosis.

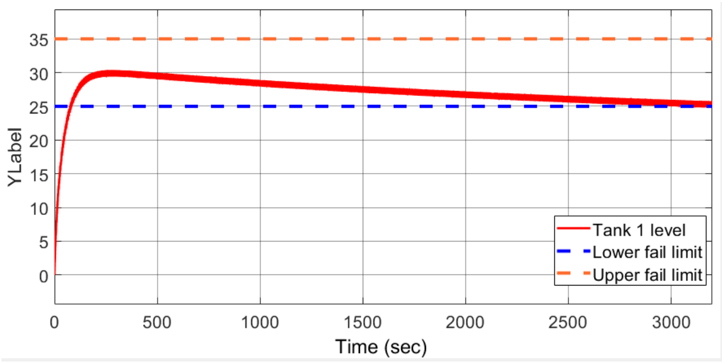

Figure 5.16: Measured height in tank 1.

height of fluid level in tank 1 is given fig 5.16. It is observed that the failure alarm is activated at 2986 sec. Hence, the proposed methodology is able to correctly predict the time of failure.

5.5 Conclusion of the chapter

The chapter improves the previously introduced framework for integrated fault diagnosis and prognosis to accommodate model and measurement uncertainties. The model uncertainties are measurement uncertainties are incorporated in the framework using Interval Extension of Functions and known model noise information.

The in depth analysis of fault diagnosis using energy activity in uncertain systems establishes the advantages of using integral function and initial conditions for fault diagnosis. With the availability of initial conditions the system is able to detect minute faults

Table 5.6: End of Life estimation.

	Estimation		Actual
	Minimum	Maximum	
End of Life	2177 sec	4994 sec	2989 sec

that are not detected using traditional methods of fault diagnosis.

The complete framework is tested for fault diagnosis and prognosis in a two-tank benchmark system. The framework is able to timely detect the occurrence of fault and predict accurately the range of end of life.

Chapter 6

Conclusions and Prospective

Contents

6.1 General Conclusion

The primary purpose of this thesis is to introduce a new approach for creating the integrated fault diagnosis and prognosis by extending a parameter fit for prognosis for diagnosis instead of the traditionally used approach of using diagnosis technique for prognosis. The primary motivation for the use a prognosis parameter for diagnosis lies in the availability of initial conditions (full or partial) which can be used in the diagnosis process thereby improving the diagnosis and hence the overall PHM process.

Energy Activity(EA) is recognised as a suitable metric for the integrated framework of fault diagnosis and prognosis. This is due to the following properties:

1. EA can never decrease over time therefore is suited for as a prognosis parameter as suggested in previous literature.

2. EA is a parameter with a physical meaning and is therefore gives an intuitive sense for application.

3. EA is a variant of energy and is therefore suited for multi-domain application.

4. EA can be defined for every component therefore fault isolation is possible.

EA is the integral of absolute product of generalised effort and generalised flow. Therefore a modelling technique that can directly deal with these is suitable for the framework proposed in this thesis. Bond graph and Energetic Macroscopic Representation are two most suited techniques as both use generalised effort and flow for modelling. Bond graph is structural approach while energetic macroscopic representation is a functional approach. A structural approach can be highly beneficial in the modelling and analysis process therefore, bond graph is used for the development and application of the framework.

The framework consists of two phases i.e. an offline phase for generation of fault signature database and an online phase for fault diagnosis and prognosis of the system.

In the offline phase a faulty system and a fault free system are simulated in parallel. Virtual measurements corresponding to that from the real system are obtained for comparison. Simulations are done for a range of faults in every component. Fault is simulated one component at a time. The residual EAI for the components is not directly usable.

To obtain a fault signature, the frequency components of the residuals are obtained. The frequency signatures for all the fault simulations are used to train a classification neural network to be applicable in the online phase.

In the online phase a virtual, fault free system is run in parallel to the real system. The online phase consists of three sequential steps i.e. fault detection, fault isolation and prognosis. Fault detection is model based and is performed by comparing the energy activities of the real and virtual system. Fault isolation is data based. Once a fault is detected, the fault isolation is performed. The residuals based on energy activity index are classified using the neural network. Once the fault is classified, model based fault prognosis is performed. Prognosis equation depends on the component undergoing a fault. Therefore, prognosis uses the results of fault isolation and system dynamic model to predict the degradation rate. This degradation rate can be used along with the known degradation law to obtain the remaining useful life

The framework is also updated to incorporate model and measurement uncertainties. The model uncertainties are incorporated using interval extension of functions. The measurement uncertainties are incorporated by injecting noise with similar traits in the virtual system.

6.1.1 Benefits of the method

A careful analysis of the proposed work highlights the following benefits of the proposed framework of integrated fault diagnosis and prognosis using Energy Activity:

1. A common parameter can be used for both fault diagnosis and prognosis therefore solving a common problem of data fusion between fault diagnosis and prognosis algorithms.

2. As the framework is based on an energy metric, it can be used for multi-domain systems.

3. The historic information in EA allows for better fault detection and problem of missed detection is solved.

4. The initial condition information available during prognosis is used during diagnosis thereby further improving the diagnosis capabilities.

5. The proposed framework is able to handle model and measurement uncertainties.

6. The offline phase does not require actual failure data as the failures can be easily simulated if an accurate model is available.

6.1.2 Limitation of the methods

A careful analysis of the proposed work highlights the following benefits of the proposed framework of integrated fault diagnosis and prognosis using Energy Activity:

1. The framework is not able to handle sensor faults.

2. The ability of framework to handle coupled energy systems needs to be checked as EA is not well developed for coupled energy systems.

3. The framework requires a prior knowledge of failure limits and degradation law.

4. The framework is developed under single fault assumption therefore, the framework can not handle multiple faults in the system.

5. The performance of framework under uncertain model conditions depends on interval extension functions. The range of these functions depends highly on the form of equation used.

6. The prognosis algorithm is applied in an R-element. The R-elements represent the energy losses. The numeric component value of these elements can be difficult to find in many situations.

7. The prognosis equation selected and the end of life that is estimated depends on accurate fault isolation which depends data based. This is the weakest point in the algorithm with no feedback mechanism in the framework to check the accuracy of fault isolation or the accuracy of the degradation law.

6.2 Future Works

Based on the above discussion it is observed that the framework has lots of room for improvement. The following are suggested topics which can be used to improve the proposed framework.

1. The data based fault isolation remains the weakest point of the proposed framework therefore the following are proposed to improve the fault isolation:

   (a) The concept of Junction Activity and Junction Activity Index can be utilized to generate a fault signature matrix to improve fault isolation.
   (b) The frequency formulation of EA can be used to directly generate fault signatures in the offline phase instead of simulation.
   (c) For the current work the neural network architecture was selected based on trial and error. A comprehensive study of best suited neural network architecture can be done to improve the performance of fault isolation.
   (d) In the current proposition, the fault isolation in online phase only accommodates measurement uncertainties. A drawback of not accommodating model uncertainties evident by a delay between fault detection and fault isolation under uncertain conditions. Therefore, model uncertainties should be accommodated in the offline phase of fault isolation.

2. The ability of the proposed algorithm to detect minute faults depends highly on the time window if the initial states of the system is not known. A longer time window allows more time for the fault to concatenate and generate alarm but it also increases the thresholds which most be overcome to generate an alarm. This trade-off can be fixed by finding an optimum window of integration used for fault detection.

3. Multiple thresholds using relative activity can be generated to improve fault detection.

4. Just as the neural network is trained for fault isolation, a neural network can be trained for also approximating the extent of fault. This can act as a feedback for prognosis algorithm.

5. A mathematical framework is proposed to make the framework entirely model based. For a system with n elements and m sensors:

$$EA = \begin{Bmatrix} EA_1 \\ EA_2 \\ .... \\ EA_n \end{Bmatrix}_{n\times 1} \tag{6.1}$$

The input signals to all the elements in the system can be represented with a vector S. Components of S are a function of the system parameters Φ.

$$S_{n\times 1} = \big[M\big]_{n\times m} \begin{bmatrix} s_1 = f_1(\Phi) \\ s_2 = f_2(\Phi) \\ .... \\ s_m = f_m(\Phi) \end{bmatrix}_{m\times 1} \tag{6.2}$$

Φ can be represented as a vector containing the numeric component values of individual components.

$$\Phi = \begin{bmatrix} \phi_1 \\ \phi_2 \\ .... \\ \phi_n \end{bmatrix}_{n\times 1} \tag{6.3}$$

For any system

$$EA = f(\Phi, t) \tag{6.4}$$

$$\mathrm{d}EA = \frac{\partial EA}{\partial S}\frac{\partial S}{\partial \Phi}\mathrm{d}\Phi + \frac{\partial EA}{\partial t}\mathrm{dt} \tag{6.5}$$

$$\frac{\mathrm{d}EA}{\mathrm{dt}} = \frac{\partial EA}{\partial S}\frac{\partial S}{\partial \Phi}\frac{\mathrm{d}\Phi}{\mathrm{dt}} + \frac{\partial EA}{\partial t} \tag{6.6}$$

$$\frac{\mathrm{d}\Phi}{\mathrm{dt}} = \left[\tfrac{\partial EA}{\partial S}\tfrac{\partial S}{\partial \Phi}\right]^{-1}\left[\tfrac{\mathrm{d}EA}{\mathrm{dt}} - \tfrac{\partial EA}{\partial t}\right] \tag{6.7}$$

Here $\frac{\mathrm{d}EA}{\mathrm{dt}}$ is calculated using the live date calculation.
$\frac{\partial EA}{\partial t}$ is calculated using reference Energy activity.
$\frac{\partial S}{\partial \Phi}$ is a jacobian calculated from model information.
$\frac{\partial EA}{\partial S}$ is a jacobian calculated as follows
Case 1 For energy storage element in derivative causality with numeric component value θ.

$$EA = \int_a^b \left| s.\theta\frac{\mathrm{d}s}{\mathrm{dt}} \right| dt \tag{6.8}$$

$$EA = \frac{\theta}{2}\int_a^b \left| \frac{\mathrm{d}s^2}{\mathrm{dt}} \right| dt \tag{6.9}$$

$$\dot{EA}_{t=b} = \left(\frac{\theta}{2}\left|\frac{\mathrm{d}s^2}{\mathrm{d}t}\right|\right)_b \tag{6.10}$$

$$\dot{EA}_{t=b} = \left(c\frac{\theta}{2}\frac{\mathrm{d}s^2}{\mathrm{d}t}\right)_b \tag{6.11}$$

where

$$c = \begin{cases} 1, & \frac{\mathrm{d}s^2}{\mathrm{d}t} \geq 0 \\ -1, & \frac{\mathrm{d}s^2}{\mathrm{d}t} < 0 \end{cases} \tag{6.12}$$

continuing from eq. 6.11

$$\frac{\mathrm{d}\dot{EA}}{\mathrm{d}s} = c\frac{\theta}{2}\frac{\mathrm{d}}{\mathrm{d}s}\left(\frac{\mathrm{d}s^2}{\mathrm{d}t}\right) = c\frac{\theta}{2}\frac{\mathrm{d}}{\mathrm{d}t}\left(\frac{\mathrm{d}s^2}{\mathrm{d}s}\right) \tag{6.13}$$

$$\frac{\mathrm{d}}{\mathrm{d}s}\left(\frac{\mathrm{d}EA}{\mathrm{d}t}\right) = \frac{\mathrm{d}}{\mathrm{d}t}\left(\frac{\mathrm{d}EA}{\mathrm{d}s}\right) = c\theta\frac{\mathrm{d}s}{\mathrm{d}t} \tag{6.14}$$

Integrating w.r.t time

$$\frac{\mathrm{d}EA}{\mathrm{d}s} = \theta\int_a^b \left(c\frac{\mathrm{d}s}{\mathrm{d}t}\right) dt \tag{6.15}$$

As the signal processing is done on live data hence, the expression is not reduced further.

Case 2 For energy storage element in integral causality with numeric component value θ.

$$EA = \int_a^b \left| s\theta\left(\int_a^b s\mathrm{d}t + I\right)\right| \mathrm{d}t \tag{6.16}$$

$$EA = \int_a^b cs\theta\left(\int_a^b s\mathrm{d}t + I\right)\mathrm{d}t \tag{6.17}$$

where

$$c = \begin{cases} 1, & s\left(\int_a^b s\mathrm{d}t + I\right) \geq 0 \\ -1, & s\left(\int_a^b s\mathrm{d}t + I\right) < 0 \end{cases} \tag{6.18}$$

continuing from equation 6.17

$$\frac{\partial EA}{\partial s} = \theta\int_a^b \left[c\frac{\partial}{\partial s}\left(s\left(\int_a^b s\mathrm{d}t + I\right)\right)\right]\mathrm{d}t \tag{6.19}$$

$$\frac{\partial EA}{\partial s} = \theta\int_a^b c\frac{\partial}{\partial s}\left(s\int_a^b s\mathrm{d}t + sI\right) dt \tag{6.20}$$

$$\frac{\partial EA}{\partial s} = \theta\int_a^b c\left(\int_a^b s\mathrm{d}t + s\frac{\partial\int_a^b s\mathrm{d}t}{\partial s} + I\right)\mathrm{d}t \tag{6.21}$$

$$\frac{\partial EA}{\partial s} = \theta\int_a^b c\left(\int_a^b s\mathrm{d}t + \int_a^b \Delta s\mathrm{d}t + I\right)\mathrm{d}t \tag{6.22}$$

$$\frac{\partial EA}{\partial s} = \theta \int_a^b c \left(\int_a^b (s + \Delta s)\, \mathrm{d}t + I \right) \mathrm{d}t \tag{6.23}$$

Case 3 For energy dissipator with numeric component value θ.

$$EA = \int_a^b |s.\theta s|\, \mathrm{d}t = \int_a^b \left|\theta s^2\right| \mathrm{d}t \tag{6.24}$$

As s^2 is always positive and θ is a physical parameter the absolute sign can be removed.

$$EA = \int_a^b \theta s^2 \mathrm{d}t \tag{6.25}$$

$$\frac{\partial EA}{\partial s} = \theta \int_a^b \frac{\partial s^2}{\partial s} \mathrm{d}t \tag{6.26}$$

$$\frac{\partial EA}{\partial s} = 2\theta \int_a^b s \mathrm{d}t \tag{6.27}$$

Appendix A

Bond Graph

A.1 Bond Graph

Bond Graph is a graphic tool that can be used to model and analyse any type of dynamic system. 'Bond' graph is named so because in this framework, the system is represented as a set of bonds representing the various elements in the system. Bond graph models work on the law of conservation of energy. This can be of great advantage for modelling multi-domain systems. However, as the dynamics of the system need to be studied, the rate of change of energy i.e. power is used to model the system.

In the bond graph framework, energy is measured as a product of a physical phenomenon bringing about a change in the system called generalised *effort* (e) and the total observed change called generalised *displacement* (Q). Similarly, power is defined as a product of a physical phenomenon bringing about a change in the system called generalised *effort* (e) and the rate of observed change called generalised *flow* (f). The effort and flow entities in various physical domains is shown in Table A.1.

In bond graph framework the different inputs and system elements interact with each other through two types of junctions i.e. $1-$junction or $0-$junction while also maintaining the causal relationship. The causal relationship is indicated by a causal stroke. The causal stroke represents the direction of flow of information about the *effort*. Hence, the direction without the causal stroke represents the direction of flow of information about the *flow*. The direction of power flow is indicated by a half arrow on the bond representing interaction between system and element. The general structure of a bond is shown in fig A.1.

A.1.1 Junctions

As discussed previously the different elements of the system interact with each other through junctions. In bond graph there are two types of junctions i.e. $1-$junction and $0-$junction. Each of the junction represent a specific physical condition that is being

Table A.1: Effort and Flow in various domains.

Domain	Effort	flow
Mechanical	Force	Velocity
	Torque	Angular Velocity
Electrical	Voltage	Current
Hydraulic	Pressure	Volume flow rate
Thermal	Temperature	Entropy change rate
	Pressure	Volume change rate
Chemical	Chemical potential	Mass flow rate
	Enthalpy	Mass flow rate
Magnetic	Magnetic-motive force	Magnetic flux rate

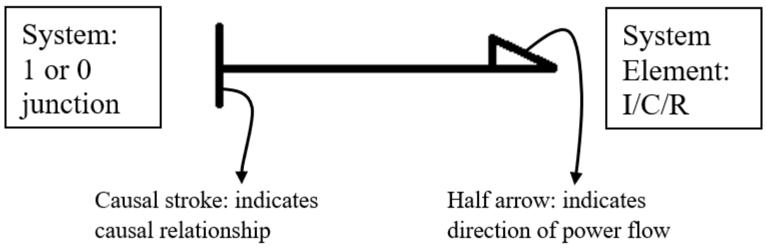

Figure A.1: General structure of a bond.

imposed on the interacting elements. It must also be noted that the power at a junction is conserved irrespective of it's type.

A.1.1.1 1-junction

A 1−junction represents an equality of generalised flow among the elements i.e. all the bonds the join at a 1−junction have same flow associated with them. Therefore, the following can be inferred:

- The flow in the n bonds attached to the junction is the same i.e.

$$f_1 = f_2 = f_3 ... = f_n \tag{A.1}$$

- As the power at the junction is conserved:

$$e_1 f_1 + e_2 f_2 + e_3 f_3 ... + e_n f_n = 0$$

  as the flow in all bonds are equal therefore,

$$e_1 + e_2 + e_3 ... + e_n = 0 \tag{A.2}$$

  It can be concluded that 1−junction is also an effort sum junction.

- As the flow is same in the bonds there should be only one source of flow information. Therefore the causal stroke of all but one bonds is directed towards the 1−junction.

A physical condition representing 1-junction is electrical components attached in series. In this case the generalised flow i.e. current is same in all the elements.

A.1.1.2 0-junction

A 0−junction represents an equality of generalised effort among the elements i.e. all the bonds the join at a 0−junction have same flow associated with them. Therefore, the following can be inferred:

- The effort in the n bonds attached to the junction is the same i.e.

$$e_1 = e_2 = e_3 ... = e_n \tag{A.3}$$

- As the power at the junction is conserved:

$$e_1 f_1 + e_2 f_2 + e_3 f_3 ... + e_n f_n = 0$$

as the effort in all bonds are equal therefore,

$$f_1 + f_2 + f_3 ... + f_n = 0 \tag{A.4}$$

It can be concluded that $0-$junction is also a flow sum junction.

- As the effort is same in the bonds there should be only one source of effort information. Therefore the causal stroke of only one bonds should directed towards the $1-$junction.

A physical condition representing 1-junction is electrical components attached in parallel. In this case the generalised effort i.e. voltage across the elements is same in all the elements.

A.1.2 Elements

Elements in the bond graph represents the various components. Just like power in bond graph framework is defined as a product of generalised flow and effort irrespective of the physical domain, the elements that interact in the bod graph framework are also limited depending on the type of behaviour irrespective of the physical domain. The mathematical relationship that governs the behaviour an element is called it's Constitutive Law (CL). The elements in bond graph can be categorised into two categories i.e. single port elements and two port element. Single port elements can be either active or passive.

A.1.2.1 Active single port elements

'Active' single port elements are those which bring the energy into the system. They are also called 'Source' elements. They represent the energy sources like battery or actuators like motors. Source elements are of two types

1. Source of Flow (SF): As the name suggests they convey information of flow to any part of the system. No effort information is exchanged. Hence, the CL for SF is

$$f(t) = SF \tag{A.5}$$

$$e = 0 \tag{A.6}$$

2. Source of Effort (SE): Corresponding to SF, they convey information of effort to any part of the system. No flow information is exchanged. Hence, the CL for SE is

$$e(t) = SE \tag{A.7}$$

$$f = 0 \tag{A.8}$$

A.1.2.2 Passive single port elements

'Passive' elements are those which do not generate energy. So, they are the elements of the system which enable the system to function by interacting with the energy provided to the system in a set pattern. Passive elements are of three types i.e.

1. Compliance element (C): A compliance element is one which takes flow information as input from the system, to return effort to the system, when the element is in integral causality. The compliance element stores generalised potential energy.

   Therefore when the element is in integral causality, the CL is given by:

   $$e = C \int f dt \tag{A.9}$$

   and for a compliance element in differential causality, the CL is given by:

   $$f = \frac{1}{C}\frac{\mathrm{d}e}{\mathrm{d}t} \tag{A.10}$$

2. Inertia element (I): An inertia element is one which takes effort information as input from the system, to return flow to the system, when the element is in integral causality. The inertia element stores generalised kinetic energy.

   Therefore when the element is in integral causality, the CL is given by:

   $$f = \frac{1}{I}\int e dt \tag{A.11}$$

   and for a compliance element in differential causality, the CL is given by:

   $$e = I\frac{\mathrm{d}f}{\mathrm{d}t} \tag{A.12}$$

3. Resistance element (R): Unlike compliance and inertia elements, the resistance element can only dissipate the energy instead of storing it in any form. Therefore, the CL for resistance element is fundamentally different form compliance and inertia i.e. CL for resistance in algebraic in nature instead of differential/integral. The CL for resistance element is given as:

   $$e = R.f \text{ or } f = \frac{1}{R}e \tag{A.13}$$

   when the input to the resistance element is generalised flow, the element is said to be in resistive causality. Similarly when the input to the element is generalised effort, then the element is said to be in conductive causality.

I, C and R can be constants, linear or non-linear functions. For modelling of multi-physical energy interactions, I, C and R can be square matrix instead of simple functions.

A.1.3 Two port passive elements

Two port elements are different from the previously mentioned single port passive elements (SE, SF, I, C, R) because unlike the others they interact with the system through two ports i.e. they are not connected to system through one port but two ports. Therefore, they can physically interact with two different points in the system. Also unlike single port passive elements, the constitutive relationship for these is not affected by causality change.

Energy flows into the transforming element with a particular combination of generalised effort and flow, the energy leaves the element with a different combination. Therefore, they transform the distribution of generalised effort and flow from one part of the system to another.

1. Transformer element (TF): The transformer element is used when the similar energy variables (effort or flow) at both the ends of the element are governed by a physical element. In other words, if the generalised flow at the both ends are governed by a physical component, a transformer element is used. For eg, in linear mechanical systems, a lever governs the velocity transformation from one end to the other. So, a transformer element is used.

   The transformer is defined using a modulus. The modulus is defined as the ratio of the generalised flow at energy exit to the generalised flow at energy inlet. The flow equations for a transformer with modulus a, is given as:

   $$f_2 = a.f_1 \tag{A.14}$$

   where f_1 and f_2 are the generalise flow at the energy inlet point and energy outlet point of the transformer.

   As the total energy is conserved by the transformer, the relation between generalised efforts is given as

   $$e_2 = \frac{1}{a} e_1 \tag{A.15}$$

   where e_1 and e_2 are the generalise effort at the energy inlet point and energy outlet point of the transformer.

2. Gyrator element (GY): The gyrator element is used when the dissimilar energy variables (effort or flow) at both the ends of the element are governed by a physical element. In other words, if the generalised effort at one end is governed by generalised flow at the other end by a physical component, a transformer element is used. For eg, in a simple DC motor, the current (flow variable) in the coil governs the torque (effort variable) in the shaft through some motor parameter.

   The gyrator is usually using a modulus. The gyrator modulus is defined as the ratio of the generalised flow at energy exit to the generalised effort at energy inlet. The governing equations for a gyrator with modulus μ, is given as:

   $$e_2 = \mu.f_1 \tag{A.16}$$

   where f_1 and e_2 are the generalise flow at the energy inlet point and generalised effort outlet point of the gyrator respectively.

(a) I element in Integral causality. (b) I element in Differential causality.

Figure A.2: Comparison of integral and differential causality..

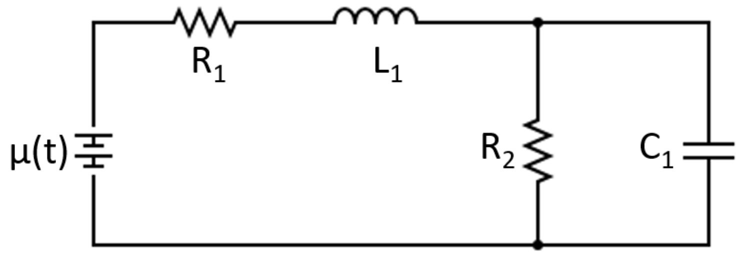

Figure A.3: Circuit diagram

As the total energy is conserved by gyrator, the relation between the remaining energy variables associated with gyrator is given as

$$f_2 = \frac{1}{\mu} e_1 \tag{A.17}$$

where e_1 and f_2 are the generalise effort at the energy inlet point and generalised flow outlet point of the gyrator respectively.

A.1.4 Causality

It has already been discussed that bond graph is used as a tool for modeling dynamic systems. In bond graph modeling, there are two type of energy storing elements that are responsible for the dynamic behavior of the system i.e. I and C element.

The system equations which represent the dynamic behavior of the system can be captured by generating the system equations either in the differential form or in the integral form. The form used for calculating the dynamics is represented using the causal stroke shown in fig A.1. The causal stroke in the bond represents the flow of effort information. For example, consider the two types of information transfer in an inertial element shown in fig A.2. For arrangement in fig A.2a, the element receives effort from the system as input and returns flow as output to the system. Hence, for an effort input and flow output in the I-element, the constitutive relationship is given by eq A.11. As this is in integral form, the energy exchange arrangement shown in fig A.2a shows the I element in integral causality. Similarly, the information exchange for I element with the constitutive relationship in in form shown by eq A.12 is represented by fig A.2b.

A.1.5 Example

A bond graph model can be understood using the following example. Figure A.3 gives an example of electrical system which needs to be modelled. The bond graph of the model is shown in fig A.4.

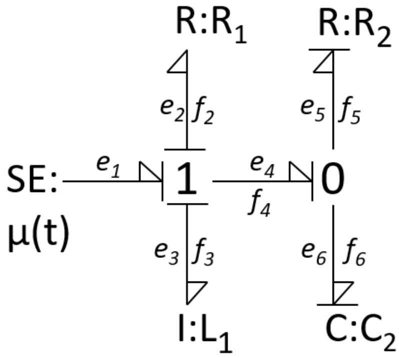

Figure A.4: Bond Graph of the electrical system

The structural relationship at the junctions i.e. equations representing the structural relation between various elements are given as:

$$1 - junction \begin{cases} e_1 - e_2 - e_3 - e_4 = 0 \\ f_2 = f_3 = f_4 \end{cases}$$
$$0 - junction \begin{cases} f_4 - f_5 - f_6 = 0 \\ e_4 = e_5 = e_6 \end{cases}$$

These equations indicate that the element R_1 and I_1 are joined on a 1 junction. This means that they have the same generalised flow, i.e. current. This is true as these elements are connected in series arrangement.

Another sub-circuit, consisting of elements R_2 and C_2 is connected in series with R_1 and I_1. The elements of sub-circuit itself are arranged in parallel arrangement. As a parallel arrangement of components indicates equal applied voltage (i.e. generalised effort), these elements are joined using a 0 junction.

The constitutive relationships i.e. the equations governing the interaction of components with the system, as represented by the bond graph are given as:

$$R_1 : e_2 = R_1 f_2$$
$$R_2 : f_2 = \frac{1}{R_1} e_5$$
$$L_1 : e_3 = L_1 \frac{\mathrm{d} f_3}{\mathrm{d} t}$$
$$C_1 : f_5 = C_1 \frac{\mathrm{d} e_5}{\mathrm{d} t}$$

The above set of equations have all the necessary information to analyse the circuit.

A.2 Modelling uncertainty in Bond Graph elements

Uncertainty in any system component θ can be modelled as either an additive uncertainty or a multiplicative uncertainty.

$$\begin{aligned} \theta &= \theta_n \pm \Delta\theta \\ \theta &= \theta_n (1 + \delta_\theta) \end{aligned} \tag{A.18}$$

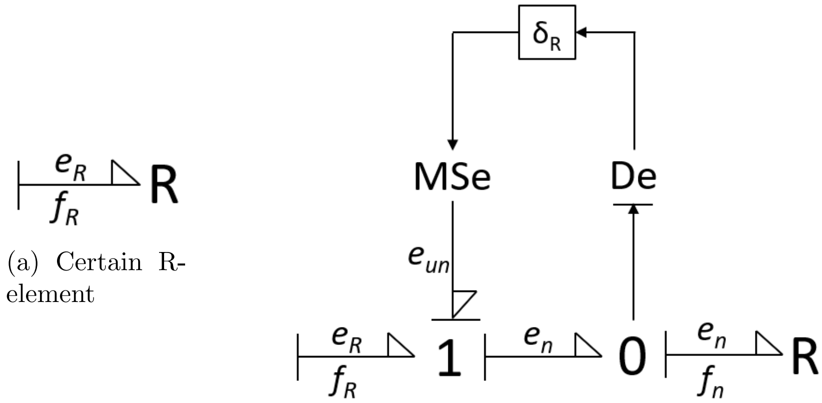

(a) Certain R-element

(b) Uncertain R-element

Figure A.5: Uncertainty modelling of an R-element in resistive causality.

where θ_n is the nominal value of the parameter, $\Delta\theta$ is the additive uncertainty and δ_θ is the multiplicative uncertainty.

Uncertainty in elements can be included in the bond graph models. Multiplicative uncertainty is included by using virtual sensor and a modulated source.

Considering an uncertain R-element, if the element is in resistive causality, the constitutive relationship is given as follows.

$$\begin{aligned}
e_R &= R f_R \\
e_R &= R_n(1+\delta_R) f_R \\
e_R &= R_n f + \delta_R R_n f_R = e_n + e_{un}
\end{aligned} \tag{A.19}$$

where e_n and e_{un} are the nominal and uncertain components of the generalised effort.

The constitutive relationship in eq A.19 can be represented on the bond graph using a modulated source MSe and virtual effort sensor De as shown in fig A.5

Similarly, for an uncertain R-element in conductive causality, the constitutive relationship and corresponding bond graph implementation is given by eq A.20 and fig A.6 respectively.

$$\begin{aligned}
f_R &= \frac{1}{R} e_R \\
f_R &= \frac{1}{R_n}(1+\delta_{1/R}) e_R \\
f_R &= \frac{e_R}{R_n} + \frac{\delta_{1/R} e_R}{R_n} = f_n + f_{un}
\end{aligned} \tag{A.20}$$

A.3 Fault detection using Analytical Redundancy Relations in Bond Graphs

The operational safety of a system is based on fault detection and isolation (FDI) process. FDI consists of the comparison of the actual behaviour of the system with reference.

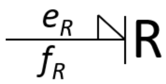

(a) Certain R-element

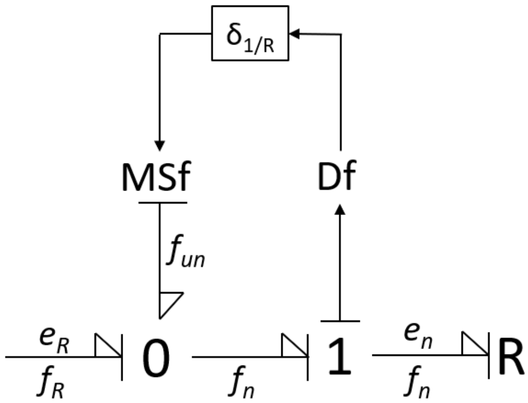

(b) Uncertain R-element

Figure A.6: Uncertainty modelling of an R-element in conductive causality.

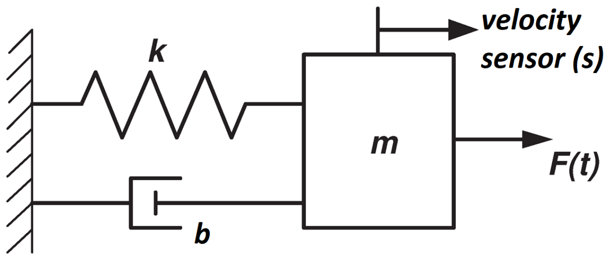

Figure A.7: Spring Mass Damper System.

Different approaches for the FDI procedures have been developed, depending on the kind of knowledge used to describe the system model. Structural monitorability analysis is based on fault signatures deduced from Analytical Redundancy Relations (ARRs)

ARRs are generated when the system is in the preferred differential causality. The structural relationship, constitutive relationship and the measured values are used to generate the ARRs directly from the bond graph model. The number of ARRs is equal to the number of sensors placed on the system.

The measurements from a system using a sensor are used by *dualising* the sensors in preferred differential causality. This means that a sensor in a bond graph model with preferred integral causality becomes a simulated source in a bond graph model with preferred differential causality. Therefore, the measured quantity is imposed on the system model in differential causality.

The above can be understood using a simple example of a spring mass damper system. For a spring mass damper system shown in fig A.7, the system bond graph model in preferred integral causality is shown in fig A.8 and system bond graph model in preferred differential causality is shown in A.9. It can be observed that the sensor (Df) for flow measurement in preferred integral causality is dualised to become a simulated source of flow (SSf) in preferred differential causality. Therefore, the flow that is measured in the real system can be imposed to perform FDI.

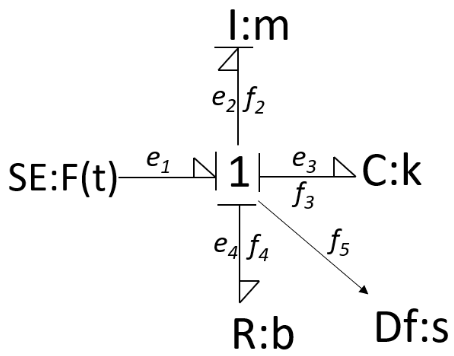

Figure A.8: Bond Graph of Spring Mass Damper System in integral causality.

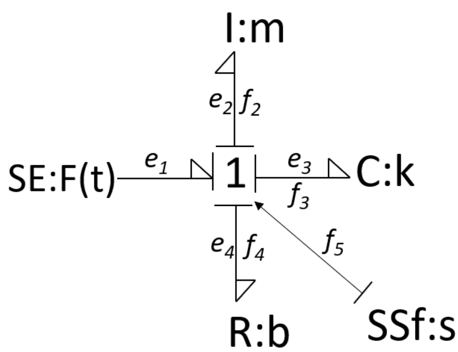

Figure A.9: Bond Graph of Spring Mass Damper System in differential causality.

A.3.1 ARR generation in bond graph

In order to perform FDI, ARRs are generated using the model in preferred differential causality. ARRs are derived using the structural relationship of the bond graph model. For the above example, the structural relationship is given as shown below.

$$e_1 - e_2 - e_3 - e_4 = 0 \tag{A.21}$$

All the generalised efforts in the structural relationship A.21 are not known but can be calculated using the constitutive relationship of the elements. For the given system, the constitutive relationships are given as follows.

$$\begin{aligned} e_1 &= F(t) \\ e_2 &= \frac{1}{m}\frac{\mathrm{d}f_2}{\mathrm{dt}} \\ e_3 &= k\int f_3 dt \\ e_4 &= bf_4 \end{aligned} \tag{A.22}$$

Substituting eq A.22 in eq A.21, the structural relationship can be expressed as follows.

$$F(t) - \frac{1}{m}\frac{\mathrm{d}f_2}{\mathrm{dt}} - k\int f_3 dt - bf_4 = 0 \tag{A.23}$$

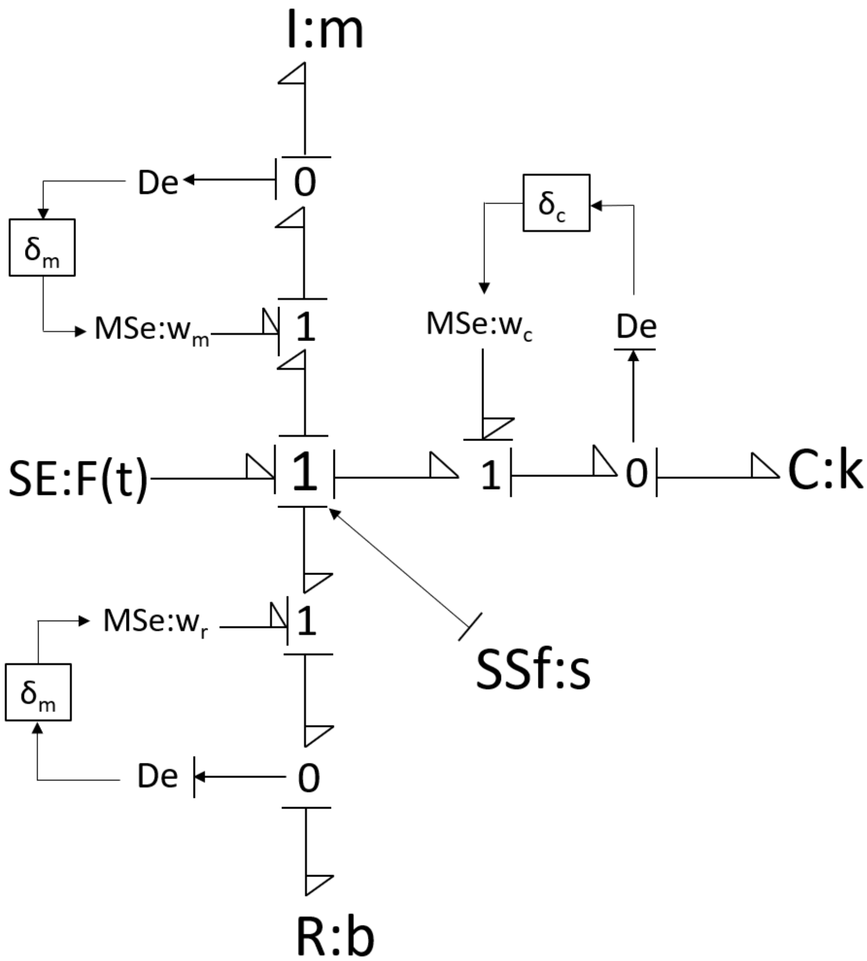

Figure A.10: Bond graph model for robust fault detection.

Finally, all the measured quantities are included to get the final ARR. In the current model the flow in the model is imposed by the measured quantity. The final ARR is obtained as follows.

$$ARR = F(t) - \frac{1}{m}\frac{\mathrm{d}s}{\mathrm{dt}} - k\int sdt - bs = 0 \tag{A.24}$$

The ARR is solved continuously to perform FDI. A non-zero value of the ARR indicated the presence of a fault.

A.3.2 Generation of robust ARR

In order to generate robust ARRs uncertainties are also modelled in the bond graph model in preferred differential causality. The bond graph model for spring mass damper system for robust fault detection is given in fig A.10.

The ARR is then generated for the model.

$$ARR = F(t) - \left(\frac{1}{m}\frac{\mathrm{d}s}{\mathrm{dt}} + w_m\right) - \left(k\int sdt + w_k\right) - (bs + w_r) = 0 \tag{A.25}$$

As the uncertain components (w_m, w_k, w_r) are know within a range and can be either positive or negative, the above equation can be rearranged as follows.

$$ARR = F(t) - \frac{1}{m}\frac{\mathrm{d}s}{\mathrm{dt}} - k\int sdt - bs \leq |w_m + w_k + w_r| \tag{A.26}$$

Appendix B

Interval Arithmetic

B.1 Interval Arithmetic

Interval arithmetic is a technique that is used to put bounds on errors in any mathematical calculation. Numerical methods that use interval arithmetic offer reliable, and mathematically correct results. In interval arithmetic, instead of representing a value as a single number, the value is recognised as a range of possibilities.

For example, manufacturing processes are always have some error associated with them. A metal component can never be manufactured for any exact dimension. Therefore, the manufacturing drawings always mention a range of tolerated dimensions.

This section introduces the basics of interval arithmetic. The details of interval arithmetic can be found in [30].

As already discussed, in interval arithmetic, values are represented as an interval. Interval is defined as set of real numbers $x|x_m \leq x \leq x_M$. Here, x_m is the minimum possible value of x, called the infinum. Also, x_M is the maximum possible value of x called the supernum.

The interval x is denoted as:

$$x = [x_m, x_M] \tag{B.1}$$

The basic properties of an interval $[x_m, x_M]$ are as follows:

- for any interval
$$x_m \leq x \leq x_M$$
- The midpoint of an interval is given as:
$$mid(x) = \frac{1}{2}(x_m + x_M)$$
- width of interval is given as:
$$width(x) = x_M - x_m$$

For any two intervals $[x_m, x_M]$ and $[y_m, y_M]$:

- Addition: $x + y = [x_m + y_m, x_M + y_M]$
- Subtraction: $x - y = [x_m - y_M, x_M - y_m]$
- Multiplication: $x \times y = [min(A), max(A)],\ where\ A = [x_m \times y_m, x_m \times y_M, x_M \times y_m, x_M \times y_M]$
- Division: $\frac{1}{x} = [\frac{1}{x_M}, \frac{1}{x_m}]$

- Calculus operations like differentiation and integration can be performed using the above basic principles.

Interval extension functions are functions whose value result is given by an interval range rather than an exact value.

Natural interval extension of an function is achieved by replacing the real values in the function by their corresponding intervals.

Rational interval function is an interval-valued function whose values are defined by a specific finite sequence of interval arithmetic operations.

B.2 Precautions while using interval arithmetic

With careful analysis of interval arithmetic, the following are observed:

- Arithmetic inverse does not hold.

$$\begin{aligned} &addition \neq substraction^{-1} \\ &division \neq multiplication^{-1} \end{aligned}$$

- Another point of concern with natural extension of functions. These extensions are dependent on the form of the function used.

  For e.g. considering the natural extension of $f(x) = x(x+1)$ for $x = [-1, 1]$

$$\begin{aligned} \text{if } f(x) &= x(x+1); [f] = [-2, 2] \\ f(x) &= xx + x; [f] = [-2, 2] \\ f(x) &= x^2 + x; [f] = [-1, 2] \end{aligned}$$

B.3 Interval extension functions in bond graph

As the interval extension of functions are used incorporate the modelling uncertainties, therefore the constitutive relationship of various elements can be modelled using natural interval extension to accommodate the system parameter uncertainties. The process is very similar to that explained in section A.2.

Considering an uncertain R-element in resistive causality. The constitutive relationship for the element is given by eq B.2, where e is the generalise effort, f is the generalised flow and R is the numeric component value of the element.

$$e = Rf \tag{B.2}$$

The natural interval extension of the above can be derived as shown in eq B.3.

$$\begin{aligned} [e_{Rm}, e_{RM}] &= [R_m, R_M][f_{Rm}, f_{RM}] \\ [e_{Rm}, e_{RM}] &= R_n(1 + [\delta_{Rm}, \delta_{RM}])[f_{Rm}, f_{RM}] \\ [e_{Rm}, e_{RM}] &= [R_n, R_n][f_{Rm}, f_{RM}] + [\delta_{Rm}, \delta_{RM}]R_n[f_{Rm}, f_{RM}] \\ [e_{Rm}, e_{RM}] &= e_n + e_{un} \end{aligned} \tag{B.3}$$

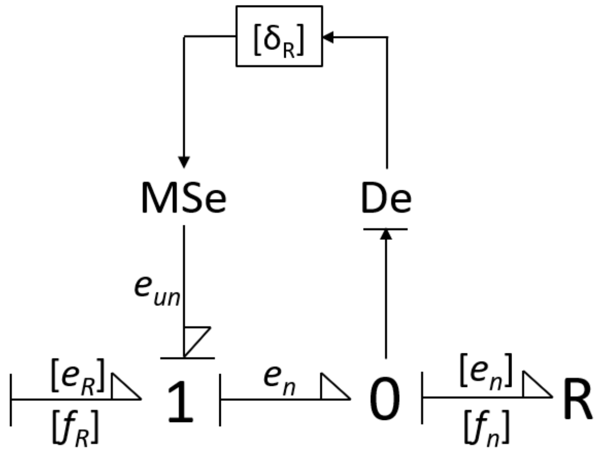

(a) Resistive R-element in interval form.

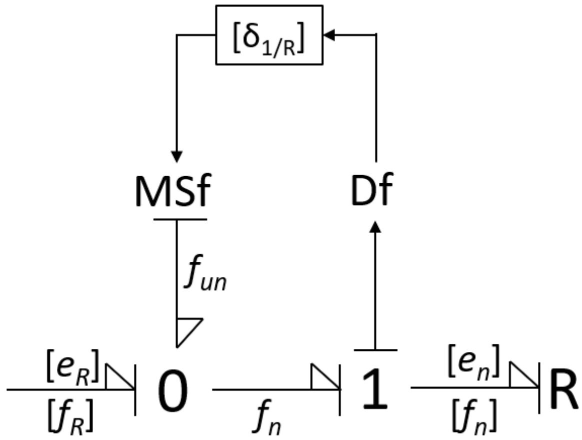

(b) Conductive R-element in interval form.

Figure B.1: Uncertainty modelling of an R-element in interval form.

Similarly, the natural interval extension of R-element in conductive causality can be derived as shown in eq B.4.

$$
\begin{aligned}
&[f_{Rm}, f_{RM}] = \frac{1}{[R_m, R_M]}[e_{Rm}, e_{RM}], \\
&[f_{Rm}, f_{RM}] = \frac{1}{R_n}(1 + [\delta_{(1/R)m}, \delta_{(1/R)M}])[e_{Rm}, e_{RM}] \\
&[f_{Rm}, f_{RM}] = \frac{[e_{Rm}, e_{RM}]}{R_n} + \frac{[\delta_{(1/R)m}, \delta_{(1/R)M}][e_{Rm}, e_{RM}]}{R_n} = f_n + f_{un}
\end{aligned}
\tag{B.4}
$$

The bond graph implementation of interval extension of R-elements in resistive and conductive causality are given in fig B.1a and fig B.1b respectively.

Bibliography

[1] Olivier Adrot, Didier Maquin, and José Ragot. “Fault detection with model parameter structured uncertainties”. In: *1999 European Control Conference (ECC)*. IEEE. 1999, pp. 475–480.

[2] Smail Bachir et al. “Diagnosis by parameter estimation of stator and rotor faults occurring in induction machines”. In: *IEEE Transactions on Industrial Electronics* 53.3 (2006), pp. 963–973.

[3] Gregory Bartram and Sankaran Mahadevan. “Prognostics and health monitoring in the presence of heterogeneous information”. In: *Proc. Annual. Conference. Prognostic. Health Management Society*. Vol. 3. 126. 2012.

[4] Andrew Bennett et al. *Lagrangian fluid dynamics*. Cambridge University Press, 2006.

[5] Tatiana Biagetti and Enrico Sciubba. “Automatic diagnostics and prognostics of energy conversion processes via knowledge-based systems”. In: *Energy* 29.12-15 (2004), pp. 2553–2572.

[6] B Ould Bouamama et al. “Derivation of constraint relations from bond graph models for fault detection and isolation”. In: *Simulation Series* 35.2 (2003), pp. 104–109.

[7] B Ould Bouamama et al. “Graphical methods for diagnosis of dynamic systems”. In: *Annual reviews in control* 38.2 (2014), pp. 199–219.

[8] Omar Bougacha, Christophe Varnier, and Noureddine Zerhouni. “Enhancing Decisions in Prognostics and Health Management Framework”. In: *International Journal of prognostics and health management* 11.7 (2020).

[9] Mathieu Bressel et al. “Extended Kalman filter for prognostic of proton exchange membrane fuel cell”. In: *Applied Energy* 164 (2016), pp. 220–227.

[10] Carl S Byington, Matthew Watson, and Doug Edwards. “Data-driven neural network methodology to remaining life predictions for aircraft actuator components”. In: *2004 IEEE Aerospace Conference Proceedings (IEEE Cat. No. 04TH8720)*. Vol. 6. IEEE. 2004, pp. 3581–3589.

[11] Steven G Chalk and James F Miller. “Key challenges and recent progress in batteries, fuel cells, and hydrogen storage for clean energy systems”. In: *Journal of Power Sources* 159.1 (2006), pp. 73–80.

[12] David Chelidze, Joseph P Cusumano, and Anindya Chatterjee. “A dynamical systems approach to damage evolution tracking, part 1: description and experimental application”. In: *J. Vib. Acoust.* 124.2 (2002), pp. 250–257.

[13] Chaochao Chen, George Vachtsevanos, and Marcos E Orchard. “Machine remaining useful life prediction: An integrated adaptive neuro-fuzzy and high-order particle filtering approach”. In: *Mechanical Systems and Signal Processing* 28 (2012), pp. 597–607.

[14] Chaochao Chen et al. “An integrated architecture for fault diagnosis and failure prognosis of complex engineering systems”. In: *Expert Systems with Applications* 39.10 (2012), pp. 9031–9040.

[15] Chaochao Chen et al. “Machine condition prediction based on adaptive neuro–fuzzy and high-order particle filtering”. In: *IEEE Transactions on Industrial Electronics* 58.9 (2010), pp. 4353–4364.

[16] ChunPing Chen et al. "Application of Fault Diagnosis Expert System for Unmanned Vehicle Safety". In: *IOP Conference Series: Materials Science and Engineering*. Vol. 608. 1. IOP Publishing. 2019, p. 012015.

[17] Huicui Chen, Pucheng Pei, and Mancun Song. "Lifetime prediction and the economic lifetime of proton exchange membrane fuel cells". In: *Applied Energy* 142 (2015), pp. 154–163.

[18] Jie Chen and Ron J Patton. *Robust model-based fault diagnosis for dynamic systems*. Vol. 3. Springer Science & Business Media, 2012.

[19] Jie Chen et al. "Failure prognosis of multiple uncertainty system based on Kalman filter and its application to aircraft fuel system". In: *Advances in Mechanical Engineering* 8.10 (2016), p. 1687814016671445.

[20] W Chen et al. "Energy based fault detection for dissipative systems". In: *2010 Conference on Control and Fault-Tolerant Systems (SysTol)*. IEEE. 2010, pp. 517–521.

[21] Xuefeng Chen et al. "Remaining life prognostics of rolling bearing based on relative features and multivariable support vector machine". In: *Proceedings of the Institution of Mechanical Engineers, Part C: Journal of Mechanical Engineering Science* 227.12 (2013), pp. 2849–2860.

[22] Zaigang Chen and Yimin Shao. "Dynamic simulation of spur gear with tooth root crack propagating along tooth width and crack depth". In: *Engineering failure analysis* 18.8 (2011), pp. 2149–2164.

[23] Tai-Yih Chiu. "Model reduction by the low-frequency approximation balancing method for unstable systems". In: *IEEE transactions on Automatic Control* 41.7 (1996), pp. 995–997.

[24] Luciana Balieiro Cosme et al. "A novel fault-prognostic approach based on interacting multiple model filters and fuzzy systems". In: *IEEE Transactions on Industrial Electronics* 66.1 (2018), pp. 519–528.

[25] Helen Cui. "Accelerated temperature cycle test and Coffin-Manson model for electronic packaging". In: *Annual Reliability and Maintainability Symposium, 2005. Proceedings.* IEEE. 2005, pp. 556–560.

[26] Lingli Cui et al. "A novel switching unscented Kalman filter method for remaining useful life prediction of rolling bearing". In: *Measurement* 135 (2019), pp. 678–684.

[27] Joseph P Cusumano, David Chelidze, and Anindya Chatterjee. "A dynamical systems approach to damage evolution tracking, part 2: Model-based validation and physical interpretation". In: *J. Vib. Acoust.* 124.2 (2002), pp. 258–264.

[28] Najmeh Daroogheh, Nader Meskin, and Khashayar Khorasani. "A novel particle filter parameter prediction scheme for failure prognosis". In: *2014 American Control Conference*. IEEE. 2014, pp. 1735–1742.

[29] Liu Datong, Peng Yu, and Peng Xiyuan. "Fault prediction based on time series with online combined kernel SVR methods". In: *2009 IEEE Instrumentation and Measurement Technology Conference*. IEEE. 2009, pp. 1163–1166.

[30] Hend Dawood. *Theories of interval arithmetic: mathematical foundations and applications*. LAP Lambert Academic Publishing, 2011.

[31] Bhupinder S Dayal and John F MacGregor. "Recursive exponentially weighted PLS and its applications to adaptive control and prediction". In: *Journal of Process control* 7.3 (1997), pp. 169–179.

[32] Xiao-Wen Deng et al. “Rule-based Fault Diagnosis Expert System for Wind Turbine”. In: *ITM Web of Conferences*. Vol. 11. EDP Sciences. 2017, p. 07005.

[33] Mohand Arab Djeziri et al. “Robust fault diagnosis by using bond graph approach”. In: *IEEE/ASME Transactions on Mechatronics* 12.6 (2007), pp. 599–611.

[34] Phuc Do et al. “A proactive condition-based maintenance strategy with both perfect and imperfect maintenance actions”. In: *Reliability Engineering & System Safety* 133 (2015), pp. 22–32.

[35] Ming Dong and David He. “Hidden semi-Markov model-based methodology for multi-sensor equipment health diagnosis and prognosis”. In: *European Journal of Operational Research* 178.3 (2007), pp. 858–878.

[36] Shichang Du, Jun Lv, and Lifeng Xi. “Degradation process prediction for rotational machinery based on hybrid intelligent model”. In: *Robotics and Computer-Integrated Manufacturing* 28.2 (2012), pp. 190–207.

[37] Bashir Mahdi Ebrahimi and Jawad Faiz. “Feature extraction for short-circuit fault detection in permanent-magnet synchronous motors using stator-current monitoring”. In: *IEEE Transactions on Power Electronics* 25.10 (2010), pp. 2673–2682.

[38] Thushara Ekanayake et al. “Model-based fault diagnosis and prognosis of dynamic systems: a review”. In: *Procedia Manufacturing* 30 (2019), pp. 435–442.

[39] Daniel Foito et al. “An Eigenvalue/Eigenvector 3D current reference method for detection and fault diagnosis in a voltage source inverter”. In: *2009 35th Annual Conference of IEEE Industrial Electronics*. IEEE. 2009, pp. 190–194.

[40] Royce G Forman, VE Kearney, and RM Engle. “Numerical analysis of crack propagation in cyclic-loaded structures”. In: (1967).

[41] Paul M Frank and Xianchun Ding. “Survey of robust residual generation and evaluation methods in observer-based fault detection systems”. In: *Journal of process control* 7.6 (1997), pp. 403–424.

[42] Michael L Fugate, Hoon Sohn, and Charles R Farrar. “Vibration-based damage detection using statistical process control”. In: *Mechanical Systems and Signal Processing* 15.4 (2001), pp. 707–721.

[43] Nagi Gebraeel et al. “Residual life predictions from vibration-based degradation signals: a neural network approach”. In: *IEEE Transactions on industrial electronics* 51.3 (2004), pp. 694–700.

[44] Nagi Z Gebraeel et al. “Residual-life distributions from component degradation signals: A Bayesian approach”. In: *IiE Transactions* 37.6 (2005), pp. 543–557.

[45] Cristian Ghiaus. “Fault diagnosis of air conditioning systems based on qualitative bond graph”. In: *Energy and buildings* 30.3 (1999), pp. 221–232.

[46] Kai Goebel and Neil Eklund. “Prognostic fusion for uncertainty reduction”. In: *AIAA Infotech@ Aerospace 2007 Conference and Exhibit*. 2007, p. 2843.

[47] Kai Goebel, Neil Eklund, and Pierino Bonanni. “Fusing competing prediction algorithms for prognostics”. In: *2006 IEEE Aerospace Conference*. IEEE. 2006, 10–pp.

[48] Felix O Heimes. “Recurrent neural networks for remaining useful life estimation”. In: *2008 international conference on prognostics and health management*. IEEE. 2008, pp. 1–6.

[49] Timothy Hickey, Qun Ju, and Maarten H Van Emden. "Interval arithmetic: From principles to implementation". In: *Journal of the ACM (JACM)* 48.5 (2001), pp. 1038–1068.

[50] Ding Hong, Gui Xiuwen, and Yang Shuzi. "An approach to state recognition and knowledge-based diagnosis for engines". In: *Mechanical Systems and Signal Processing* 5.4 (1991), pp. 257–266.

[51] Sheng Hong and Zheng Zhou. "Application of gaussian process regression for bearing degradation assessment". In: *2012 6th International Conference on New Trends in Information Science, Service Science and Data Mining (ISSDM2012)*. IEEE. 2012, pp. 644–648.

[52] Sheng Hong and Zheng Zhou. "Remaining useful life prognosis of bearing based on Gauss process regression". In: *2012 5th International Conference on BioMedical Engineering and Informatics*. IEEE. 2012, pp. 1575–1579.

[53] Xiheng Hu. "FF-Padé method of model reduction in frequency domain". In: *IEEE transactions on automatic control* 32.3 (1987), pp. 243–246.

[54] Runqing Huang et al. "Residual life predictions for ball bearings based on self-organizing map and back propagation neural network methods". In: *Mechanical systems and signal processing* 21.1 (2007), pp. 193–207.

[55] P Irving, O Eker, and F Camci. "Prognostics control of cracking in structures and components operating in hydrogen environments". In: *Proc. Int. Hydrogen Conf.* 2012.

[56] Rolf Isermann. "Process fault detection based on modeling and estimation methods—A survey". In: *automatica* 20.4 (1984), pp. 387–404.

[57] Amin Torabi Jahromi et al. "Sequential fuzzy clustering based dynamic fuzzy neural network for fault diagnosis and prognosis". In: *Neurocomputing* 196 (2016), pp. 31–41.

[58] Kshitij Jerath, Sean Brennan, and Constantino Lagoa. "Bridging the gap between sensor noise modeling and sensor characterization". In: *Measurement* 116 (2018), pp. 350–366.

[59] Mayank Shekhar Jha. "Diagnostics and Prognostics of Uncertain Dynamical Systems in a Bond Graph Framework". PhD thesis. 2015.

[60] Mayank Shekhar Jha, Geneviève Dauphin-Tanguy, and B Ould Bouamama. "Robust FDI based on LFT BG and relative activity at junction". In: *2014 European Control Conference (ECC)*. IEEE. 2014, pp. 938–943.

[61] Yuanyuan Jiang et al. "Fault prognostic of electronics based on optimal multi-order particle filter". In: *Microelectronics Reliability* 62 (2016), pp. 167–177.

[62] Marine Jouin et al. "Estimating the end-of-life of PEM fuel cells: Guidelines and metrics". In: *Applied energy* 177 (2016), pp. 87–97.

[63] Mojtaba Kordestani et al. "A modular fault diagnosis and prognosis method for hydro-control valve system based on redundancy in multisensor data information". In: *IEEE Transactions on Reliability* 68.1 (2018), pp. 330–341.

[64] Mojtaba Kordestani et al. "Failure Prognosis and Applications—A Survey of Recent Literature". In: *IEEE transactions on reliability* (2019).

[65] Sachin Kumar, IV Singh, and BK Mishra. "A homogenized XFEM approach to simulate fatigue crack growth problems". In: *Computers & Structures* 150 (2015), pp. 1–22.

[66] Tze Leung Lai. "Sequential multiple hypothesis testing and efficient fault detection-isolation in stochastic systems". In: *IEEE Transactions on Information Theory* 46.2 (2000), pp. 595–608.

[67] Pradeep Lall, Ryan Lowe, and Kai Goebel. “Extended Kalman filter models and resistance spectroscopy for prognostication and health monitoring of leadfree electronics under vibration”. In: *IEEE Transactions on Reliability* 61.4 (2012), pp. 858–871.

[68] Yves Langeron, Antoine Grall, and Anne Barros. “A modeling framework for deteriorating control system and predictive maintenance of actuators”. In: *Reliability Engineering & System Safety* 140 (2015), pp. 22–36.

[69] David Leung and Jose Romagnoli. “Dynamic probabilistic model-based expert system for fault diagnosis”. In: *Computers & Chemical Engineering* 24.11 (2000), pp. 2473–2492.

[70] Bo Li et al. “Neural-network-based motor rolling bearing fault diagnosis”. In: *IEEE transactions on industrial electronics* 47.5 (2000), pp. 1060–1069.

[71] Gang Li et al. “Reconstruction based fault prognosis for continuous processes”. In: *Control Engineering Practice* 18.10 (2010), pp. 1211–1219.

[72] Linxia Liao and Felix Köttig. “Review of hybrid prognostics approaches for remaining useful life prediction of engineered systems, and an application to battery life prediction”. In: *IEEE Transactions on Reliability* 63.1 (2014), pp. 191–207.

[73] Chi Keong Reuben Lim and David Mba. “Switching Kalman filter for failure prognostic”. In: *Mechanical Systems and Signal Processing* 52 (2015), pp. 426–435.

[74] Chi Keong Reuben Lim and David Mba. “Switching Kalman filter for failure prognostic”. In: *Mechanical Systems and Signal Processing* 52-53 (2015), pp. 426–435. ISSN: 0888-3270.

[75] Xiao Lin et al. “Condition based spare parts supply”. In: *Reliability Engineering & System Safety* 168 (2017), pp. 240–248.

[76] Hongmei Liu, Lianfeng Li, and Jian Ma. “Rolling bearing fault diagnosis based on STFT-deep learning and sound signals”. In: *Shock and Vibration* 2016 (2016).

[77] J Liu et al. “A data-model-fusion prognostic framework for dynamic system state forecasting”. In: *Engineering Applications of Artificial Intelligence* 25.4 (2012), pp. 814–823.

[78] Qinming Liu et al. “Manufacturing system maintenance based on dynamic programming model with prognostics information”. In: *Journal of Intelligent Manufacturing* 30.3 (2019), pp. 1155–1173.

[79] Ruonan Liu, Boyuan Yang, and Alexander G Hauptmann. “Simultaneous Bearing Fault Recognition and Remaining Useful Life Prediction Using Joint-Loss Convolutional Neural Network”. In: *IEEE Transactions on Industrial Informatics* 16.1 (2019), pp. 87–96.

[80] Tongshun Liu, Kunpeng Zhu, and Liangcai Zeng. “Diagnosis and prognosis of degradation process via hidden semi-markov model”. In: *IEEE/ASME Transactions on Mechatronics* 23.3 (2018), pp. 1456–1466.

[81] Zhijuan Liu et al. “A hybrid LSSVR/HMM-based prognostic approach”. In: *Sensors* 13.5 (2013), pp. 5542–5560.

[82] Xinsheng Lou and Kenneth A Loparo. “Bearing fault diagnosis based on wavelet transform and fuzzy inference”. In: *Mechanical systems and signal processing* 18.5 (2004), pp. 1077–1095.

[83] Loucas S Louca. “A frequency-based interpretation of energy-based model reduction of linear systems”. In: *Journal of Dynamic Systems, Measurement, and Control* 138.12 (2016).

[84] Loucas S Louca, Jeffrey L Stein, and Gregory M Hulbert. “A physical-based model reduction metric with an application to vehicle dynamics”. In: *IFAC Proceedings Volumes* 31.17 (1998), pp. 585–590.

[85] Loucas S Louca, Jeffrey L Stein, and Gregory M Hulbert. "Energy-based model reduction methodology for automated modeling". In: *Journal of dynamic systems, measurement, and control* 132.6 (2010).

[86] Loucas S Louca and JL Stein. "Ideal physical element representation from reduced bond graphs". In: *Proceedings of the Institution of Mechanical Engineers, Part I: Journal of Systems and Control Engineering* 216.1 (2002), pp. 73–83.

[87] Jianhui Luo et al. "Model-based prognostic techniques [maintenance applications]". In: *Proceedings AUTOTESTCON 2003. IEEE Systems Readiness Technology Conference.* Ieee. 2003, pp. 330–340.

[88] Jianhui Luo et al. "Model-based prognostic techniques applied to a suspension system". In: *IEEE Transactions on Systems, Man, and Cybernetics-Part A: Systems and Humans* 38.5 (2008), pp. 1156–1168.

[89] Jie Ma, Gang Li, and Donghua Zhou. "Fault prognosis technology for non-Gaussian and nonlinear processes based on KICA reconstruction". In: *The Canadian Journal of Chemical Engineering* 96.2 (2018), pp. 515–520.

[90] Jie Ma et al. "Reconstruction-based fault prognosis for flue gas turbines with independent component analysis". In: *Asia-Pacific Journal of Chemical Engineering* 9.2 (2014), pp. 205–213.

[91] A Majidian and MH Saidi. "Comparison of fuzzy logic and neural network in life prediction of boiler tubes". In: *International Journal of Fatigue* 29.3 (2007), pp. 489–498.

[92] Henri-Jean Marais, George Van Schoor, and Kenneth R Uren. "Energy-based fault detection for an autothermal reformer". In: *IFAC-PapersOnLine* 49.7 (2016), pp. 353–358.

[93] AJ McEvily, D Eifler, and E Macherauch. "An analysis of the growth of short fatigue cracks". In: *Engineering Fracture Mechanics* 40.3 (1991), pp. 571–584.

[94] Kamal Medjaher and Noureddine Zerhouni. "Residual-based failure prognostic in dynamic systems". In: *IFAC Proceedings Volumes* 42.8 (2009), pp. 716–721.

[95] Subhasish Mohanty et al. "Mixed Gaussian process and state-space approach for fatigue crack growth prediction". In: *International workshop on structural heath monitoring.* Vol. 2. Citeseer. 2007, pp. 1108–1115.

[96] Aslan Mojallal and Saeed Lotfifard. "Multi-physics graphical model-based fault detection and isolation in wind turbines". In: *IEEE transactions on smart grid* 9.6 (2017), pp. 5599–5612.

[97] Amalendu Mukherjee, Ranjit Karmakar, and Arun Kumar Samantaray. *Bond graph in modeling, simulation and fault identification.* IK International New Delhi, 2006.

[98] Kevin Murphy and Stuart Russell. "Rao-Blackwellised particle filtering for dynamic Bayesian networks". In: *Sequential Monte Carlo methods in practice.* Springer, 2001, pp. 499–515.

[99] Hasan Ocak and Kenneth A Loparo. "HMM-based fault detection and diagnosis scheme for rolling element bearings". In: (2005).

[100] Aˆ Y Orbak et al. "Model reduction in the physical domain". In: *Proceedings of the Institution of Mechanical Engineers, Part I: Journal of Systems and Control Engineering* 217.6 (2003), pp. 481–496.

[101] Rolf F Orsagh, Jeremy Sheldon, and Christopher J Klenke. "Prognostics/diagnostics for gas turbine engine bearings". In: *ASME Turbo Expo 2003, collocated with the 2003 International Joint Power Generation Conference.* American Society of Mechanical Engineers Digital Collection. 2003, pp. 159–167.

[102] M Ch Pan, Paul Sas, and Hendrik Van Brussel. "Machine condition monitoring using signal classification techniques". In: *Journal of Vibration and Control* 9.10 (2003), pp. 1103–1120.

[103] Pe Paris and Fazil Erdogan. "A critical analysis of crack propagation laws". In: (1963).

[104] Jong I Park et al. "Dual features functional support vector machines for fault detection of rechargeable batteries". In: *IEEE Transactions on Systems, Man, and Cybernetics, Part C (Applications and Reviews)* 39.4 (2009), pp. 480–485.

[105] Romano Patrick et al. "An integrated approach to helicopter planetary gear fault diagnosis and failure prognosis". In: *2007 IEEE Autotestcon.* IEEE. 2007, pp. 547–552.

[106] Leto Peel. "Data driven prognostics using a Kalman filter ensemble of neural network models". In: *2008 International Conference on Prognostics and Health Management.* IEEE. 2008, pp. 1–6.

[107] Ying Peng and Ming Dong. "A hybrid approach of HMM and grey model for age-dependent health prediction of engineering assets". In: *Expert Systems with Applications* 38.10 (2011), pp. 12946–12953.

[108] Marie-Cécile Pera et al. *Electrochemical components.* John Wiley & Sons, 2013.

[109] Eduardo Bento Pereira, Roberto Kawakami Harrop Galvão, and Takashi Yoneyama. "Model predictive control using prognosis and health monitoring of actuators". In: *2010 ieee international symposium on industrial electronics.* IEEE. 2010, pp. 237–243.

[110] V Fernão Pires, JF Martins, and AJ Pires. "Eigenvector/eigenvalue analysis of a 3D current referential fault detection and diagnosis of an induction motor". In: *Energy conversion and management* 51.5 (2010), pp. 901–907.

[111] Om Prakash and AK Samantaray. "Model-based diagnosis and prognosis of hybrid dynamical systems with dynamically updated parameters". In: *Bond graphs for modelling, control and fault diagnosis of engineering systems.* Springer, 2017, pp. 195–232.

[112] Om Prakash et al. "Adaptive prognosis for a multi-component dynamical system of unknown degradation modes". In: *IFAC-PapersOnLine* 51.24 (2018), pp. 184–191.

[113] Karkulali Pugalenthi and Nagarajan Raghavan. "A holistic comparison of the different resampling algorithms for particle filter based prognosis using lithium ion batteries as a case study". In: *Microelectronics Reliability* 91 (2018), pp. 160–169.

[114] L. R. Rodrigues et al. "Use of PHM Information and System Architecture for Optimized Aircraft Maintenance Planning". In: *IEEE Systems Journal* 9.4 (2015), pp. 1197–1207.

[115] Yasmine Rosunally et al. "Prognostics framework for remaining life prediction of cutty sark iron structures". In: *Proc. Annu. Conf. Prognost. Health Management Soc.* 2009.

[116] Miguel Á Sainz, Joaquim Armengol, and Josep Vehı. "Fault detection and isolation of the three-tank system using the modal interval analysis". In: *Journal of process control* 12.2 (2002), pp. 325–338.

[117] Arun Kumar Samantaray and Belkacem Ould Bouamama. *Model-based process supervision: a bond graph approach.* Springer Science & Business Media, 2008.

[118] A Sánchez-Fernández et al. "Fault detection based on time series modeling and multivariate statistical process control". In: *Chemometrics and Intelligent Laboratory Systems* 182 (2018), pp. 57–69.

[119] B Satish and NDR Sarma. "A fuzzy BP approach for diagnosis and prognosis of bearing faults in induction motors". In: *IEEE Power Engineering Society General Meeting, 2005.* IEEE. 2005, pp. 2291–2294.

[120] JZ Sikorska, Melinda Hodkiewicz, and Lin Ma. "Prognostic modelling options for remaining useful life estimation by industry". In: *Mechanical systems and signal processing* 25.5 (2011), pp. 1803–1836.

[121] IV Singh et al. "The numerical simulation of fatigue crack growth using extended finite element method". In: *International Journal of Fatigue* 36.1 (2012), pp. 109–119.

[122] Manarshhjot Singh et al. "Bond graph model for prognosis and health management of mechatronic systems based on energy activity". In: *2018 7th International Conference on Systems and Control (ICSC).* IEEE. 2018, pp. 430–434.

[123] Rodney K Singleton, Elias G Strangas, and Selin Aviyente. "Extended Kalman filtering for remaining-useful-life estimation of bearings". In: *IEEE Transactions on Industrial Electronics* 62.3 (2014), pp. 1781–1790.

[124] Haithem Skima et al. "Post-prognostics decision making in distributed MEMS-based systems". In: *Journal of Intelligent Manufacturing* 30.3 (2019), pp. 1125–1136.

[125] Hoon Sohn, Keith Worden, and Charles R Farrar. "Statistical damage classification under changing environmental and operational conditions". In: *Journal of intelligent material systems and structures* 13.9 (2002), pp. 561–574.

[126] Abdenour Soualhi et al. "Hidden Markov models for the prediction of impending faults". In: *IEEE Transactions on Industrial Electronics* 63.5 (2016), pp. 3271–3281.

[127] JK Spoerre. "Application of the cascade correlation algorithm (CCA) to bearing fault classification problems". In: *Computers in industry* 32.3 (1997), pp. 295–304.

[128] Marcel Staroswiecki and G Comtet-Varga. "Analytical redundancy relations for fault detection and isolation in algebraic dynamic systems". In: *Automatica* 37.5 (2001), pp. 687–699.

[129] C Sueur and G Dauphin-Tanguy. "Bond graph approach to multi-time scale systems analysis". In: *Journal of the Franklin Institute* 328.5-6 (1991), pp. 1005–1026.

[130] Bo Sun et al. "Benefits and challenges of system prognostics". In: *IEEE Transactions on reliability* 61.2 (2012), pp. 323–335.

[131] David C Swanson. "A general prognostic tracking algorithm for predictive maintenance". In: *2001 IEEE Aerospace Conference Proceedings (Cat. No. 01TH8542).* Vol. 6. IEEE. 2001, pp. 2971–2977.

[132] RF Swati et al. "Extended finite element method (XFEM) analysis of fiber reinforced composites for prediction of micro-crack propagation and delaminations in progressive damage: a review". In: *Microsystem Technologies* 25.3 (2019), pp. 747–763.

[133] Babak Vaseghi, Noureddine Takorabet, and Farid Meibody-Tabar. "Fault analysis and parameter identification of permanent-magnet motors by the finite-element method". In: *IEEE Transactions on Magnetics* 45.9 (2009), pp. 3290–3295.

[134] Venkat Venkatasubramanian et al. "A review of process fault detection and diagnosis: Part III: Process history based methods". In: *Computers & chemical engineering* 27.3 (2003), pp. 327–346.

[135] Kim Verbert, Bart De Schutter, and Robert Babuška. "A multiple-model reliability prediction approach for condition-based maintenance". In: *IEEE Transactions on Reliability* 67.3 (2018), pp. 1364–1376.

[136] Jay Govind Verma, Sachin Kumar, and Pavan Kumar Kankar. "Crack growth modeling in spur gear tooth and its effect on mesh stiffness using extended finite element method". In: *Engineering Failure Analysis* 94 (2018), pp. 109–120.

[137] Gaetano Vilasi. *Hamiltonian dynamics*. World Scientific, 2001.

[138] Chih-Chung Wang and Gee-Pinn James Too. "Rotating machine fault detection based on HOS and artificial neural networks". In: *Journal of intelligent manufacturing* 13.4 (2002), pp. 283–293.

[139] Dong Wang et al. "Support vector data description for fusion of multiple health indicators for enhancing gearbox fault diagnosis and prognosis". In: *Measurement Science and Technology* 22.2 (2010), p. 025102.

[140] Hua WANG, Huan-min LIU, and Hui-fen DUAN. "Case-based reasoning method in fault diagnosis expert system of inertial navigation system". In: *Journal of Chinese Inertial Technology* 17.5 (2009), pp. 614–617.

[141] Jinjiang Wang et al. "An integrated fault diagnosis and prognosis approach for predictive maintenance of wind turbine bearing with limited samples". In: *Renewable Energy* 145 (2020), pp. 642–650.

[142] L Wang, Z Zhang, and C Xu RF Circuit Design. "Theory and applications". In: *Support Vector Machines, Springer-Verlag, Berlin Heidelber* (2005).

[143] X. Wang et al. "A Data Analytic Approach to Automatic Fault Diagnosis and Prognosis for Distribution Automation". In: *IEEE Transactions on Smart Grid* 9.6 (2018), pp. 6265–6273.

[144] ZeFeng Wang, Jean-Luc Zarader, and Sylvain Argentieri. "A novel aircraft fault diagnosis and prognosis system based on Gaussian mixture models". In: *2012 12th International Conference on Control Automation Robotics & Vision (ICARCV)*. IEEE. 2012, pp. 1794–1799.

[145] Yuxin Wen et al. "Degradation modeling and RUL prediction using Wiener process subject to multiple change points and unit heterogeneity". In: *Reliability Engineering & System Safety* 176 (2018), pp. 113–124.

[146] Qi Wu. "Fault diagnosis model based on Gaussian support vector classifier machine". In: *Expert Systems with Applications* 37.9 (2010), pp. 6251–6256.

[147] Siyan Wu, Ming J Zuo, and Anand Parey. "Simulation of spur gear dynamics and estimation of fault growth". In: *Journal of Sound and Vibration* 317.3-5 (2008), pp. 608–624.

[148] Jiuping Xu and Lei Xu. "Health management based on fusion prognostics for avionics systems". In: *Journal of Systems Engineering and Electronics* 22.3 (2011), pp. 428–436.

[149] Yuan Xu, Ying Liu, and Qunxiong Zhu. "Multivariate time delay analysis based local KPCA fault prognosis approach for nonlinear processes". In: *Chinese Journal of Chemical Engineering* 24.10 (2016), pp. 1413–1422.

[150] Zhengguo Xu, Yindong Ji, and Donghua Zhou. "A new real-time reliability prediction method for dynamic systems based on on-line fault prediction". In: *IEEE transactions on reliability* 58.3 (2009), pp. 523–538.

[151] Jihong Yan and Jay Lee. “A hybrid method for on-line performance assessment and life prediction in drilling operations”. In: *2007 IEEE International Conference on Automation and Logistics*. IEEE. 2007, pp. 2500–2505.

[152] Bo-Suk Yang and Achmad Widodo. “Support vector machine for machine fault diagnosis and prognosis”. In: *journal of system design and dynamics* 2.1 (2008), pp. 12–23.

[153] Yuan Yao and Furong Gao. “Statistical monitoring and fault diagnosis of batch processes using two-dimensional dynamic information”. In: *Industrial & engineering chemistry research* 49.20 (2010), pp. 9961–9969.

[154] Ming Yu. “Fault diagnosis and prognosis of hybrid systems using bond graph models and computational intelligence”. PhD thesis. 2012.

[155] Ming Yu, Danwei Wang, and Ming Luo. “An integrated approach to prognosis of hybrid systems with unknown mode changes”. In: *IEEE Transactions on Industrial Electronics* 62.1 (2014), pp. 503–515.

[156] Zhenyou Zhang, Yi Wang, and Kesheng Wang. “Fault diagnosis and prognosis using wavelet packet decomposition, Fourier transform and artificial neural network”. In: *Journal of Intelligent Manufacturing* 24.6 (2013), pp. 1213–1227.

[157] Chunhui Zhao and Furong Gao. “Online fault prognosis with relative deviation analysis and vector autoregressive modeling”. In: *Chemical Engineering Science* 138 (2015), pp. 531–543.

[158] Kai Zhong, Min Han, and Bing Han. “Data-driven based fault prognosis for industrial systems: a concise overview”. In: *IEEE/CAA Journal of Automatica Sinica* (2019).

[159] Zhe Zhou, Chenglin Wen, and Chunjie Yang. “Fault isolation based on k-nearest neighbor rule for industrial processes”. In: *IEEE Transactions on Industrial Electronics* 63.4 (2016), pp. 2578–2586.

[160] Zhi-Jie Zhou et al. “A model for real-time failure prognosis based on hidden Markov model and belief rule base”. In: *European Journal of Operational Research* 207.1 (2010), pp. 269–283.

[161] Zhiyu Zhu et al. “A convolutional neural network based on a capsule network with strong generalization for bearing fault diagnosis”. In: *Neurocomputing* 323 (2019), pp. 62–75.